

104p

19

MTP-P&VE-S-62-3
April 26, 1962

N64-16709

Code 1

NASA.

GEORGE C. MARSHALL

**SPACE
FLIGHT
CENTER**

HUNTSVILLE, ALABAMA

(NASA TMX-54641)

EXPERIMENTAL VIBRATION PROGRAM ON A FULL SCALE SATURN SPACE VEHICLE

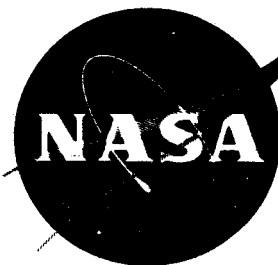
By and

Charles E. Watson & Kay W. Slayden

26 Apr. 1962

104p on file

OTS: \$9.10/
\$3.32



RQT 4710

GEORGE C. MARSHALL SPACE FLIGHT CENTER

MTP-P&VE-S-62-3

EXPERIMENTAL VIBRATION PROGRAM ON A FULL SCALE SATURN SPACE VEHICLE

By

Charles E. Watson & Kay W. Slayden

16709

ABSTRACT

A

The Saturn Block I Dynamic Test Vehicle (SA-D1) was subjected to lateral, torsional, and longitudinal bending mode tests. Transfer functions, relating sensor output to shaker force input, were obtained to aid the Astrionics Division in the design of vehicle control system networks.

The report contains bending mode shapes and frequencies with damping factors associated with each mode.

Tests were performed at five separate weight conditions as follows: Lift-off, 10 seconds, 35 seconds, Q max, and Cut-off.

Test results indicate a factor of six exists between engine control frequency and the lowest vehicle bending frequency, thus minimizing the possibility of severe engine-vehicle coupling.

AUTHOR

GEORGE C. MARSHALL SPACE FLIGHT CENTER

MTP-P&VE-S-62-3

EXPERIMENTAL VIBRATION PROGRAM ON A FULL SCALE SATURN SPACE VEHICLE

By

Charles E. Watson & Kay W. Slayden

EXPERIMENTAL STRUCTURES SECTION
STRUCTURES BRANCH
PROPULSION & VEHICLE ENGINEERING DIVISION
GEORGE C. MARSHALL SPACE FLIGHT CENTER
NATIONAL AERONAUTICS AND SPACE ADMINISTRATION
HUNTSVILLE, ALABAMA

TABLE OF CONTENTS

Section	Page
I. INTRODUCTION.....	1
II. DESCRIPTION.....	2
A. Test Setup.....	2
B. Instrumentation and Control.....	4
C. Test Results.....	5
1. General.....	5
2. Lateral Tests.....	7
3. Torsional Vibration Tests.....	9
4. Longitudinal Tests.....	10
5. Structural Damping.....	10
6. Cable Resonances.....	13
III. CONCLUSIONS AND RECOMMENDATIONS.....	13
APPENDIX.....	92

LIST OF ILLUSTRATIONS

Figure	Title	Page
1.	Drawing of SA-D1 in the Test Tower.....	15
2.	Installation in the Test Tower.....	16
3.	Spring Cluster.....	17
4.	Original Lower Connecting Link.....	18
5.	New Lower Connection Link.....	19
6.	Instrumentation Trailer.....	20
7.	Electro-Dynamic Shakers.....	21
8.	Pitch Bending Mode Frequencies VS. Flight Time....	22
9.	SA-D1 and SA-1 Weight and CG VS. Flight Time.....	23
10.	Suspension and Shaker Orientation.....	24
11.	Vehicle Frequency Response Curves.....	25
12.	Vehicle Frequency Response Curves.....	26
13.	Vehicle Frequency Response Curves.....	27
14.	Vehicle Frequency Response Curves.....	28
15.	Extrapolation to the Free-Free Frequency.....	29
16.	Lateral Bending Modes (Pitch Plane).....	30
17.	Lateral Bending Modes (Pitch Plane).....	31
18.	Lateral Bending Modes (Pitch Plane).....	32
19.	Lateral Bending Modes (Pitch Plane).....	33
20.	Lateral Bending Modes (Pitch Plane).....	34
21.	Lateral Bending Modes (Pitch Plane).....	35
22.	Lateral Bending Modes (Pitch Plane).....	36

LIST OF ILLUSTRATIONS (Con't)

Figure	Title	Page
23.	Lateral Bending Modes (Pitch Plane).....	37
24.	Lateral Bending Modes (Pitch Plane).....	38
25.	Lateral Bending Modes (Pitch Plane).....	39
26.	Lateral Bending Modes (Pitch Plane).....	40
27.	Lateral Bending Modes (Pitch Plane).....	41
28.	Lateral Bending Modes (Pitch Plane).....	42
29.	Lateral Bending Modes (Pitch Plane).....	43
30.	Lateral Bending Modes (Pitch Plane).....	44
31.	Lateral Bending Modes (Pitch Plane).....	45
32.	Lateral Bending Modes (Pitch Plane).....	46
33.	Lateral Bending Modes (Pitch Plane).....	47
34.	Lateral Bending Modes (Pitch Plane).....	48
35.	Lateral Bending Modes (Pitch Plane).....	49
36.	Lateral Bending Modes (Pitch Plane).....	50
37.	Lateral Bending Modes (Pitch Plane).....	51
38.	Lateral Bending Modes (Pitch Plane).....	52
39.	Lateral Bending Modes (Pitch Plane).....	53
40.	Lateral Bending Modes (Pitch Plane).....	54
41.	Lateral Bending Modes (Pitch Plane).....	55
42.	Lateral Bending Modes (Pitch Plane).....	56
43.	Lateral Bending Modes (Pitch Plane).....	57
44.	Lateral Bending Modes (Pitch Plane).....	58
45.	Lateral Bending Modes (Pitch Plane).....	59

LIST OF ILLUSTRATIONS (Con't)

Figure	Title	Page
46.	Lateral Bending Modes (Yaw Plane).....	60
47.	Lateral Bending Modes (Yaw Plane).....	61
48.	Lateral Bending Modes (Yaw Plane).....	62
49.	Lateral Bending Modes (Yaw Plane).....	63
50.	Lateral Bending Modes (Yaw Plane).....	64
51.	Lateral Bending Modes (Yaw Plane).....	65
52.	Lateral Bending Modes (Yaw Plane).....	66
53.	Lateral Bending Modes (Yaw Plane).....	67
54.	Lateral Bending Modes (Yaw Plane).....	68
55.	Lateral Bending Modes (Yaw Plane).....	69
56.	Lateral Bending Modes (Yaw Plane).....	70
57.	Lateral Bending Modes (Yaw Plane).....	71
58.	Lateral Bending Modes (Yaw Plane).....	72
59.	Lateral Bending Modes (Yaw Plane).....	73
60.	Lateral Bending Modes (Yaw Plane).....	74
61.	Lateral Bending Modes (Yaw Plane).....	75
62.	Lateral Bending Modes (Yaw Plane).....	76
63.	Lateral Bending Modes (Yaw Plane).....	77
64.	Lateral Bending Modes (Yaw Plane).....	78
65.	Lateral Bending Modes (Yaw Plane).....	79
66.	Lateral Bending Modes (Yaw Plane).....	80
67.	Lateral Bending Modes (Yaw Plane).....	81

LIST OF ILLUSTRATIONS (Con't)

Figure	Title	Page
68.	Lateral Bending Modes (Yaw Plane).....	82
69.	Lateral Bending Modes (Yaw Plane).....	83
70.	Lateral Bending Modes (Yaw Plane).....	84
71.	Lateral Bending Modes (Yaw Plane).....	85
72.	Lateral Bending Modes (Yaw Plane).....	86
73.	Lateral Bending Modes (Yaw Plane).....	87
74.	Lateral Bending Modes (Yaw Plane).....	88
75.	Torsional Bending Modes.....	89
76.	Torsional Bending Modes.....	90
77.	Torsional Bending Modes.....	91
A-1.	Cable Resonant Response (SA-D5).....	93
A-2.	Cable Frequency VS. Cable Tension (SA-D5).....	94

DEFINITION OF SYMBOLS

SYMBOL	DEFINITION
f	Resonant frequency - cycles per second
G	Number of gravities of acceleration
g	Structural damping factor - $2 \frac{C}{C_c}$
ω_n	Circular resonant frequency - radians per second
K	Torsional spring constant in-lbs. per radian
(P-P)	Peak to peak
cps	Cycles per second

GEORGE C. MARSHALL SPACE FLIGHT CENTER

MTP-P&VE-S-62-3

EXPERIMENTAL VIBRATION PROGRAM ON A FULL SCALE SATURN SPACE VEHICLE

By

Charles E. Watson & Kay W. Slayden

SUMMARY

The Saturn Block I Dynamic Test Vehicle (SA-D1) was subjected to a ground vibration survey in the simulated free-free condition. Transfer functions obtained were used to aid the Astrionics Division in the design of control system networks.

Lateral bending mode frequencies increased from 2.20 cps, the Lift-off first mode, to near 12 cps, the Q max third mode. A great deal of interaction and coupling was derived from separate outer tank bending mode frequencies which at Q max (flight condition corresponding to max dynamic pressure) obscured the second bending mode entirely. First torsional bending mode increased from 5.69 cps at Lift-off to 7.91 cps at Cut-off. All frequencies found are sufficiently above the expected control frequency.

Damping factors obtained averaged "g" - 2.40 percent.

SECTION I. INTRODUCTION

The Saturn Block I Dynamic Test Vehicle (SA-D1) is a full scale prototype of SA-1, NASA's first Saturn Flight Test Vehicle. The vehicle consists of a 75-foot booster (S-I) composed of a 105-in. diameter center LOX tank encircled by eight 70-in. diameter alternating fuel and LOX containers. Mounted aft of the containers and through the thrust frame section are eight liquid rocket engines rated at 165,000 lb thrust each. Forward of the booster and second stage adapter are two dummy stages, S-IV and S-V respectively, containing water ballast tanks representing the correct weight, center of gravity and moment of inertia of future powered upper stages. The most forward portion of the vehicle is an instrument compartment and a dummy payload making the entire vehicle

163 ft long, weighing 305,614 lb empty and 933,730 lbs at Lift-off. FIGURE 9 shows a comparison of the variation in weight and center of gravity between SA-1 and SA-D1 versus flight time.

The purpose of the experimental vibration program is to excite the vehicle through a frequency range sufficient to determine the significant free-free lateral, torsional and longitudinal mode shapes, frequencies, and associated damping coefficients. Knowledge of these is required because of their effects on the vehicle control stabilizing networks.

In cooperation with Flight Dynamics personnel in the Astrionics Division, transfer functions were obtained for the first three bending modes and the first torsional mode expressing amplitude and phase of rate gyro outputs at four locations versus lateral force input at the engine gimbal plane.

Five vehicle conditions were tested to obtain the variation of bending frequencies during powered flight. Flight time conditions tested are as follows:

T = 0 (Lift-off)
T = 10 seconds
T = 35 seconds
T = 63 seconds (Q max)
T = 119 seconds (Cut-off)

The tanks were filled with deionized water and the correct weight was simulated within 3 percent at each flight time mentioned.

SECTION II. DESCRIPTION

A. TEST SETUP

To simulate a free-free condition the vehicle was suspended in the Dynamic Test Stand, shown in the photograph, FIGURE 2. The suspension system consisted of cables running upward from the outrigger points located in the tail section of the vehicle through a group of twelve springs to a hydraulic cylinder fastened at the 72-ft level of the tower. Eight hydraulic cylinders were used to raise the vehicle clear of its hold-down structure, a distance of approximately 1-1/4 inches. See the photographs, FIGURES 3, 4, and 5 and the drawing in FIGURE 1. FIGURE 4 shows the new lower suspension link developed during the test program. The new connecting link has only 1/5 the weight of the original connecting link, but because of its late introduction into the test program, only the 10-second and Empty time conditions were tested with it. The springs

present in each of the eight suspension assemblies provided a relatively soft suspension system having a total maximum lateral spring rate of 626#/in. and a total vertical spring rate of 625,500#/in.

Calculations done prior to the test showed that a ratio of at least 20 to 1 existed between expected first bending mode frequencies and the rigid body translational frequency of the vehicle and suspension system. This ratio was satisfactory, because normally an attempt is made to keep the ratio at 10 to 1 or greater. However; the rigid body rocking frequency of the vehicle about its center of gravity proved to be somewhat higher, thus lowering the ratio of separation. In order to keep the ratio as high as possible, the suspension was varied along with the various time points tested.

First bending mode frequency to rocking frequency ratios determined during lateral tests are listed in Table I, below.

TABLE I

<u>TIME</u>	<u>PITCH</u>	<u>YAW</u>
L. O.	6.41	7.20
10 sec.	6.96	7.63
35 sec.	8.02	8.56
Q max	11.55	9.12
Empty	6.70	6.08

The rigid body rotational frequency to first torsional mode ratio was satisfactory and remained above 20 to 1 for all torsional tests performed.

This ratio for the longitudinal test conducted was 5.16 to 1. This value is low because it is in direct line of the spring suspension system and when considering the large mass involved, the ratio is rather good.

The sketch shown in FIGURE 10 gives a description of the seven variations in suspension used for all test results included in this report. This sketch also shows the two principal planes of excitation, namely, the yaw plane and the pitch plane + $22\frac{1}{2}^{\circ}$ referred to as the pitch plane throughout the report.

B. INSTRUMENTATION AND CONTROL

Instrumentation used on previous vibration tests was composed of velocity pickups, having natural frequency of 6 cps, mounted on the vehicle in critical locations and roving pickups were used to establish nodal points. Their use in this test was prohibited because of the frequency range in which the major portion of the investigation was carried out, namely, 0 - 10 cps.

Strain gage bridge type, one "G", accelerometers were used with reasonable success during this test. The amplitude ratio of the calibrating accelerometer and a typical test accelerometer was equal to 1.0 (flat response) up to 10 cps; above this the ratio varied between 1.05 and 0.95 at 15 cps, or 1.0 and 0.90 at 20 cps. The phase lag equalled 30 degrees at 12 cps. Sufficient calibration data was available to correct original test data for these effects. The majority of testing was done at less than 10 cps, at "G" levels between 0.1 and 0.5 G's vector. Accelerometer outputs were put through amplifier and associated galvanometers and read on two direct writing oscillographs, shown in the photograph, FIGURE 6.

Power to drive the shakers was supplied from a 40-ampere amplidyne generator modified to deliver constant current with an increased response time for operation in the frequency range of 0 - 15 cps and an electronic power amplifier for use above 15 cps.

A system of four shakers was available for use in determining lateral and torsional mode shapes. Each new time condition was investigated using two or three shakers, depending on the mode in question, at 300 to 400 lb vector each; and by varying the phase of the shakers, mode shapes were established.

Original mode shape studies were followed by transfer function determinations during which either the 1500-lb shaker or two 500-lb long stroke shakers, located at the gimbal plane, were operated at force levels of approximately 1000 lb vector. The 1500-lb shaker and the two 500-lb shakers were used in the pitch and yaw planes, respectively. The photograph in FIGURE 7 shows the 1500-lb shaker in the center and one of the 500-lb shakers on the left.

The two 500-lb shakers were operated out of phase for torsional tests and in phase beneath the Fin I and II outriggers for the longitudinal tests performed.

Resonant frequencies were determined, during these runs, with rate gyro and armature current output on an oscilloscope. The rate gyro was used in preference to an accelerometer because it has no appreciable phase lag below 25 cps. The bending mode diagrams presented in this report were taken from these runs.

The frequency response curves shown were obtained from incremental sweeps run through the first bending mode. Increments of $0.01 \pm .002$ cps were converted to the period (T) in seconds, and during a sweep, an electronic counter was used to establish periods within the required tolerance. Usually, sweeps were limited to a bandwidth of one cycle.

C. TEST RESULTS

1. General. The most distinct mode shapes, taken with the softest suspension system, are shown plotted on an outline of the vehicle in FIGURES 16 - 77. The curves coordinates are "G" (peak to peak) versus vehicle station and pickup location. Node points are marked on the left of the station ordinates. Mode shapes of the outer tanks instrumented are shown adjacent to the primary structural mode.

A comparison of SA-D1, Langley model and single beam theoretical mode shapes and frequencies is made for first and second bending modes at the Lift-off, Q max, and Empty flight time conditions. These data are plotted on the corresponding SA-D1 mode shape in FIGURES 16, 21, 38, 40, 43, and 44.

The first bending mode shapes agree closely from the three sources; however, theoretical first bending frequencies are lower than both SA-D1 and Langley. There exists considerable difference in the second bending mode shapes, with both Langley and the theoretical showing notably more response than SA-D1. It is suspected that outboard engine activity throughout this frequency range may be causing this difference in response, which is representative of the flight vehicle. The second bending frequency values have less percent difference than the first mode values, with the theoretical second bending values being lowest.

The Langley model exhibits a characteristic second bending at the Q max time condition, while the SA-D1 mode shape shows the outer tanks out of phase with the primary structure. Test results indicate the outer propellant tanks of the Langley model have greater stiffness than those in SA-D1.

FIGURE 8 shows how lateral bending frequencies vary with increasing flight time. Table II gives a comparison of lateral resonant frequencies obtained with hard and soft suspension systems and torsional resonant frequencies obtained with a soft suspension system.

An experimental indication of the effect of vehicle suspension stiffness on the true free-free first bending resonant frequency is given by FIGURE 15. In one case the vehicle (first stage empty) was suspended from four suspension points producing a restoring moment of 3.15×10^9 in. - #/radian. The corresponding first bending resonant frequency was 3.12 cps. In the other case the restoring moment was $.538 \times 10^9$ in. - #/radian with a corresponding first bending resonant frequency of 2.95 cps.

TABLE II

RESONANT BENDING MODE FREQUENCIES OBTAINED WITH
SOFT & HARD SUSPENSIONS IN THE PITCH & YAW PLANES

MODE	L. O.						10 Sec.						35 Sec.						Q max						Cutoff					
	PITCH			YAW			PITCH			YAW			PITCH			YAW			PITCH			YAW			PITCH			YAW		
	S	H	S	S	H	S	S(N)	H(N)	S	S	H	S	S	H	S	S	H	S	S	H	S	S	H	S	S(N)	H	S	H	S	H
Rocking	.343	.392	.304	.354	.354	.304	.334	.392	.304	.354	.354	.334	.394	.392	.245	.415	.317	.406	.44	.591	.501	.584								
1st Bending	2.20	2.26	2.19	2.25	2.25	2.32	2.39	2.43	2.32	2.34	2.34	2.68	2.66	2.68	2.83	2.94	2.89	2.96	2.95	3.20	3.05	3.22								
1st Cluster	4.02	--	3.90	3.91	4.04	4.02	4.04	4.04	4.02	4.27	4.66	4.66	4.67	4.73	5.68	5.82	5.75	5.80	--	--	--	--								
2nd Cluster	5.54	--	5.50	5.51	5.85	5.78	5.69	5.69	5.78	5.76	7.09	8.36	8.40	8.52	7.83	7.97	7.79	7.87	--	--	--	--								
2nd Bending	6.74	--	6.80	6.80	6.94	6.87	10	10.18	10.0	10.0	10.0	10.72	10.09	11.1	10.46	10.46	10.8	10.7	--	--	--	--								
Engine	--	--	9.34	9.56	10.12	10.18	11.96	11.98	12.0	11.94	11.62	11.62	11.60	12.28	12.3	12.28	12.28	12.42	--	--	--	--								
3rd Bending	9.19	--	11.7	11.8	11.96	11.98	11.96	11.98	12.0	11.94	11.62	11.62	11.60	12.28	12.3	12.28	12.28	12.42	--	--	--	--								

(N) New Lower Suspension Link

RESONANT TORSIONAL MODE FREQUENCIES OBTAINED WITH A SOFT SUSPENSION SYSTEM				
MODE	L. O.	35 Sec.	Q max	Empty
Rigid Body	0.239	0.256	0.258	0.333
1st Torsional	5.69	6.38	6.36	7.91
Cluster	6.38	8.35	----	----
Cluster & Engine	9.47	10.73	9.73	----

Both these frequency values were obtained with the modified light-weight suspension system, and due to the fact that no interference was obtained from suspension cable "string" resonances in either case, the change in frequencies obtained was due almost entirely to change in stiffness. With the foregoing assumption, the true free-free first bending frequency can be deduced as follows:

$$\text{Since } \omega_n = \left(\frac{K}{M} \right)^{\frac{1}{2}}$$

$$d\omega_n = \frac{dK}{2(KM)^{\frac{1}{2}}}$$

or, for small changes in ω_n and K

$$\Delta\omega_n \sim \Delta K$$

This relation is plotted in FIGURE 15 yielding 2.93 for the true free-free first bending frequency as against 2.95 obtained with the soft spring restoring system.

2. Lateral Tests

a. First Bending Modes. In general, the primary mode shapes are considerably affected by coupling of the outer tanks with the vehicle when their individual resonant frequencies occur near one another. More specifically the first bending mode shapes in Figures 16, 24, 46, and 53 show there are no uncoupled first bending mode shapes at the Lift-off and 10 seconds flight time conditions. In each case there is either an outer LOX or outer fuel tank out of phase with the center tank. These modes were chosen because they are the lowest vehicle resonance found in each series. First bending modes at Q max and Empty are clean normal modes with all measured outer tanks in phase with the center tank. The first bending mode at the 35 seconds time condition, shown in FIGURE 32, appears relatively clean; however, its decay curve exhibits an abnormally high value for structural damping. The frequency response diagram in FIGURE 13 shows a resonant peak whose response is only one-half combined with a band width twice that of other time conditions plotted, and explains the occurrence of the high structural damping factor. The broad band resonant peak is maintained by closely coupled outer tank resonance and places the first bending mode at 35 seconds in a class with the Lift-off and 10 seconds first bending modes. FIGURES 11 - 15 are frequency response diagrams for the five time conditions tested, and show the relative amplitude of the primary structure and outer tanks obtained from incremental sweeps through the first vehicle resonance. These response curves aid and substantiate results determined from the mode shape diagrams, and show that the clean resonant peaks for Q max and Empty are unique, and degenerate into more complex form with increasing tank fullness.

FIGURE 11 is the frequency response curve for the first mode at Lift-off. This mode was peaked at 2.20 cps with the rate gyro, for the mode shape shown in FIGURE 16, while fuel and LOX tank individual first bending modes were established at 2.21 cps and 2.32 cps, respectively. The response curve shows the first bending mode at 2.17 cps and slightly higher at 2.18 cps is the only outer LOX tank resonance within this range. The fuel tank resonance, when coupled with the vehicle shows up at 2.28 cps. These are followed by weaker outer tank resonances between 2.4 and 2.44 cps with the next strongest resonance at 2.85 cps, the LOX tank in resonance in the tangential direction. Fuel tank tangential was not monitored during this sweep. The 10 seconds response curve, see FIGURE 12, is equally, if not more, complex than that found at Lift-off.

b. Cluster Modes. Cluster modes are apparent between the first and second bending modes at Lift-off, 10 seconds, 35 seconds, and Q max. The first cluster mode is distinguished by having only one node on the primary structure with all outer tanks measured out of phase with the center tank. The second cluster mode shows the characteristic second bending mode on the primary structure; however, in pitch, the outer LOX tank #1 and outer fuel tank #1 are in phase with the center tank, but outer fuel tank #4 is out of phase. In the yaw plane, outer LOX tank #4 and outer fuel tank #4 are in phase with the center tank but outer fuel tank #1 is out of phase. Frequency flight time curves, shown in FIGURE 8, shows the slope of the cluster mode curves increasing rapidly toward the second vehicle mode line causing complex mode coupling in the vicinity of the high end of the cluster mode curves, with the consequence that no second bending mode was found at the Q max condition. The resonant point closest to second bending at the Q max condition was found at 7.83 cps, but by definition, is a second cluster mode.

c. Second Bending Modes and Engines. All second bending modes, excluding the Q max time condition, are strong, clean modes, and in general, have low structural damping factors.

The outboard engine cantilever resonant frequencies were increased from around 6 cps to 9.0 and 8.3 cps in the pitch and yaw planes, respectively, by bracing the actuator support arms before overall vehicle tests began. Because it was impossible to increase engine resonance above 10 cps or out of the suspected critical frequency range, highly damped hydraulic control valves were placed in the engine control system to dampen or limit response peaks and cause wide resonant peaks in this frequency range. However, when coupled with vehicle resonances, engine resonances, at some degree of buildup, are found anywhere between 6 and 10.6 cps. This frequency range covers the majority of second bending frequencies; and diagrams of the second bending modes for Lift-off and 35 seconds in the pitch plane and Lift-off, 10 seconds, and 35 seconds in the yaw plane show a reversal of the mode shape below the lowest node point. This effect is attributed to strong out of phase motion of the engines acting as mechanical dampers.

d. Higher Bending Modes. The frequency range from 9 to 12 cps is complicated by outer tank second bending resonances for the Lift-off, 10 seconds, and 35 seconds flight time conditions. Between 11.5 to 12 cps the top section, from Station 1700 forward, has a strong partial cantilever resonance; and vehicle resonances existing in this frequency range, namely, 35 seconds and Q max third bending modes, tend to couple with the top section resonance (see FIGURES 37 and 42). This frequency is very easily excited and is found riding on lower multiple frequencies of 2, 3, and 4 cps, making records difficult to read, thus influencing amplitude and damping values taken from multiple and beating record traces. Mode shapes in the frequency range from 9 - 12 cps are divided into engine and third bending modes with variations of each, depending on outer tank activity.

3. Torsional Vibration Tests

a. First Torsional Modes. The first torsional mode shapes for Lift-off, 35 seconds, and Empty are shown in FIGURES 75 through 77, respectively. Each has a single node within the S-I stage, with the outer tanks in phase with the primary structure.

b. Cluster Modes. The first mode is followed by a cluster mode that is characterized in a manner similar to those found in lateral tests. There is no node on the primary structure and tangential pickups on the outer tanks show them out of phase with the primary structure. This type mode is found in the Lift-off and 35 seconds time conditions.

c. Cluster and Engine Modes. This mode is exhibited in the Lift-off and 35 seconds time condition and consists of the primary structure and outer fuel tanks being in phase while the outer LOX tanks and outboard engines are out of phase. The engine response in these modes is very strong. In the Q max condition, the lower cluster mode frequency has increased into the higher frequency range, and this condition results in a coupling of the lower cluster mode with the engines with very weak response of the primary structure.

Higher resonant points, up to 13 cps, consist of outer tank second bending modes for heavy conditions and outer tank first bending modes for the Empty condition. There are no resonant frequencies between 7.91 cps and 14.22 cps in the Empty condition.

Cluster and engine modes are accompanied by high values of structural damping, which is discussed in Section II.

4. Longitudinal Test

A brief longitudinal test was made using two 500-lb shakers mounted beneath outriggers on Fins I and III. The vehicle was at the 10 seconds weight condition, and a rigid body bouncing frequency was found at 1.61 cps. Two longitudinal modes were found, the first at 8.32 cps and the second at 11.1 cps. The 8.32 cps looks like a first mode with a node at Station 1140, but the 11.1 cps frequency also has only one node located at Station 1300. Because of the extreme time limit placed on this phase, it was impossible to instrument the vehicle sufficiently to identify the higher mode. It is suspected, however, that the outboard engines in cantilever motion may be out of phase with the base of the vehicle to give a second node at the 11.1 cps frequency, giving a second mode and a cause for the higher forward node point. Structural damping (g) equaled 8.5 percent and 1.5 percent on the first and second frequency, respectively.

5. Structural Damping

Structural damping factors ($g = \frac{2C}{Cc}$) were determined experimentally by the logarithmic decrement method. Damping values obtained are listed in Table III

As seen in Table III, the trend for damping is to decrease with increasing bending modes. The values are not consistent enough to make any statement of change with increasing tank fullness. The cluster modes show a decrease in damping from the first to the second.

Values used to obtain damping factors were taken from records of the forwardmost pickups unless their output was unsatisfactory; then values were taken from pickups located on another component that was in resonance, generally outer LOX or fuel tanks. The forwardmost pickups give a representative damping factor for the entire vehicle, but this is not necessarily true for outer tank locations.

Damping factors were obtained from all pickup locations on two first bending records, one for Lift-off in the pitch plane and the other for Lift-off in the yaw plane; the average "g" value compared with "g" from the top pickup is as follows:

$$\text{Structure Damping Factor } \%g = 2 \frac{C}{Cc} \times 100$$

	<u>Average</u>	<u>P.U. #35</u>
Pitch Plane	2.52	2.71
Yaw Plane	4.13	4.41

TABLE III

DAMPING VALUES OBTAINED DURING LATERAL AND TORSIONAL EXCITATION

LATERAL TESTS
 $\% "g" = 2 \frac{C}{Cc} \times 100$

MODE	PITCH					YAW				
	L.O.	10 Sec.	35 Sec.	Q max	Empty	L.O.	10 Sec.	35 Sec.	Q max	Empty
1st	2.62	2.36	11.6 ¹	2.27	2.41	4.41	6.15	3.62	2.48	5.0
2nd	1.0	-- 2.	1.04	--	1.82	1.07	0.982	0.864	--	3.83
3rd	1.26	1.48	1.75	1.36	--	1.18	1.8	2.7	1.61	--
1st Cluster	2.62	4.99	2.83	2.41	--	2.99	2.0	3.71	4.5	--
2nd Cluster	2.21	2.7	2.09	1.52	--	1.8	2.14	2.5	1.9	--

NOTES:

- See FIGURE 13. The wide band resonant peak, caused by tank coupling, causes this apparent high damping value.
- Output is low, making damping values unreliable.

TORSIONAL TESTS

 $\% "g" = 2 \frac{C}{Cc} \times 100$

MODE	L.O.	35 Sec.	Q max	Empty
1st	2.76	1.64	1.58	18.0
Cluster	7.8	8.15	--	--
Engine & Cluster	--1.	--2.	--2.	--

NOTES:

- Very highly damped; difficult to obtain accurate "g" value.
- All traces beating giving false "g" value.

Because structural damping is proportional to displacement, damping factors were determined from the first ten cycles after armature current cut-off so damping from separate runs would be comparable. Various influences present that might cause the damping factors listed in Table III to vary from the expected trends are as follows:

a. First and third modes already mentioned with regard to outer tank coupling, whether it be first or second bending in the outer tanks, have higher damping factors than would be expected if they were pure modes.

b. The second bending modes, in general clean modes, are affected by engine resonances which increase or decrease damping factors, depending upon the phase relation of the engines with respect to the tail of the vehicle. The phase angle can vary from 0 to 180° depending upon what part of the engine resonance curves the mode frequency coincides with.

The decrease in damping factor with increasing bending mode is due mainly to the decrease in amplitude associated with higher modes. The decrease in damping from first to second cluster mode is caused by decreased relative motion in the outer tanks in the second cluster mode.

The general increase in damping factor from the pitch plane to yaw plane is due in part to larger amplitudes of vibration caused by longer stroke shakers, but also due to the geometry of outer tanks along the two different planes of vibration. The pitch plane is the more rigid because of the symmetric location of outer LOX tanks.

Fluid movement (slosh) increases vehicle structural damping factors. Structural damping factors appear to decrease in outer propellant tanks when slosh frequencies and outer tank frequencies couple. The fluid movement supplies the energy to drive the tank after shaker cut-off, resulting in oscillograph records that show a very low rate of oscillation decay.

Damping values of the first torsional mode are comparable to those in lateral tests, except for the Empty condition. Cluster and engine modes are very highly damped, which is a characteristic of the engines and due to an increased relative motion of outer tanks in the torsional direction. The torsional test subjected connecting pins in the forward end of the fuel tank to motion in line with them as opposed to perpendicular to a line through them in radial excitation causing the increase in relative motion during torsional tests.

6. Cable Resonances

Cable resonances became annoying when they occurred near vehicle bending resonances. This was first noticed Empty with four point suspension and again at Q max with 8 point suspension; however, valid data was obtained for Q max using four point suspension. Cable resonances occurred again intermittently at the three other time conditions, depending on the suspension system used. Usually the softest suspension for 35 seconds, 10 seconds, and Lift-off raised the tension in four of the cable assemblies so that their resonances occurred between the first bending and first cluster modes. However, it was necessary to raise the cable assembly frequency, so a new lower link was designed that uses only one suspension cable and weighs only 1/5 the amount of the original lower connection link. This decrease in effective cable mass and increase in cable tension raised cable frequencies again. As explained earlier, the 10-second and Empty conditions, the two conditions felt to be most affected by cables, were rerun with the new suspension links providing reliable test results from the five time conditions tested.

Cable resonance is not expected to be a problem in SA-D5 dynamic tests and is explained in the Appendix.

SECTION III. CONCLUSIONS AND RECOMMENDATIONS

A frequency spectrum would show no resonant bending frequencies below 2 cps, thus leaving approximately a factor of 6 between the Lift-off first lateral mode and the expected vehicle control system frequency. First torsional modes start at 5.69 cps and altogether have a higher average damping factor than lateral modes. These two factors indicate that torsional modes have little effect on control problems.

Tank slosh frequencies are present in the range of the control system frequency; however, slosh baffles, present in the tanks, limit slosh buildup effectively, and the slosh frequencies increase with increase in longitudinal acceleration.

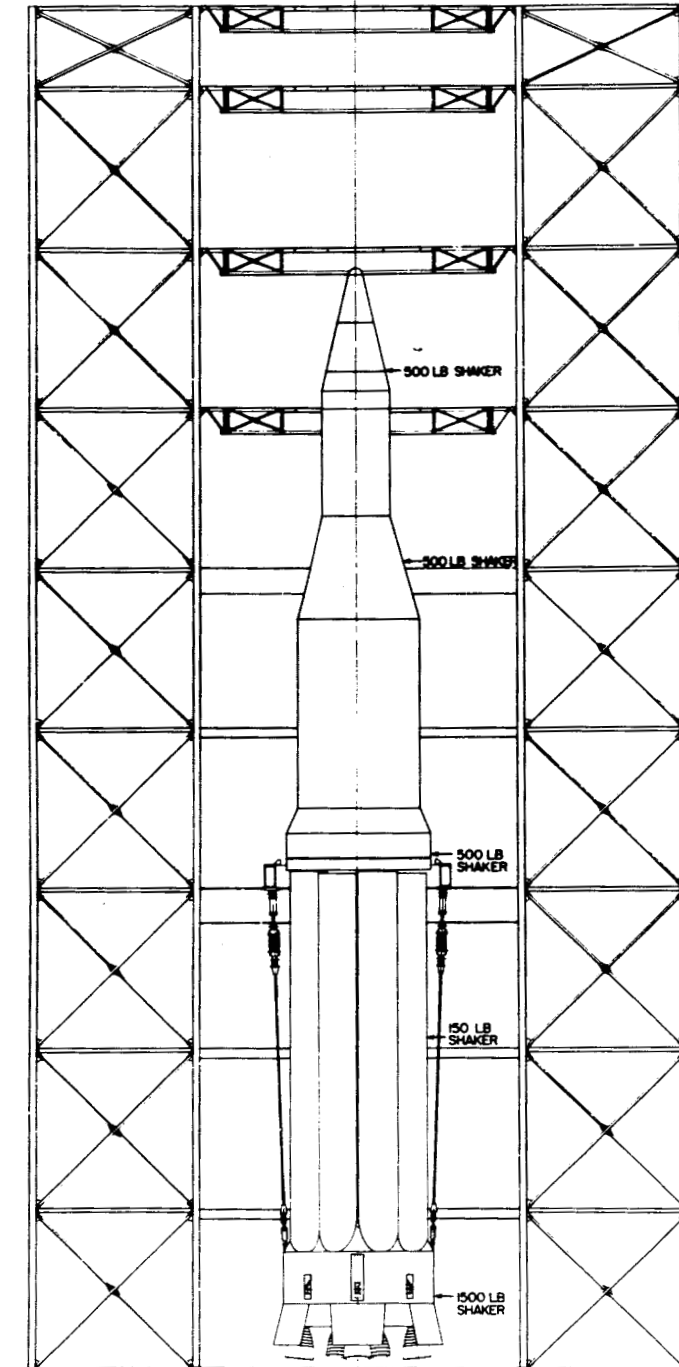
Generally speaking, lateral damping factors decrease with increasing bending mode and cluster mode frequency. The average lateral damping factor obtained during the test is "g" 2.4 percent. Average "g" values from torsional tests are 4.36 percent.

Use of the new lower connecting link raised bending frequencies approximately 1 percent because of the large weight decrease near the tail of the vehicle and because of the increased resonant frequency of the cable assemblies.

Resonant frequencies obtained, using the softest suspension allowable in each case, are estimated to be very close to actual free-free conditions by extrapolation of results obtained with hard and soft suspensions. The 0.67 percent difference, shown in the report for the Empty condition, would not increase above a maximum of 5 percent difference for the Lift-off condition.

Efforts should be made to excite SA-D5 along the true pitch plane rather than the pitch plane $+22\frac{1}{2}^{\circ}$ used in this test.

A possibly more refined suspension system, consisting of 6 degrees of freedom fluid bearings, is under consideration for use with SA-D5 (Block II Configuration). If this system proves successful, it will eliminate the necessity for avoiding cable resonances. It is felt that the suspension system used for SA-D1, however, created no significant errors, and with refinements made possible by the experience gained in the SA-D1 program, can be very successfully utilized for SA-D5.

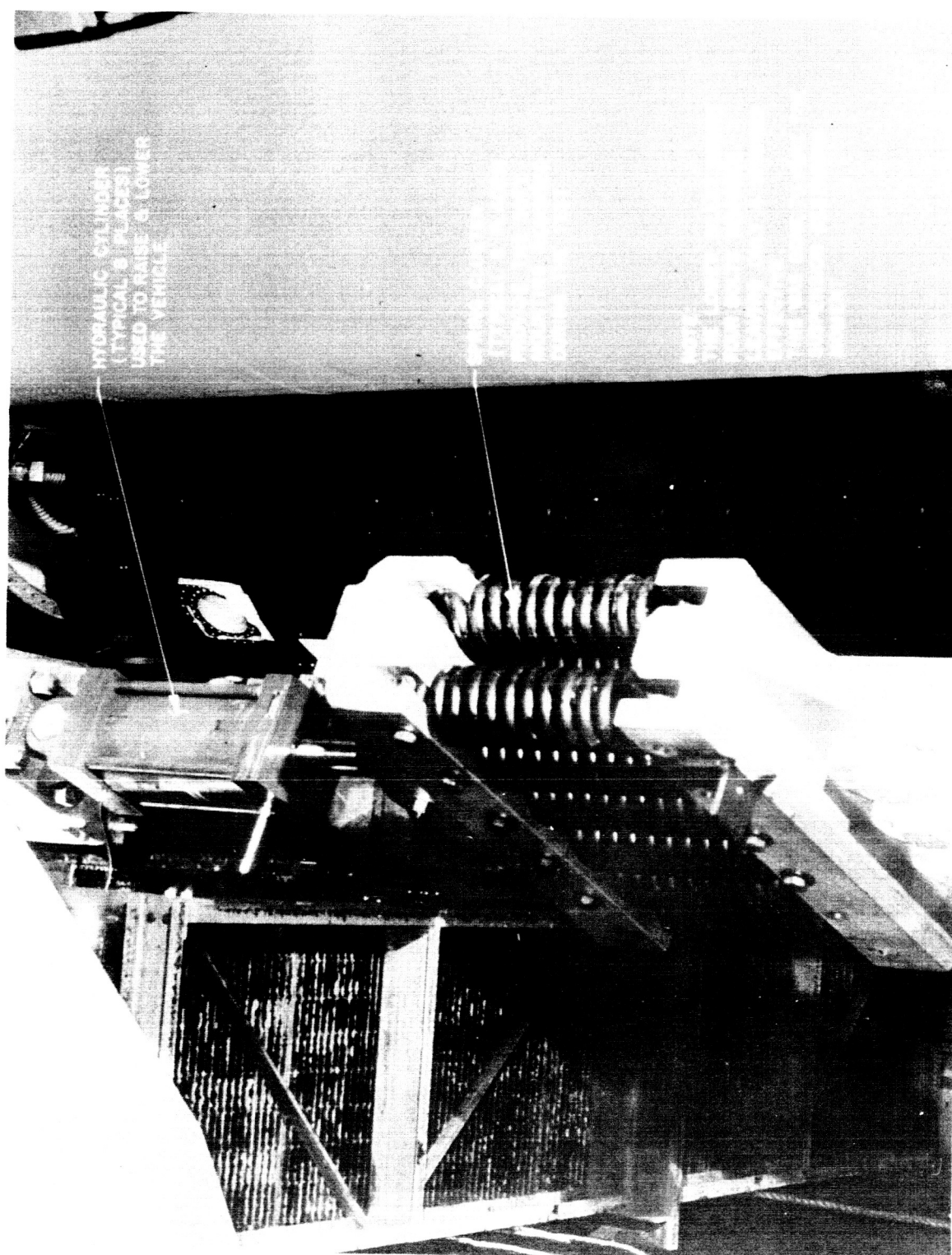


MTP-P&VE-S-62-3

FIGURE 1. DRAWING OF SA-D1 IN THE TEST TOWER



FIGURE 2. INSTALLATION IN THE TEST TOWER



MTP-P&VE-S-62-3

FIGURE 3. SPRING CLUSTER

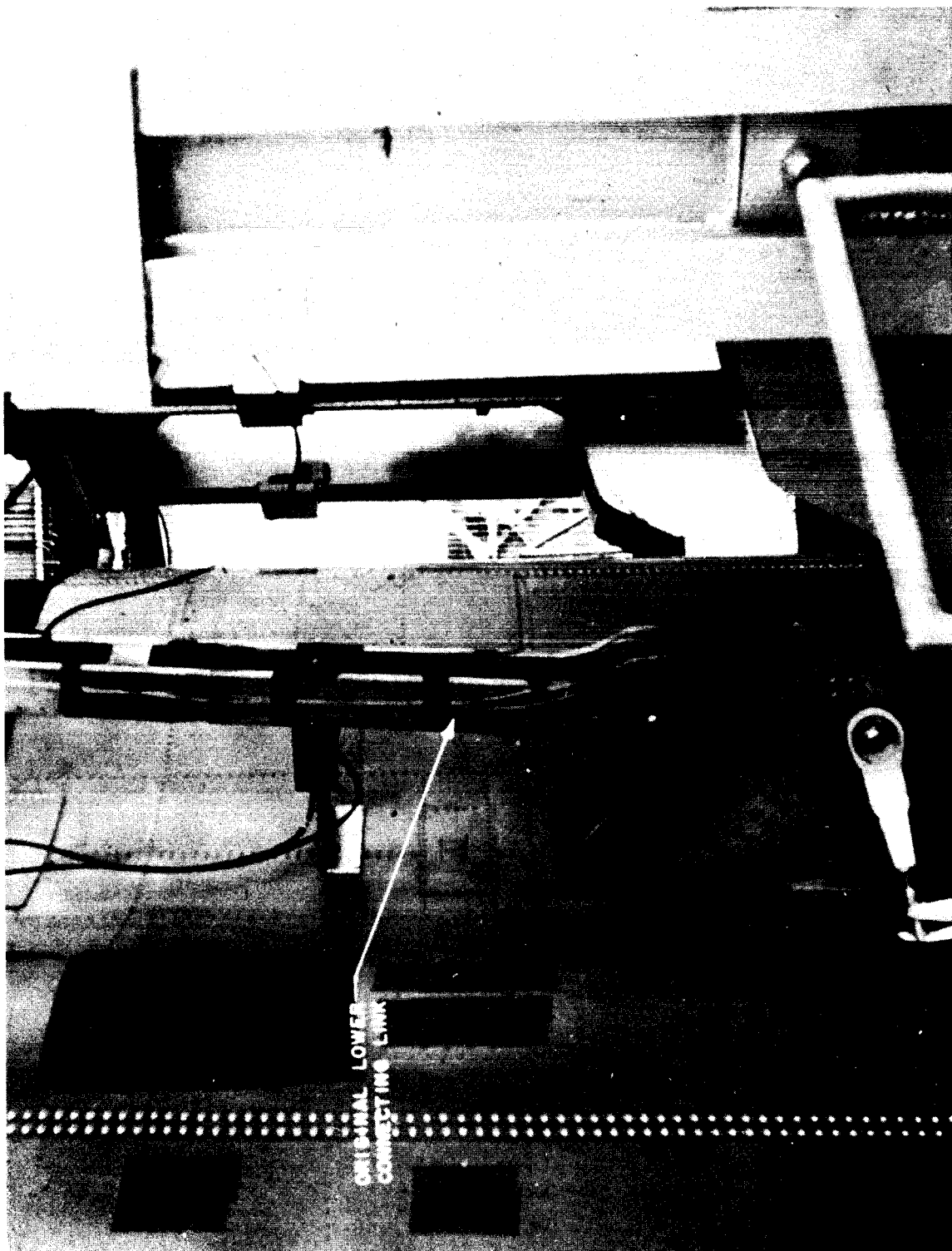
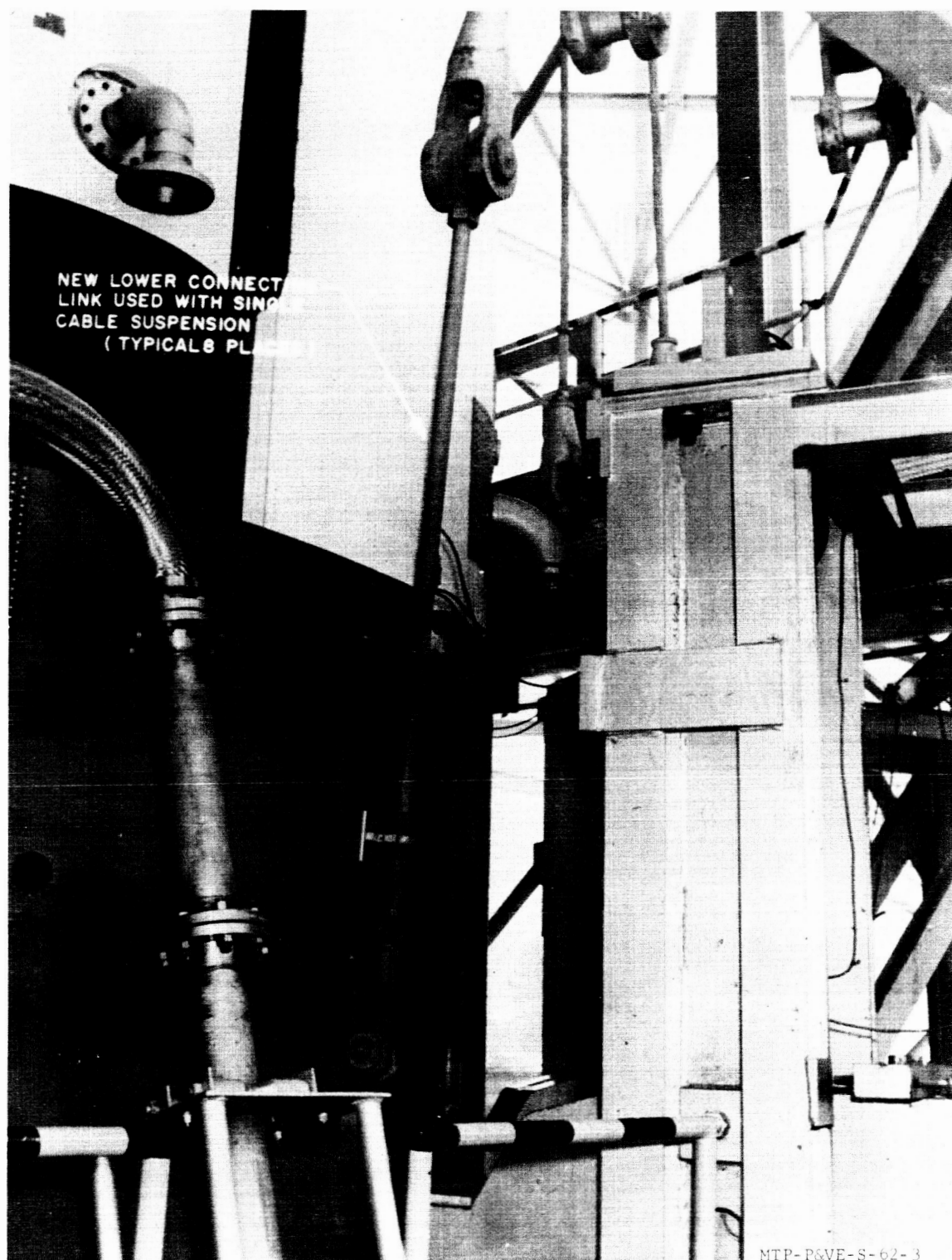


FIGURE 4. ORIGINAL LOWER CONNECTING LINK

MTP-P&VE-S-62-3



MTP-P&VE-S-62-3

FIGURE 5. NEW LOWER CONNECTION LINK



FIGURE 6. INSTRUMENTATION TRAILER

MTP-P&VE-S-62-3

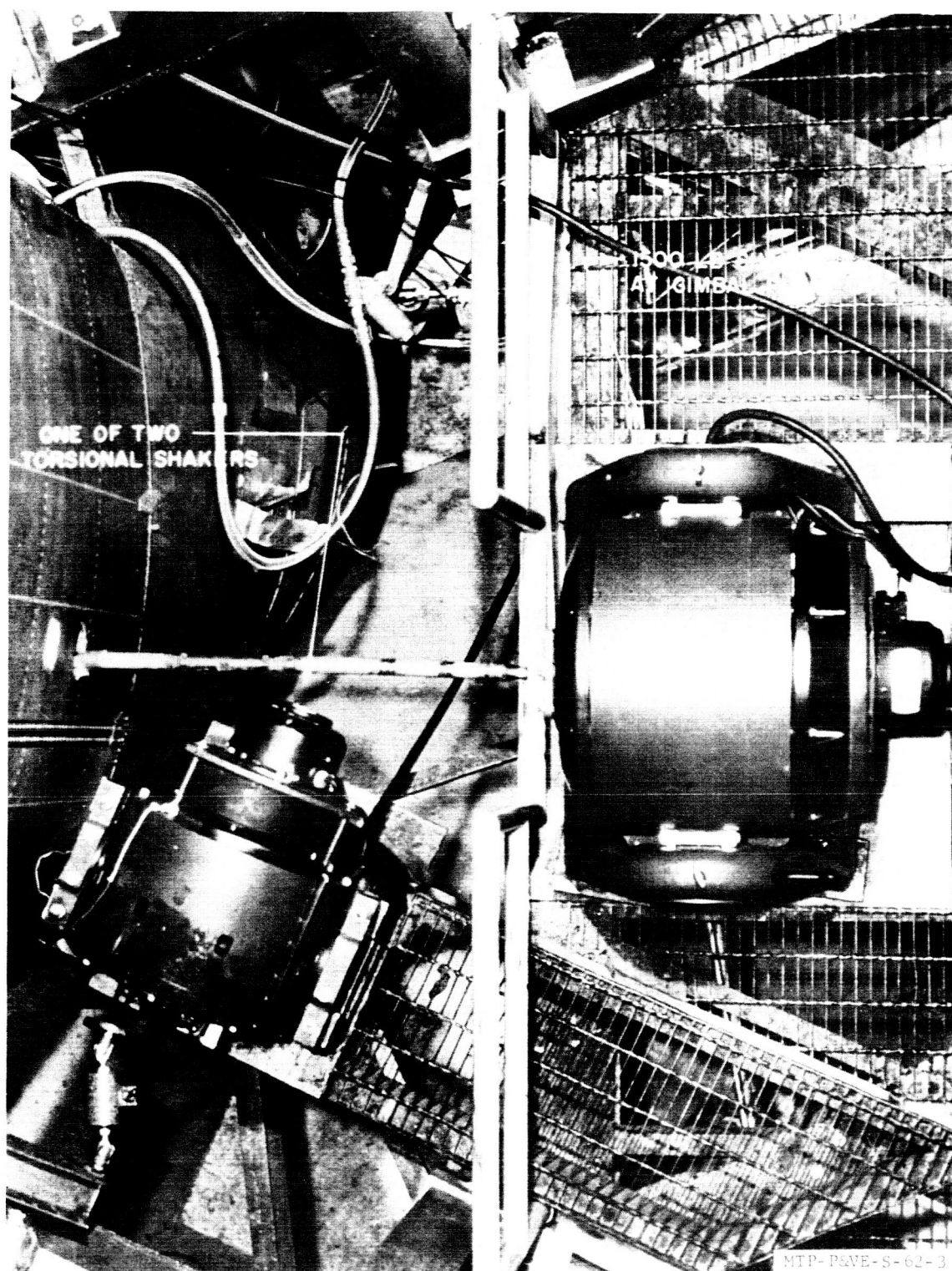
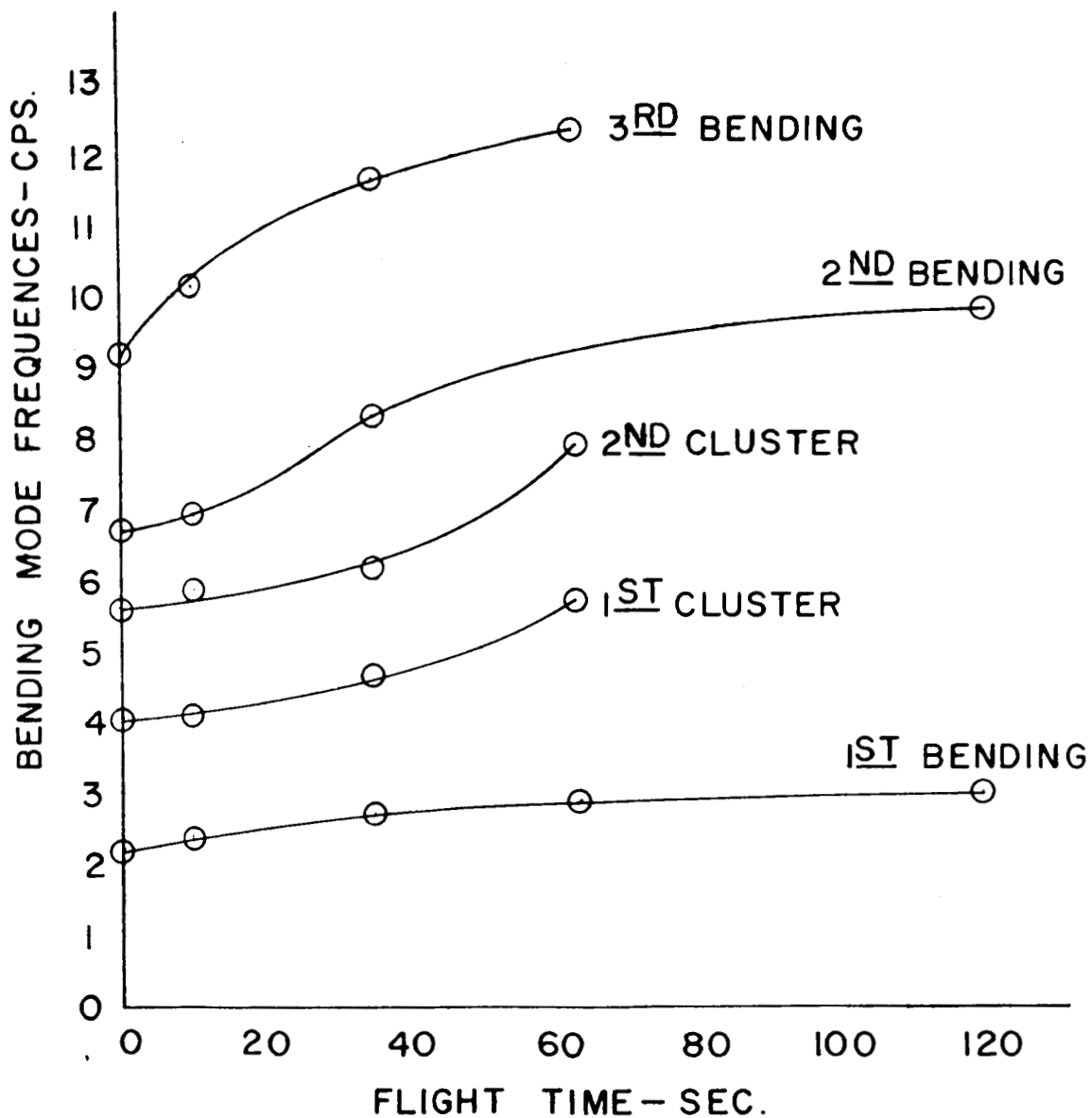
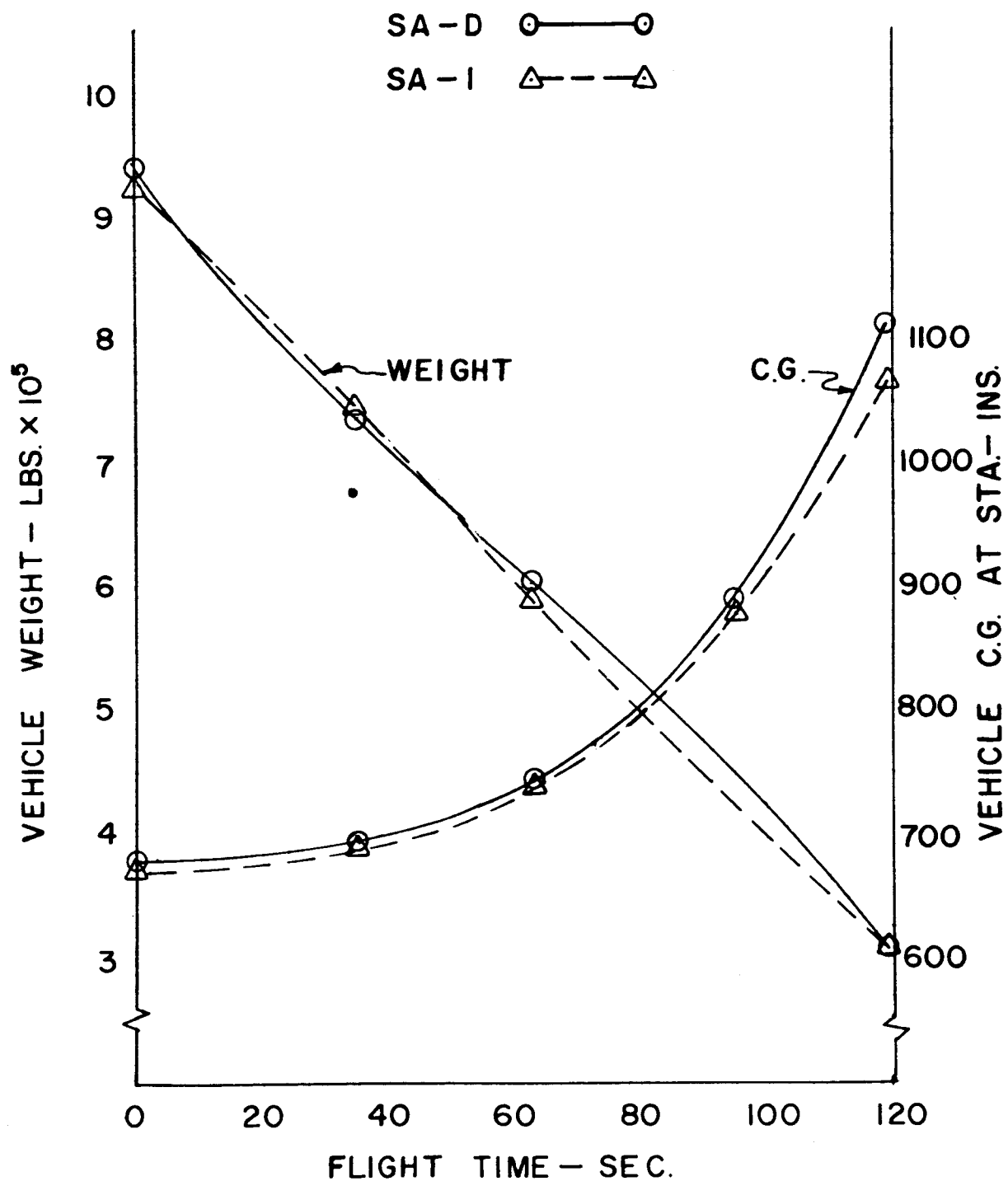


FIGURE 7. ELECTRO-DYNAMIC SHAKERS



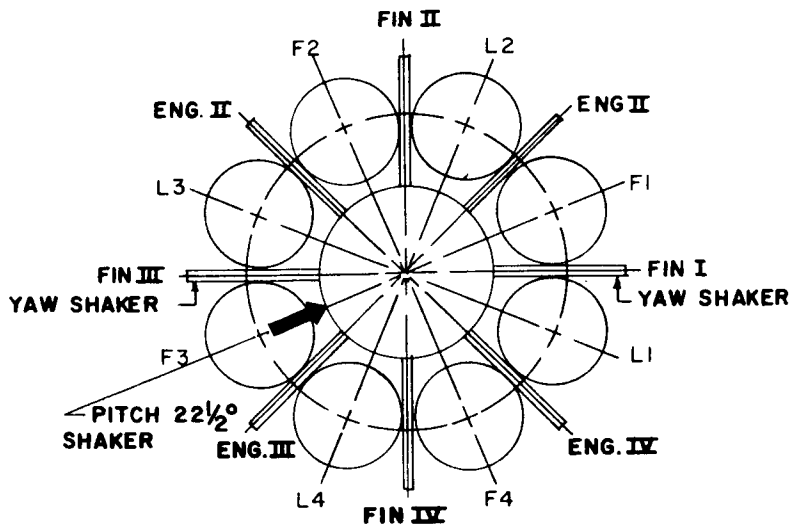
MTP-P&VE-S-62-3

FIGURE 8. PITCH BENDING MODE FREQUENCIES VS. FLIGHT TIME



MTP-P&VE-S-62-3

FIGURE 9. SA-D1 AND SA-1 WEIGHT AND CG VS. FLIGHT TIME



REFERENCE NO	DESCRIPTION	CODE
1. HARD FOR PITCH & YAW, L.O., 10 SECS, & 35 SECS		8(ODD-12S-1C & EVEN-12S-2C)
2. SOFT FOR PITCH, L.O., 40 SECS & 35 SECS		8(ODD-4S-1C & EVEN-12S-2C)
2N. SEE NOTE 1		
3. SOFT FOR PITCH, EMPTY & Q MAX		4(EVEN-12S-2C)
3N SEE NOTE 1		
4. HARD FOR PITCH, EMPTY & Q MAX		4(ODD-12S-1C)
6. SOFT FOR YAW, L.O., 10 SECS, & 35 SECS		6(ODD-12S-1C 2 EVEN ENGINES -12S-2C)
8. SOFT FOR YAW, Q MAX & EMPTY		4(4 FINS-12S { ODD-1C EVEN-2C

ODD - OUTRIGGERS I & III, ENGINES I & III

EVEN - OUTRIGGERS II & IV, ENGINES II & IV

S - SPRINGS IN INDIVIDUAL CLUSTER

C - CABLES

NOTE: 1

REFERENCE NUMBERS FOLLOWED BY (N) INDICATE
SUBSTITUTION OF THE NEW LOWER CONNECTING
LINES SHOWN IN FIGURE 5. ALL (N) RUNS
HAVE ONLY 1C OR 1 CABLE.

MTP-P&VE-S-62-3

FIGURE 10. SUSPENSION AND SHAKER ORIENTATION

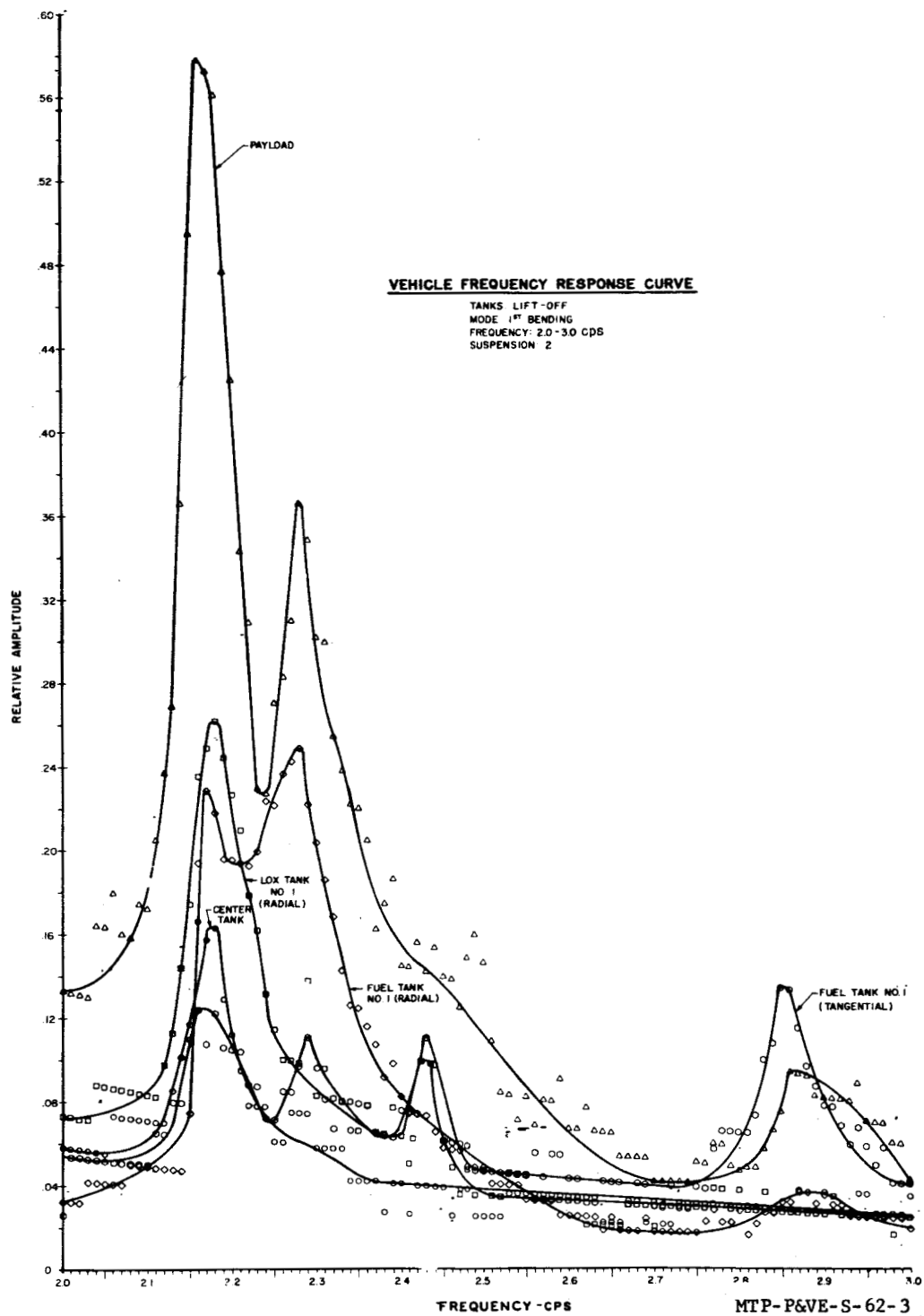


FIGURE 11. VEHICLE FREQUENCY RESPONSE CURVES

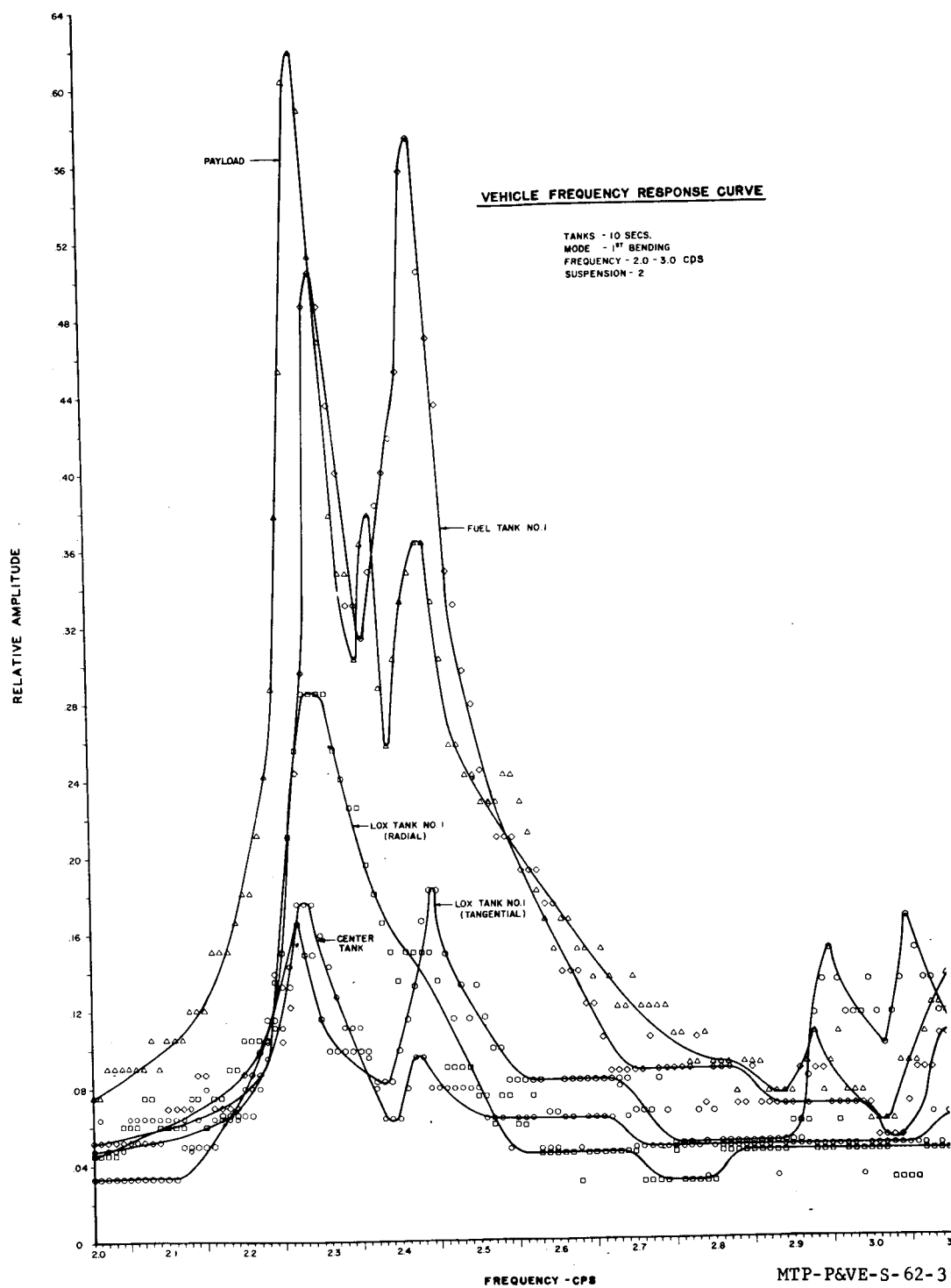


FIGURE 12. VEHICLE FREQUENCY RESPONSE CURVES

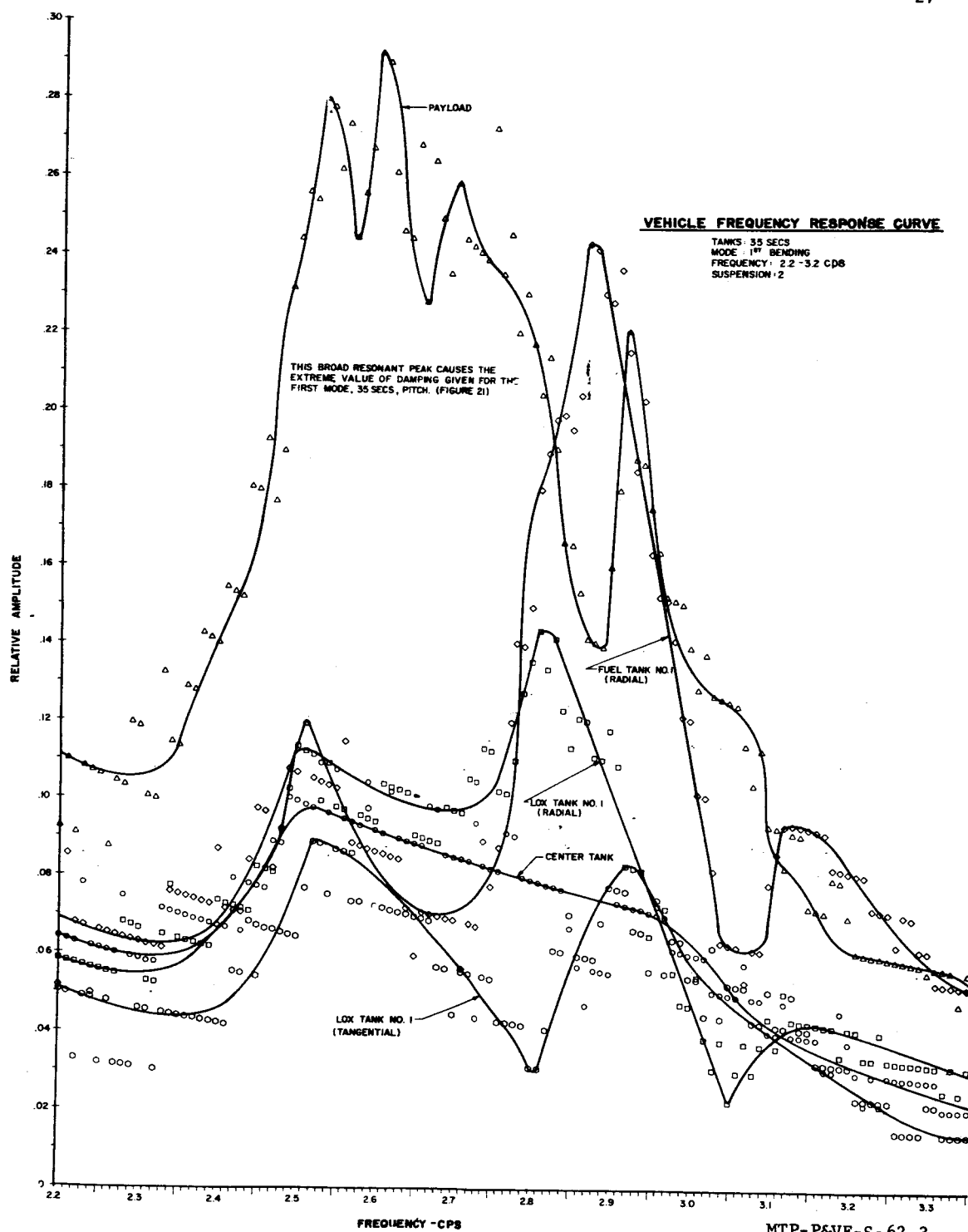
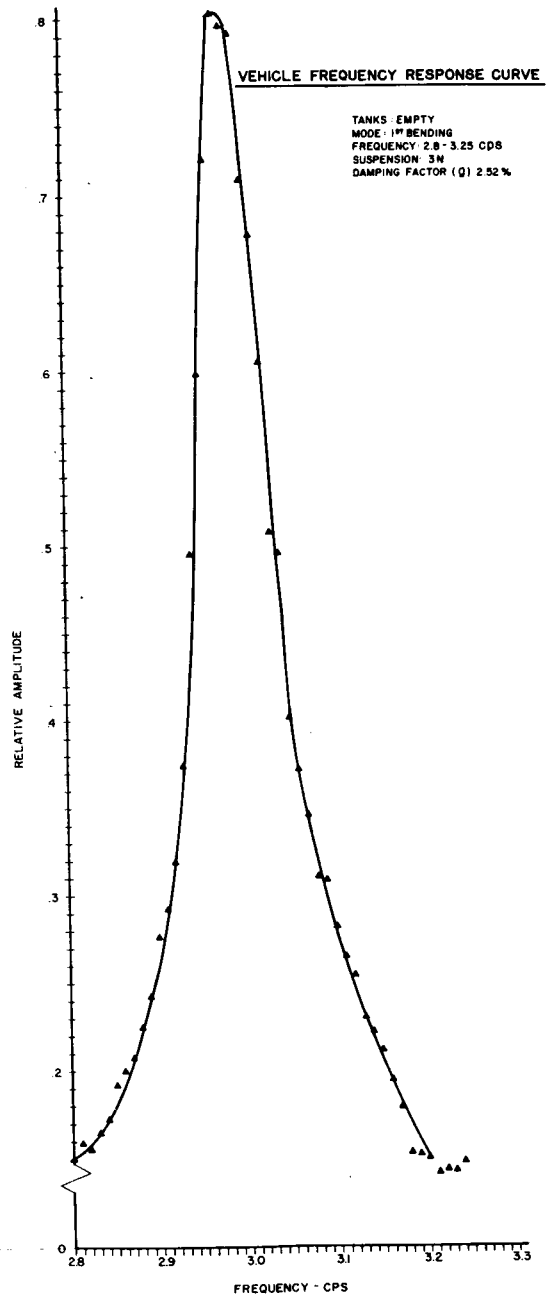
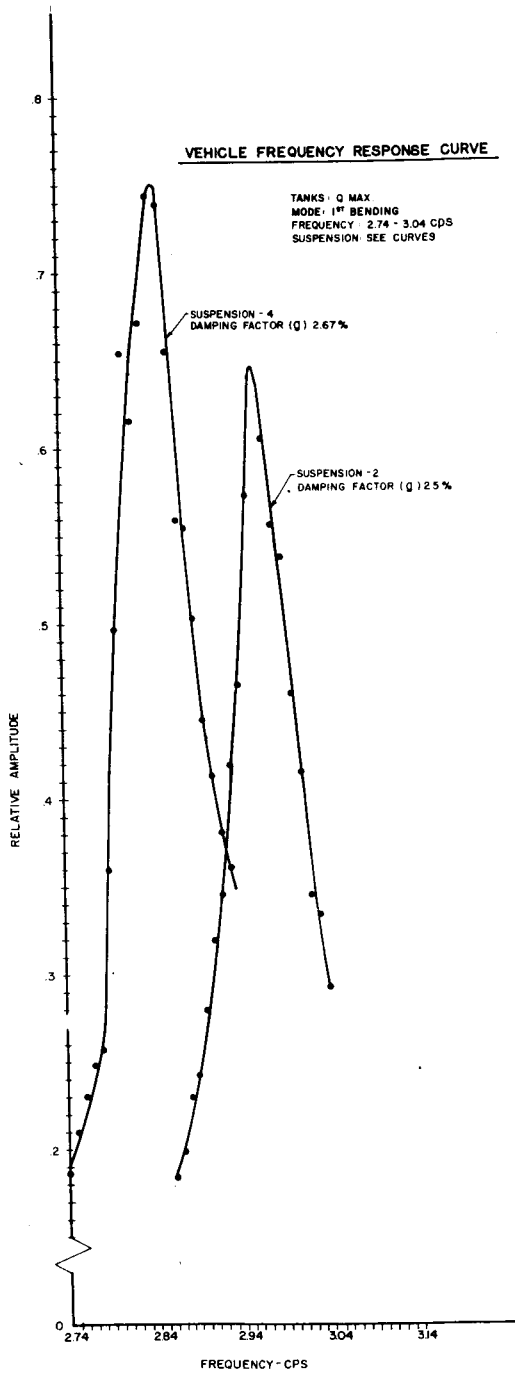
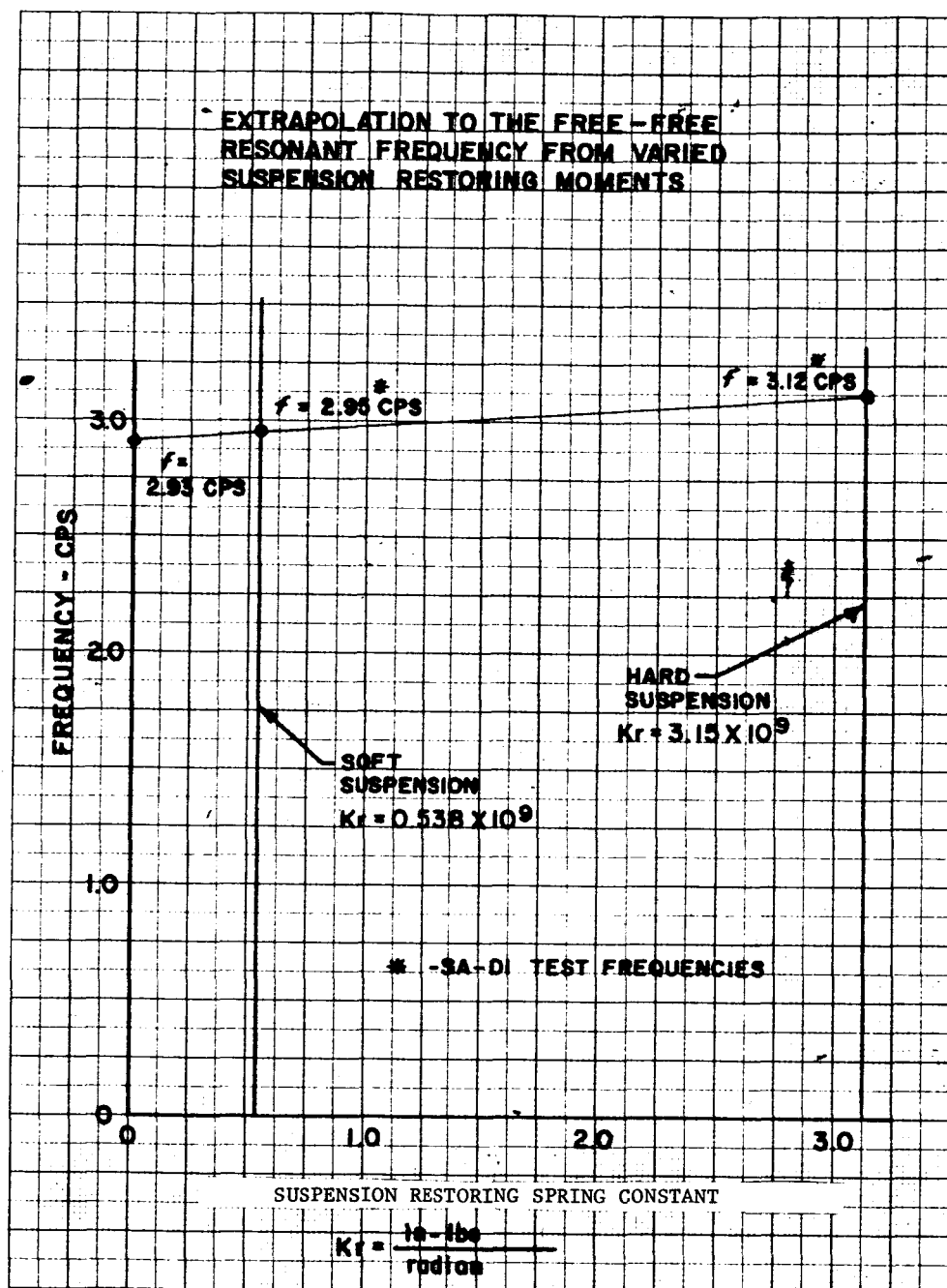


FIGURE 13. VEHICLE FREQUENCY RESPONSE CURVES



MTP-P&VE-S-62-3

FIGURE 14. VEHICLE FREQUENCY RESPONSE CURVES



MTP-P&VE-S-62-3

FIGURE 15. EXTRAPOLATION TO THE FREE-FREE FREQUENCY

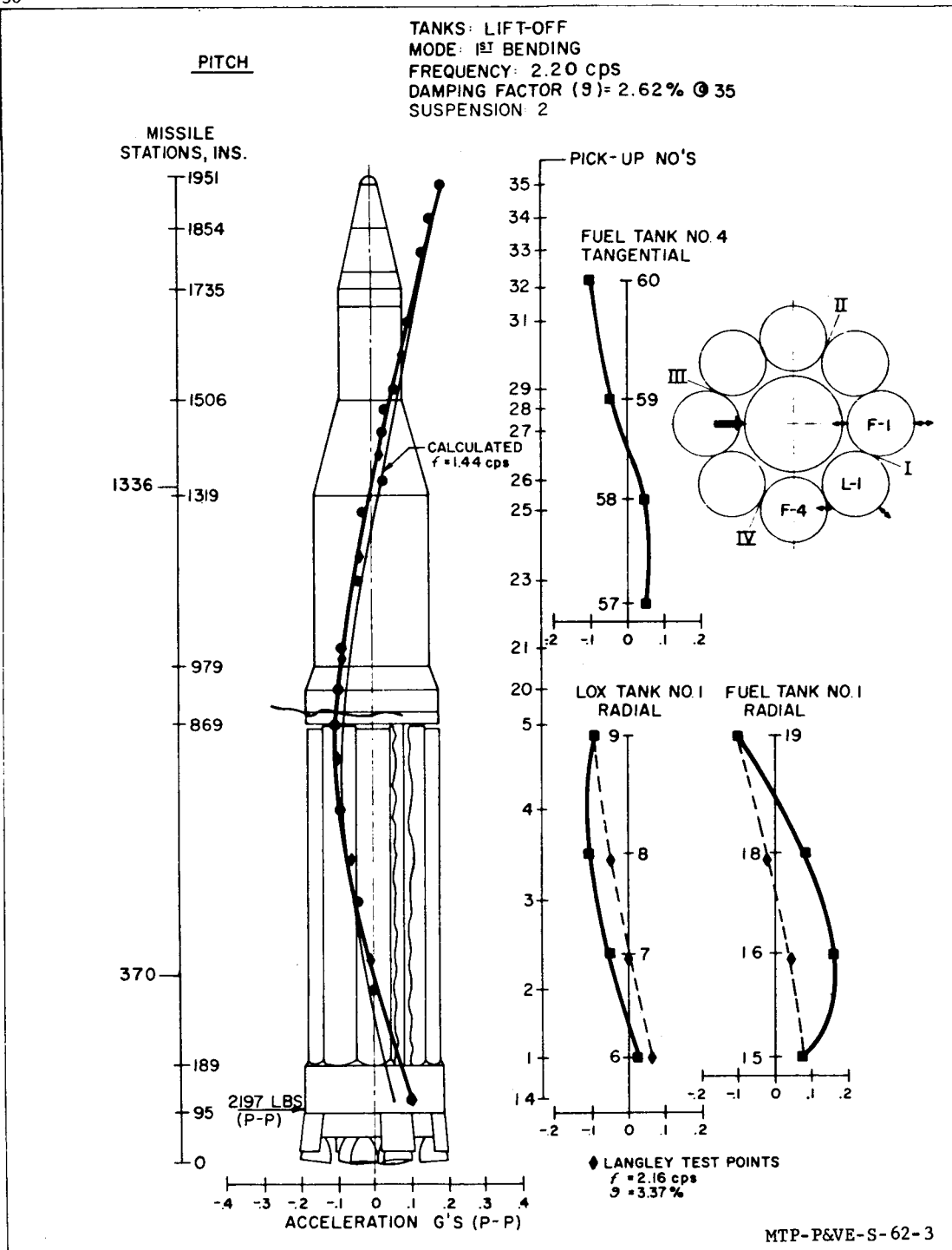


FIGURE 16. LATERAL BENDING MODES (PITCH PLANE)

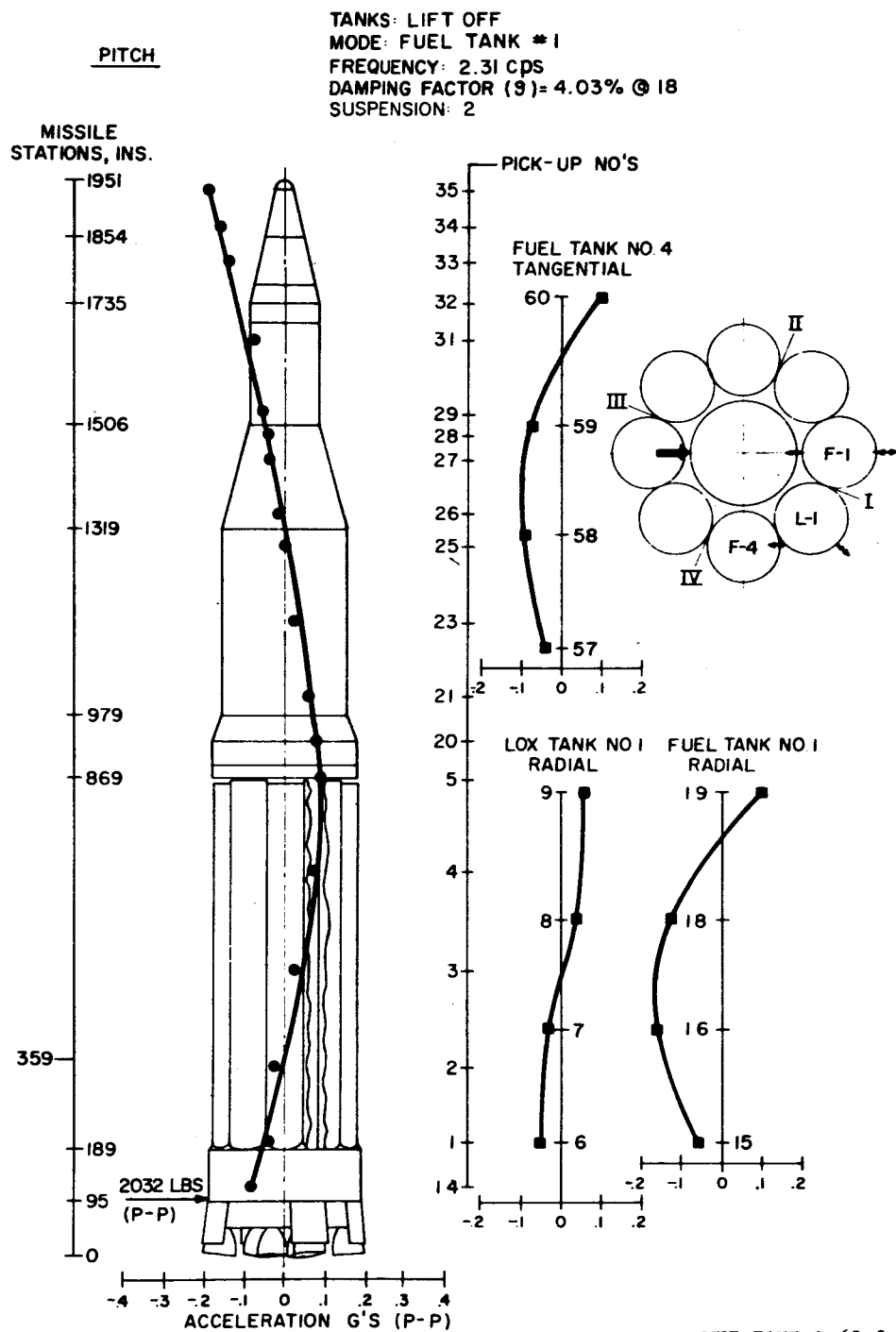


FIGURE 17. LATERAL BENDING MODES (PITCH PLANE)

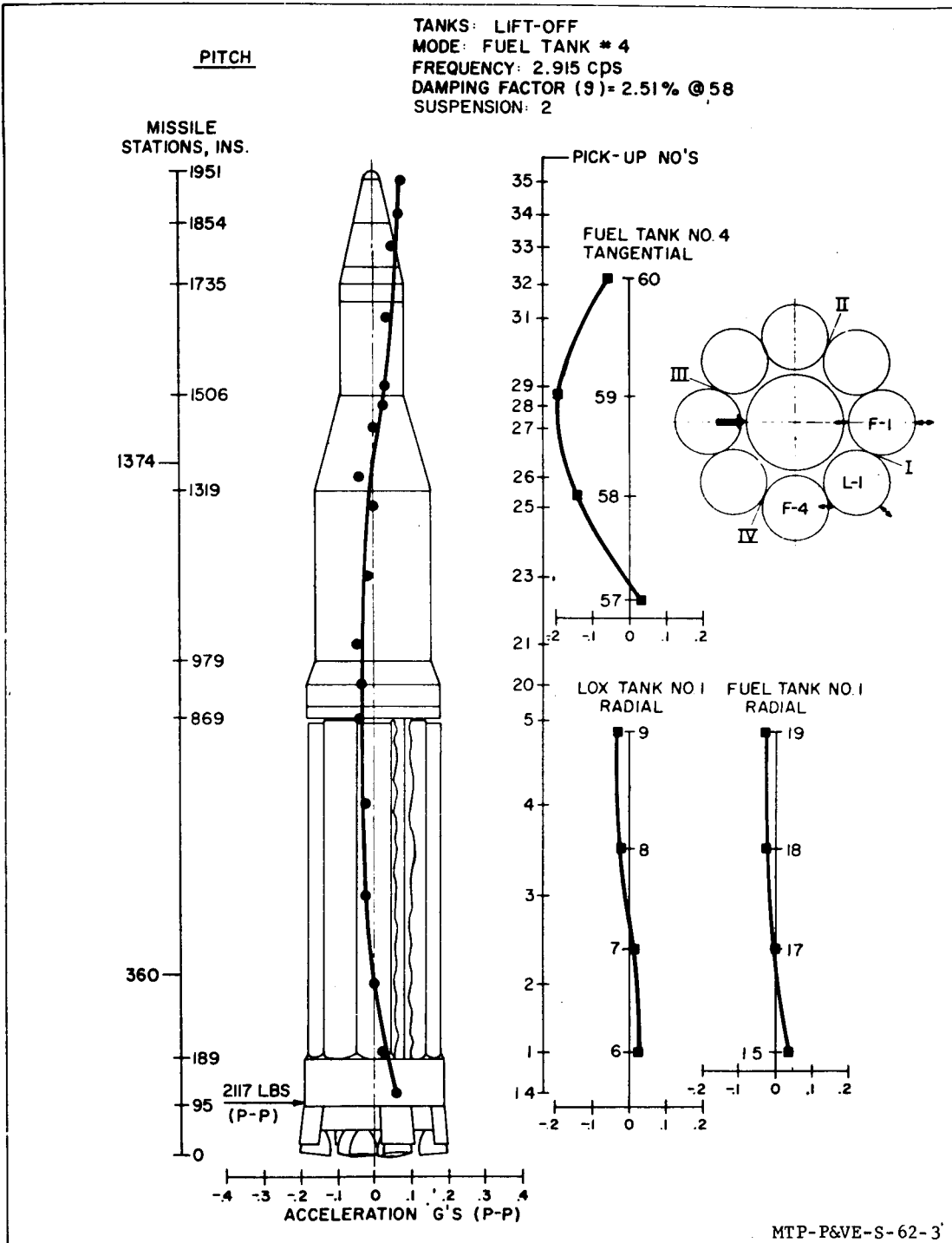


FIGURE 18. LATERAL BENDING MODES (PITCH PLANE)

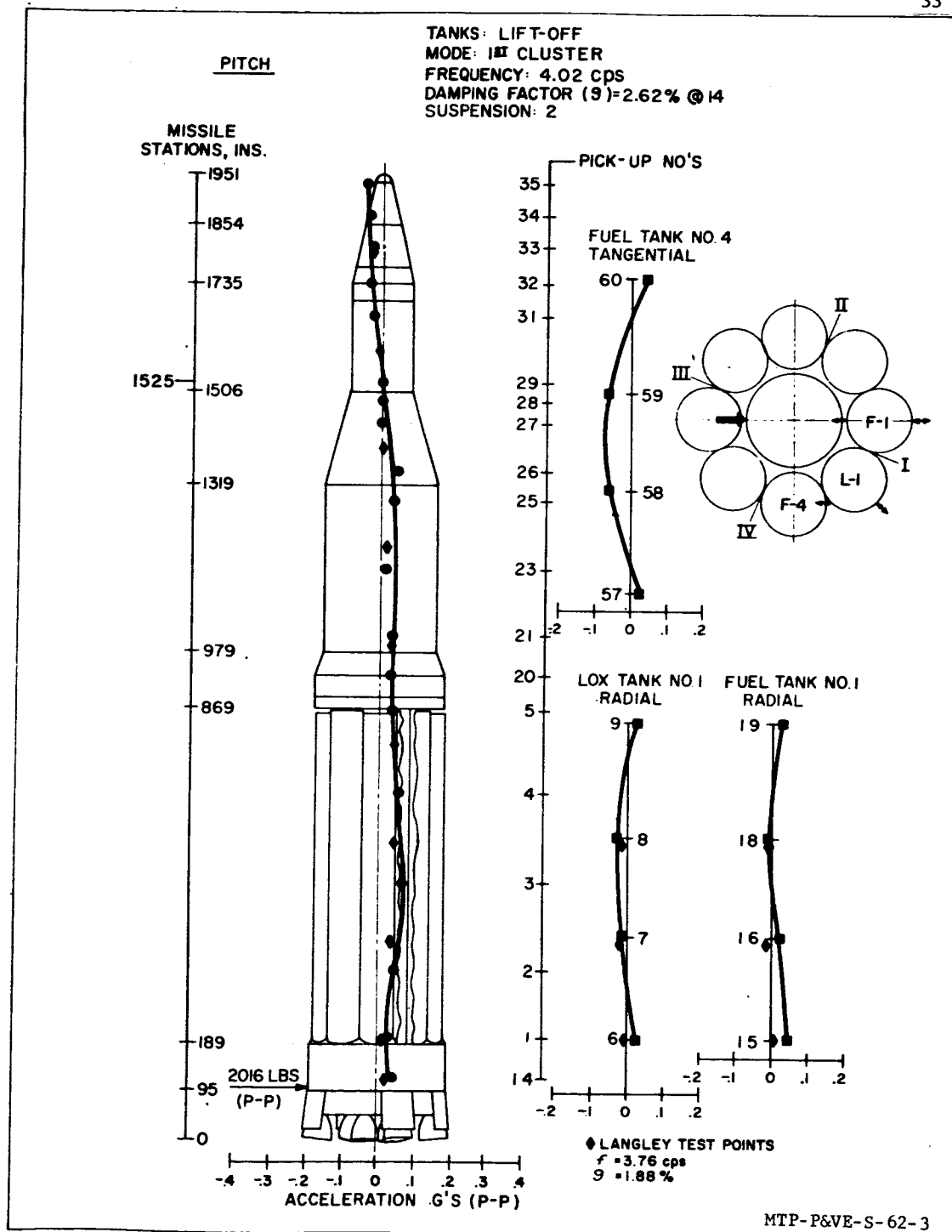


FIGURE 19. LATERAL BENDING MODES (PITCH PLANE)

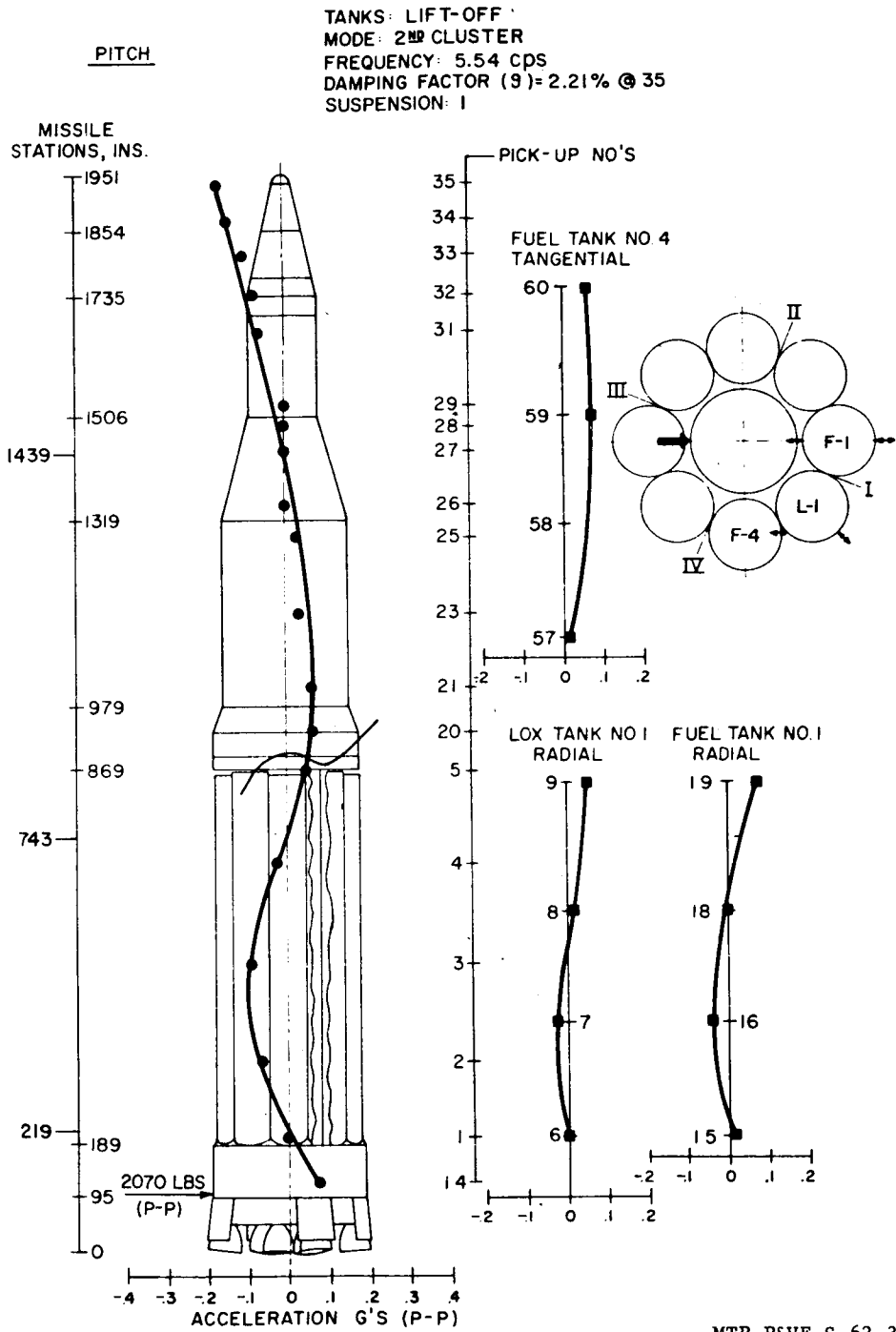


FIGURE 20. LATERAL BENDING MODES (PITCH PLANE)

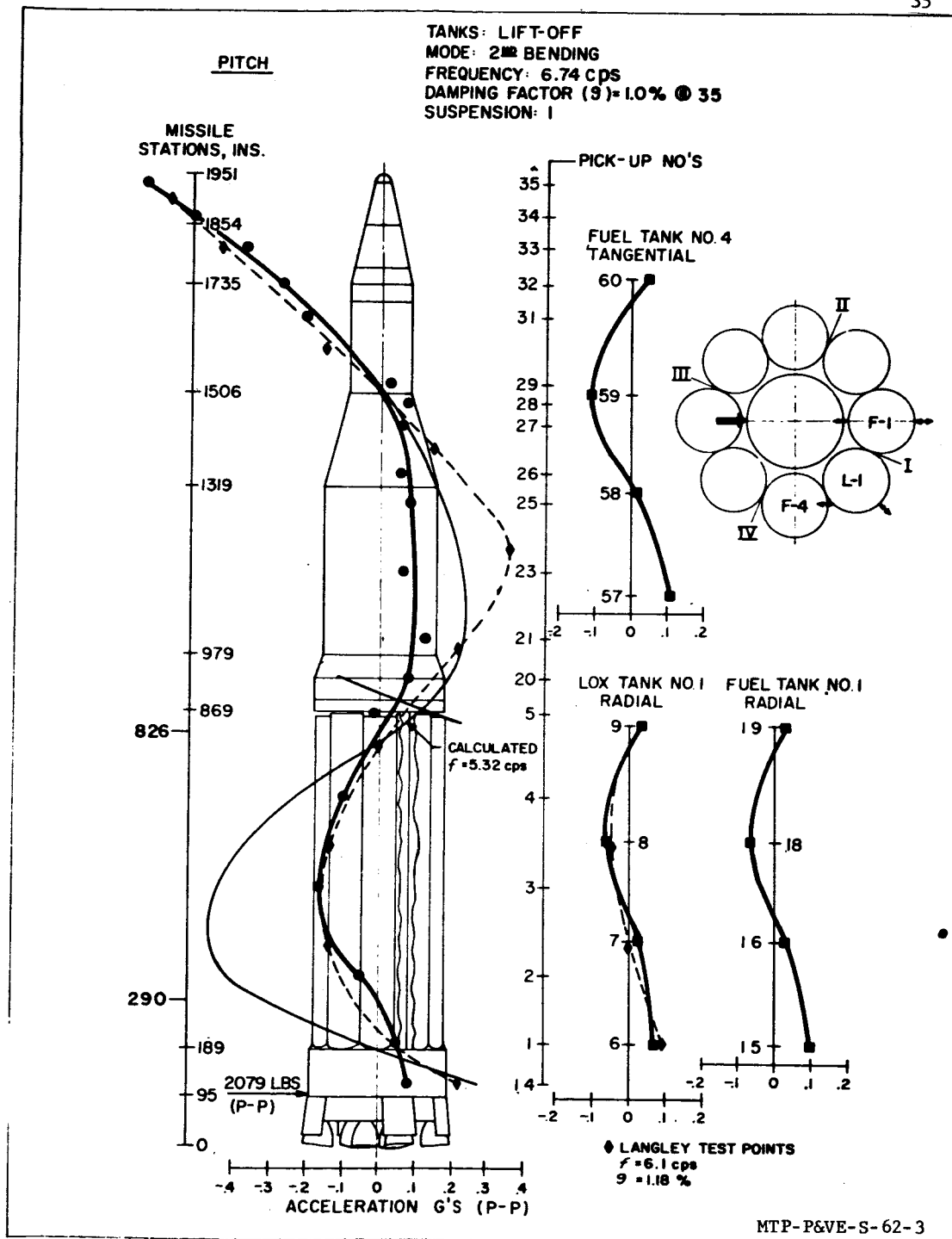


FIGURE 21. LATERAL BENDING MODES (PITCH PLANE)

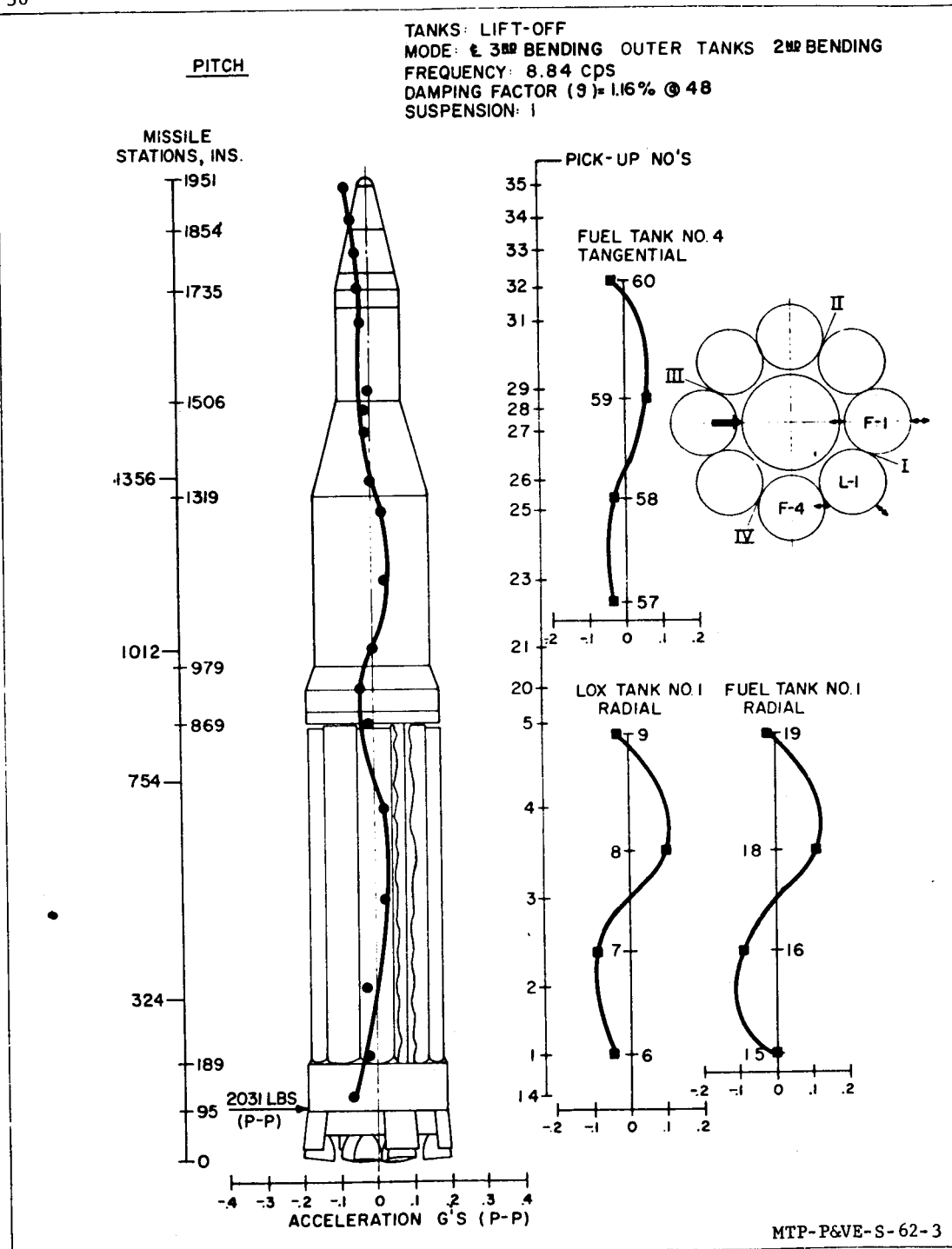


FIGURE 22. LATERAL BENDING MODES (PITCH PLANE)

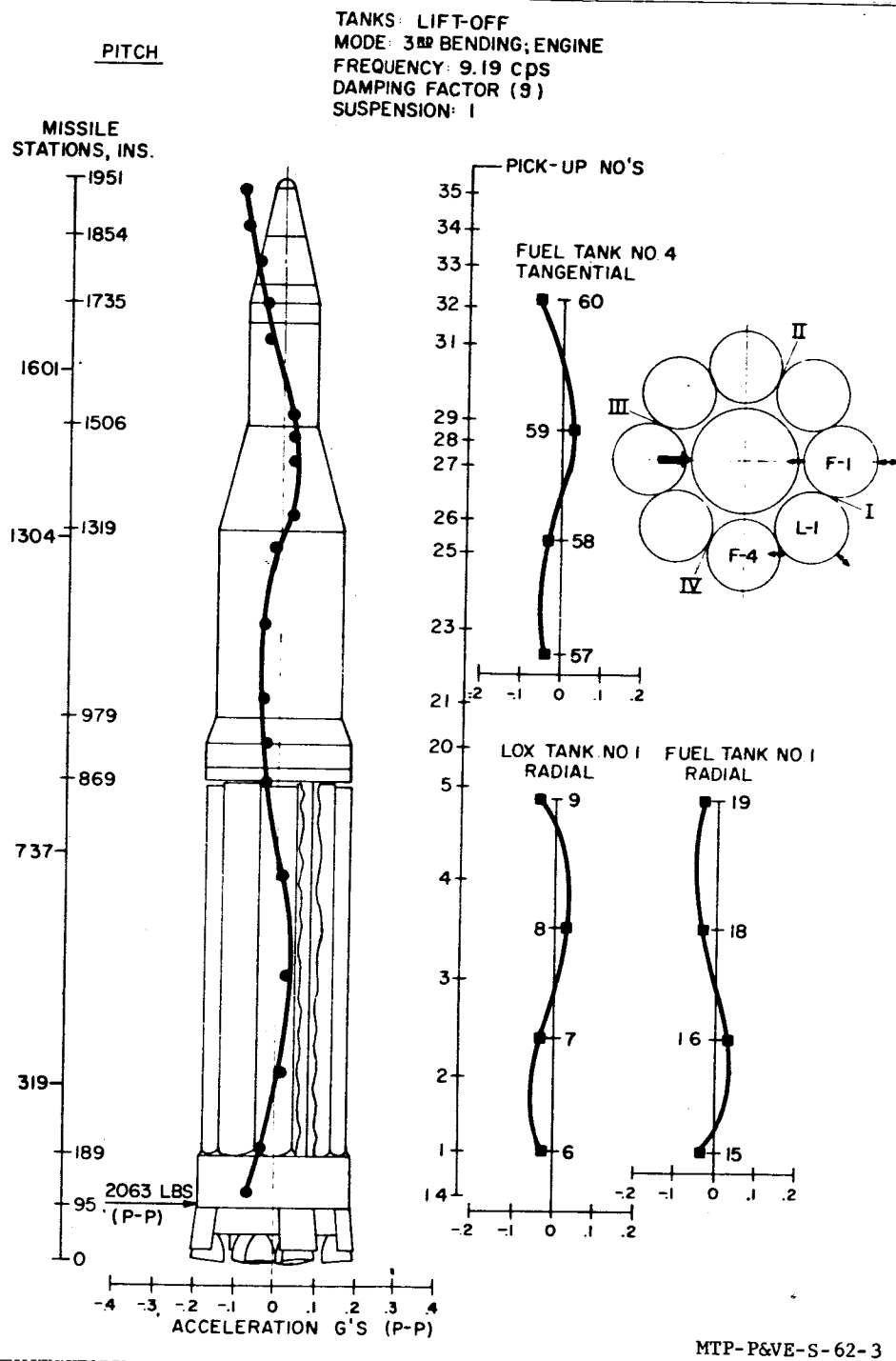


FIGURE 23. LATERAL BENDING MODES (PITCH PLANE)

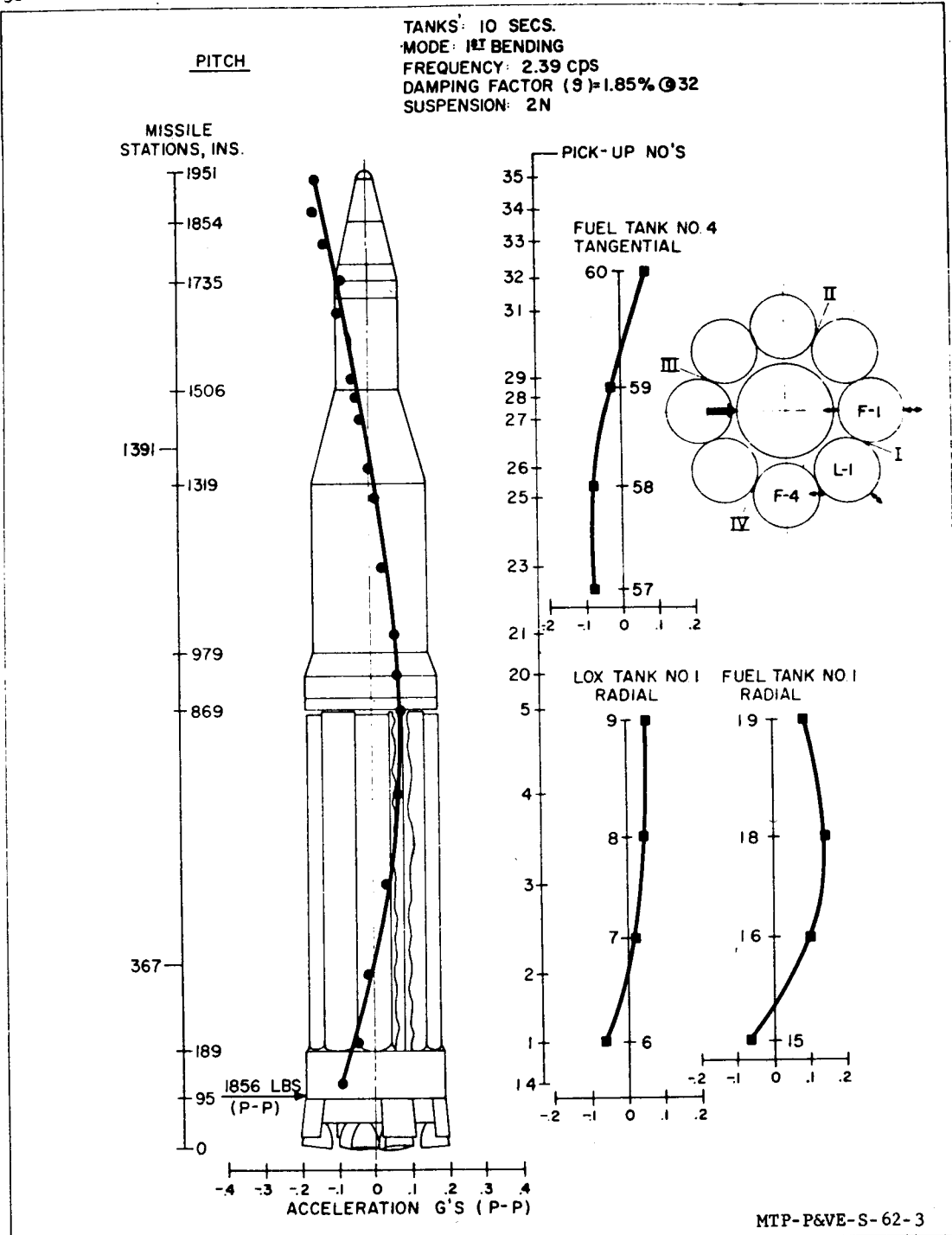


FIGURE 24. LATERAL BENDING MODES (PITCH PLANE)

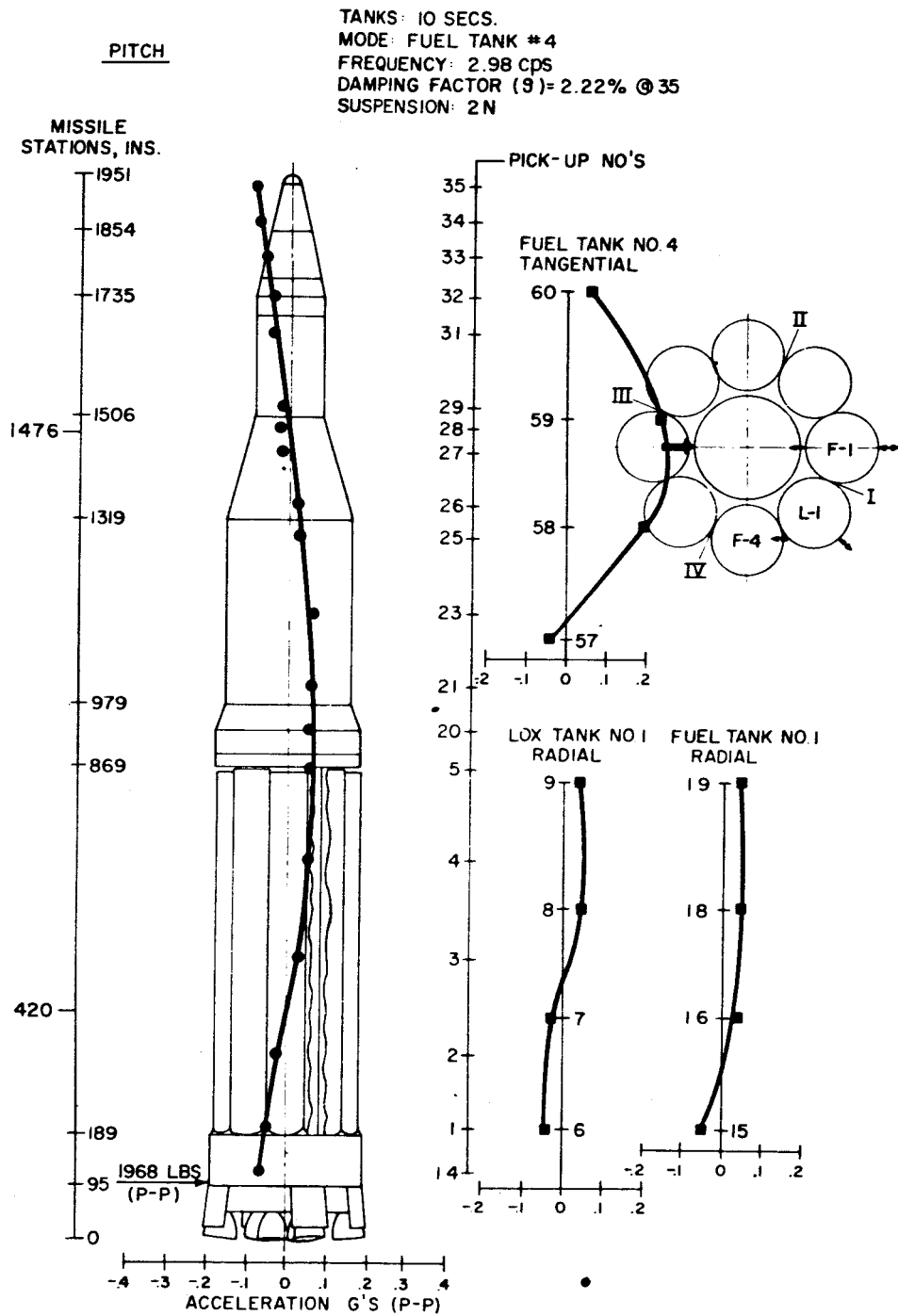


FIGURE 25. LATERAL BENDING MODES (PITCH PLANE)

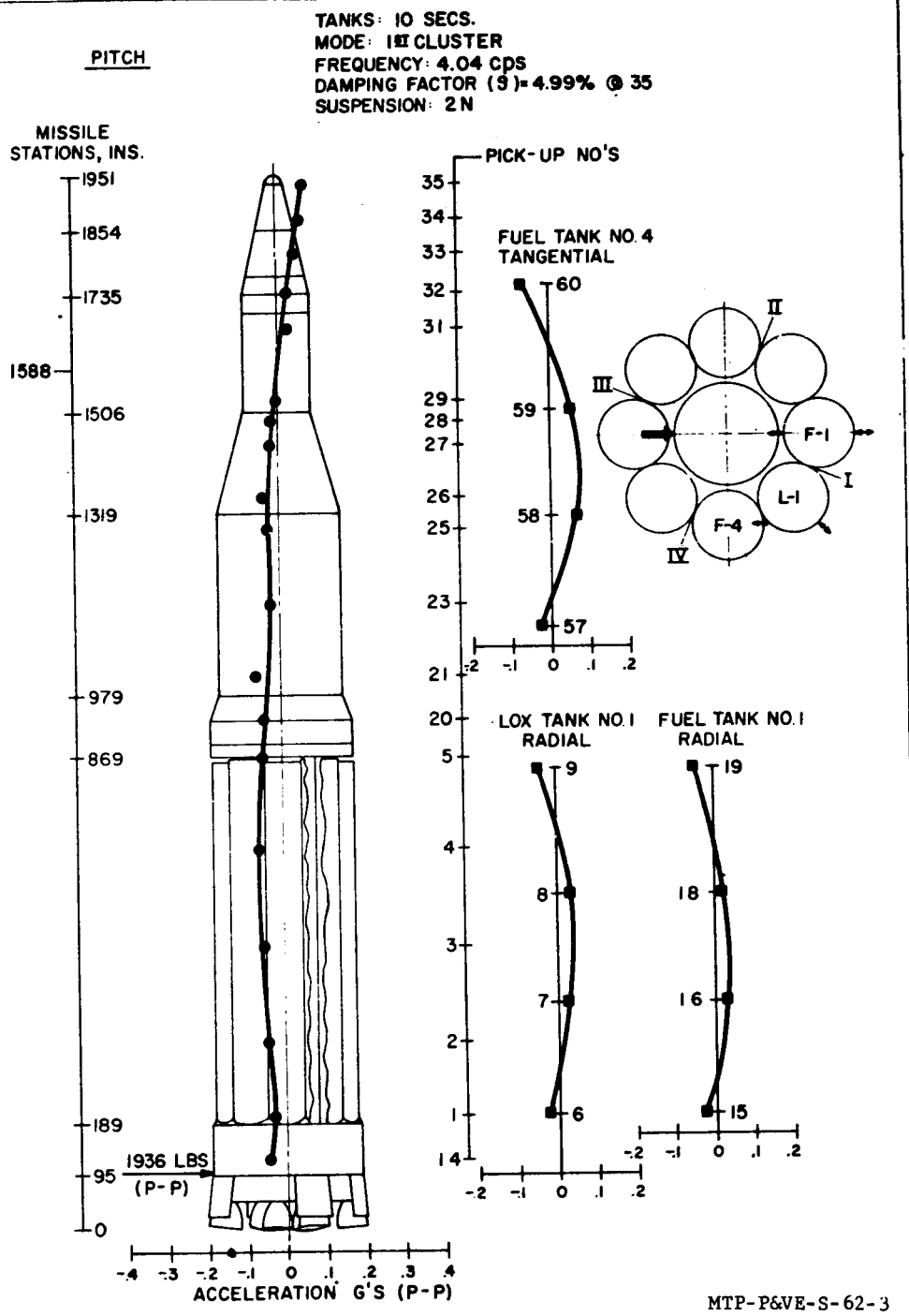


FIGURE 26. LATERAL BENDING MODES (PITCH PLANE)

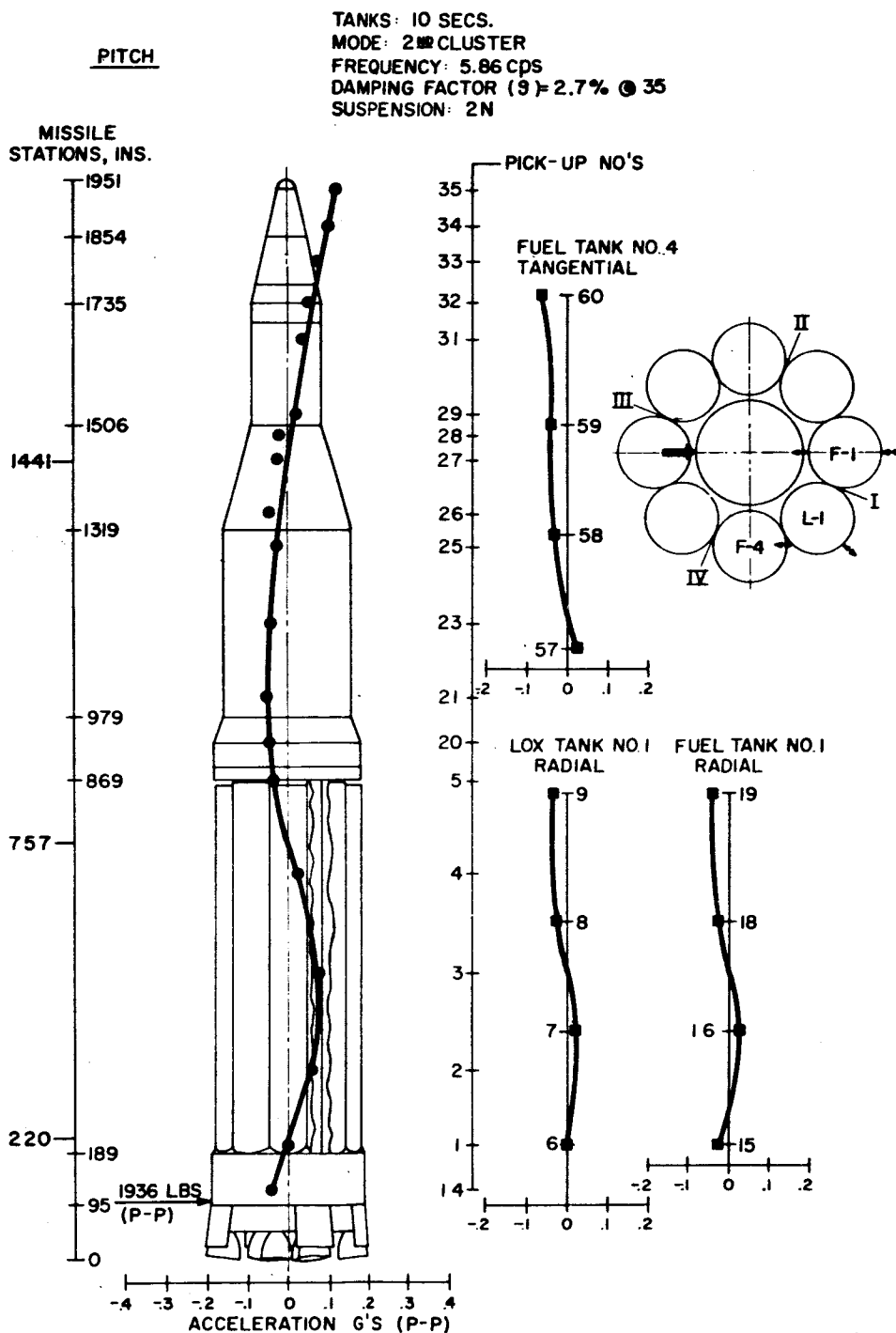


FIGURE 27. LATERAL BENDING MODES (PITCH PLANE)

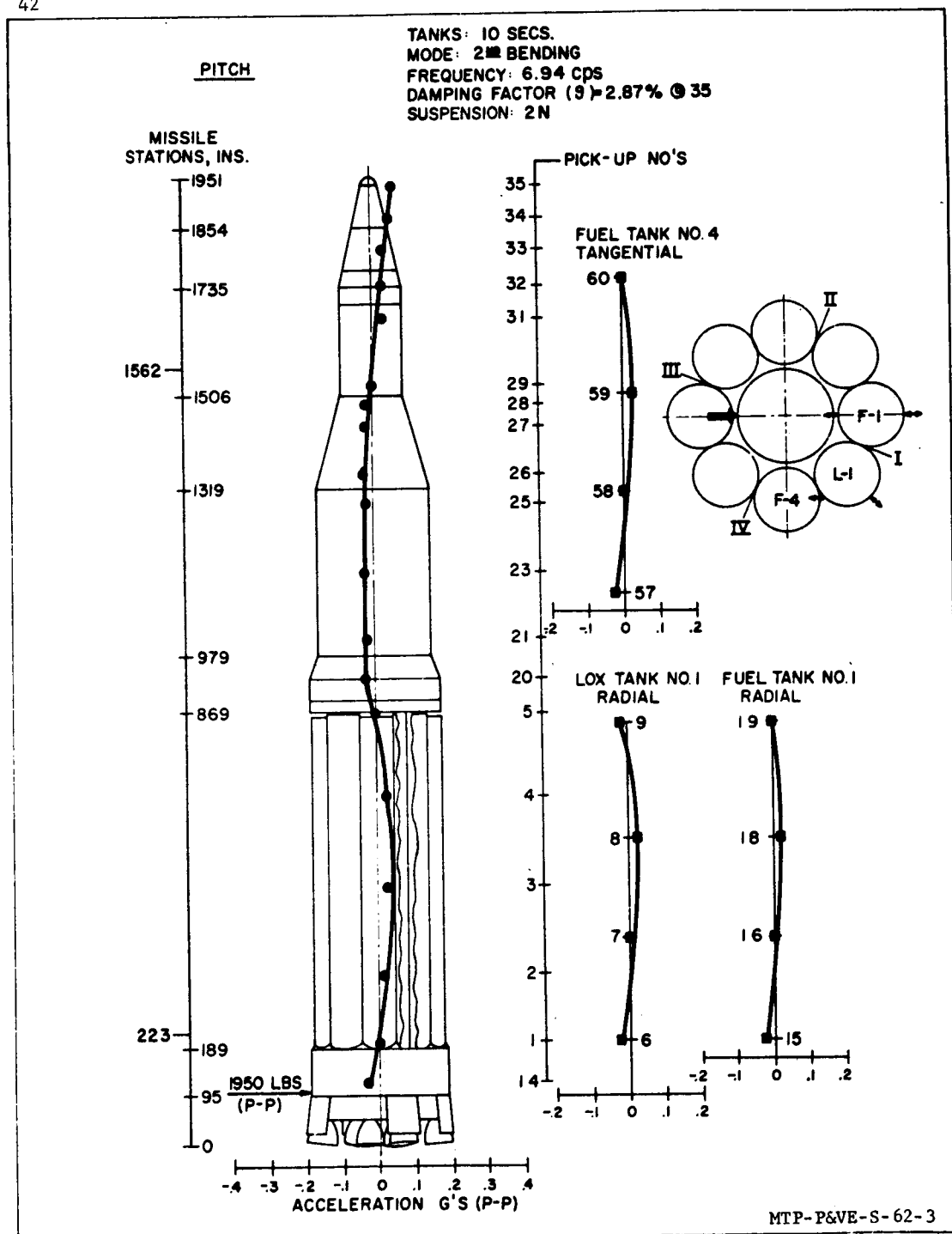


FIGURE 28. LATERAL BENDING MODES (PITCH PLANE)

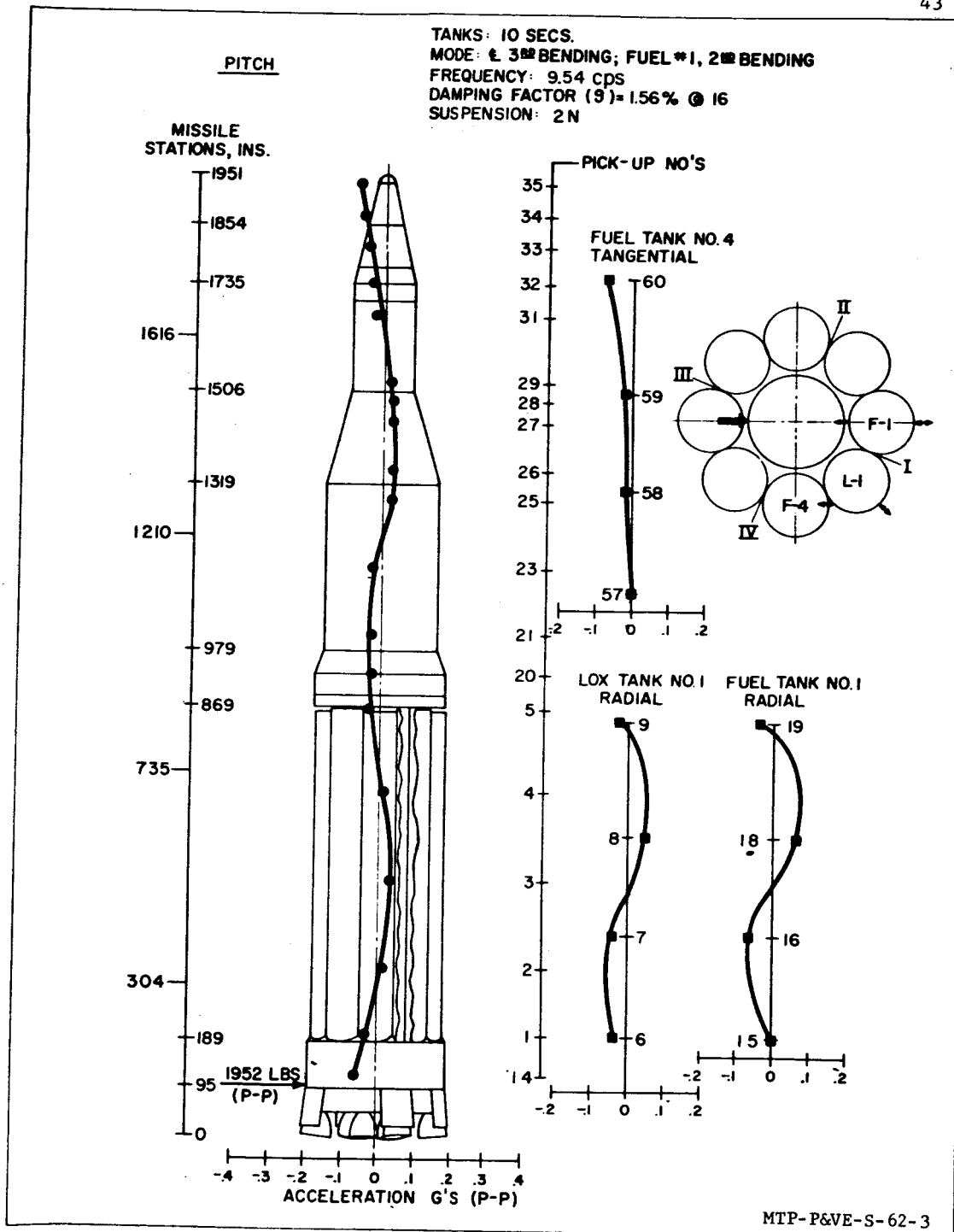
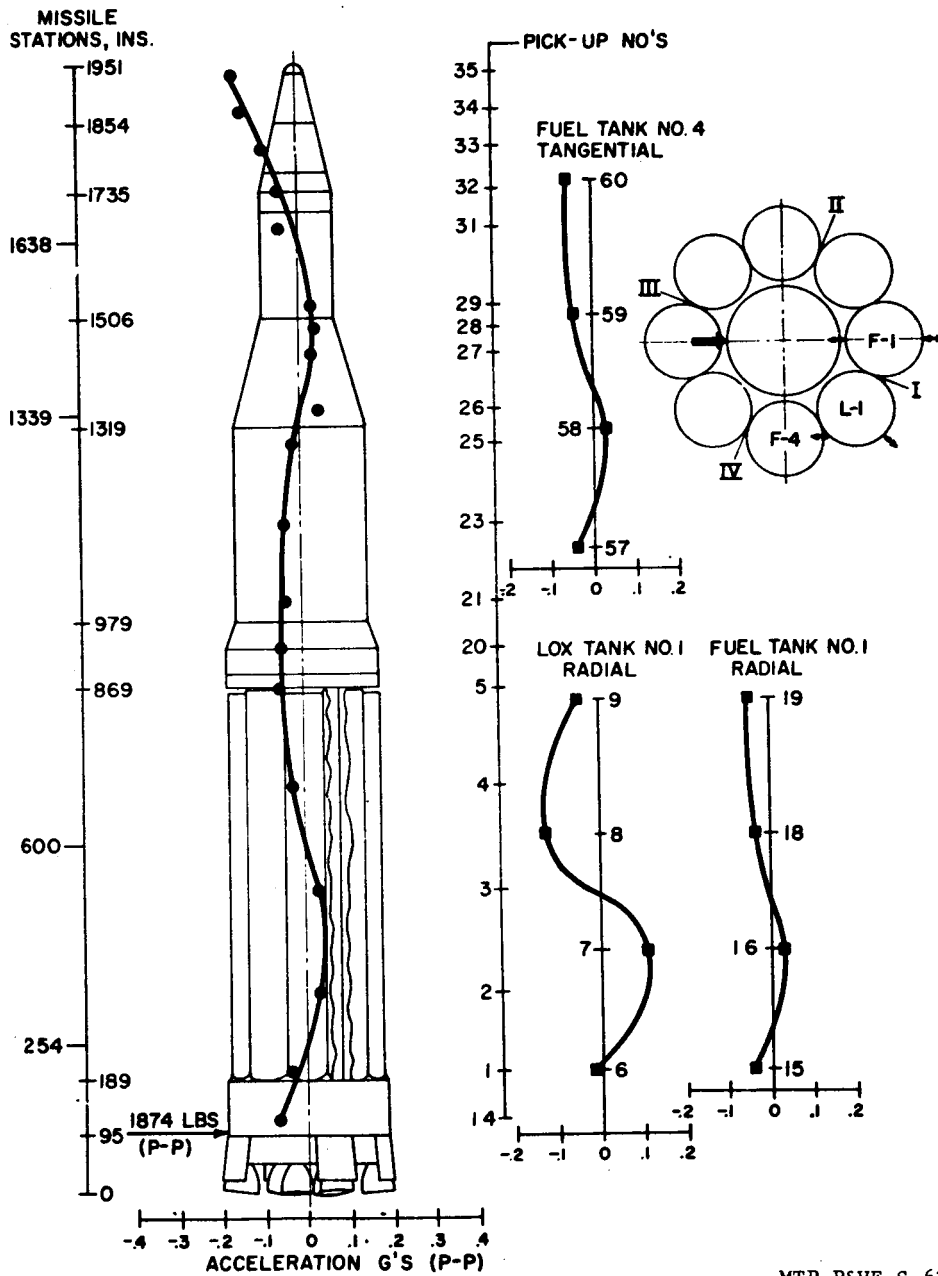


FIGURE 29. LATERAL BENDING MODES (PITCH PLANE)

PITCH

TANKS: 10 SECS.
 MODE: 3rd BENDING; LOX 1, 2nd BENDING
 FREQUENCY: 10.12 cps
 DAMPING FACTOR (9) = 2.47% @ 7
 SUSPENSION: 2N



MTP-P&VE-S-62-3

FIGURE 30. LATERAL BENDING MODES (PITCH PLANE)

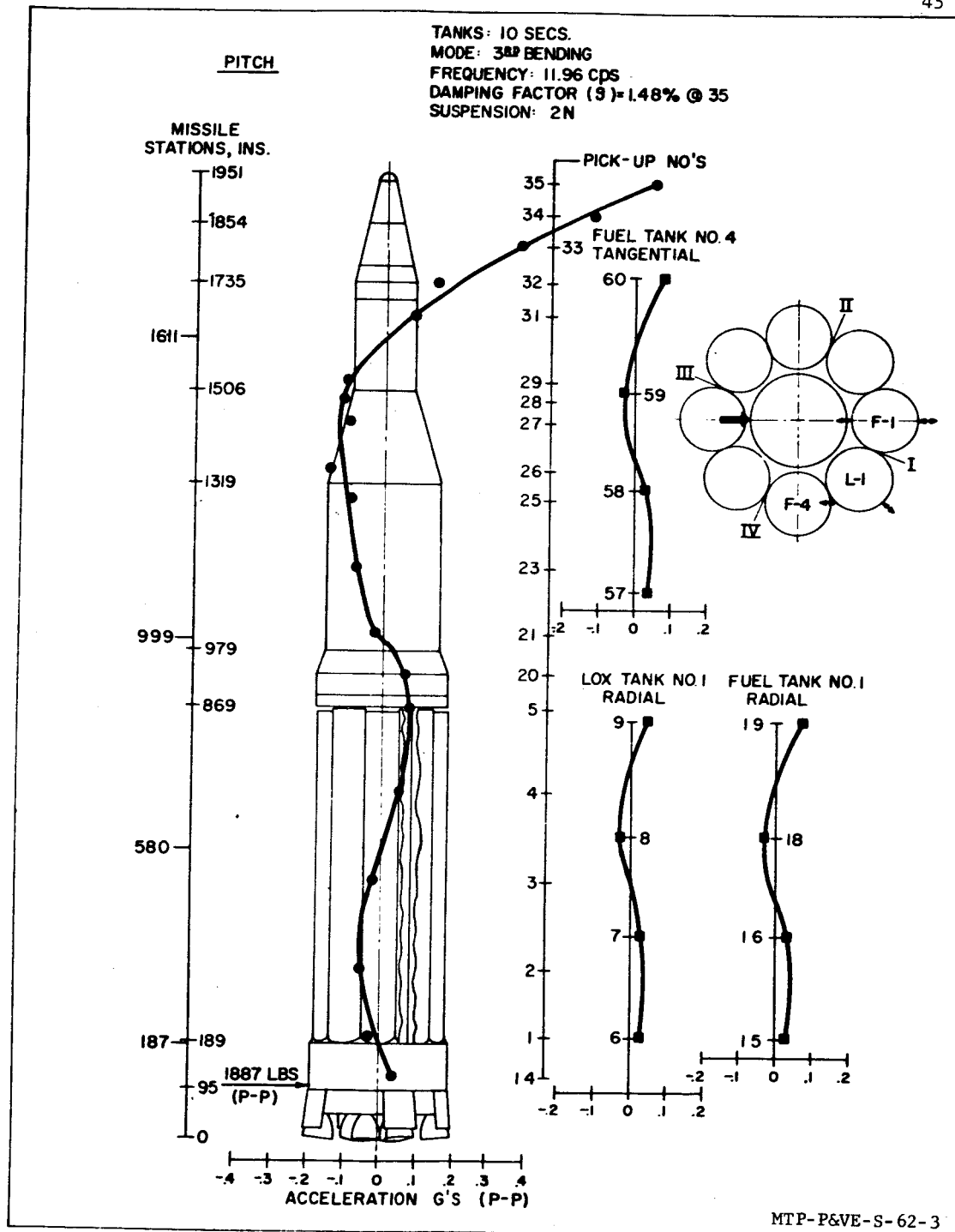


FIGURE 31. LATERAL BENDING MODES (PITCH PLANE)

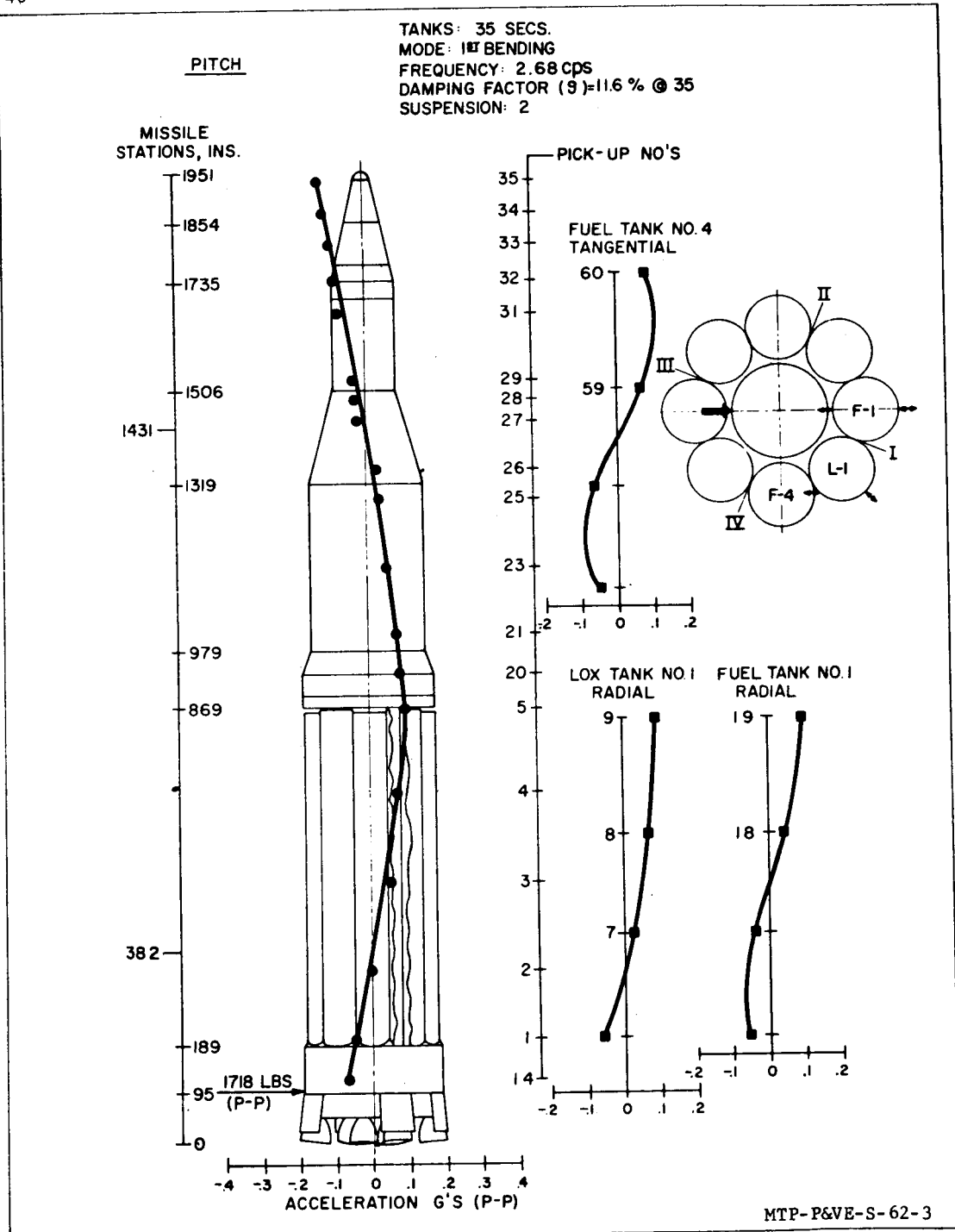


FIGURE 32. LATERAL BENDING MODES (PITCH PLANE)

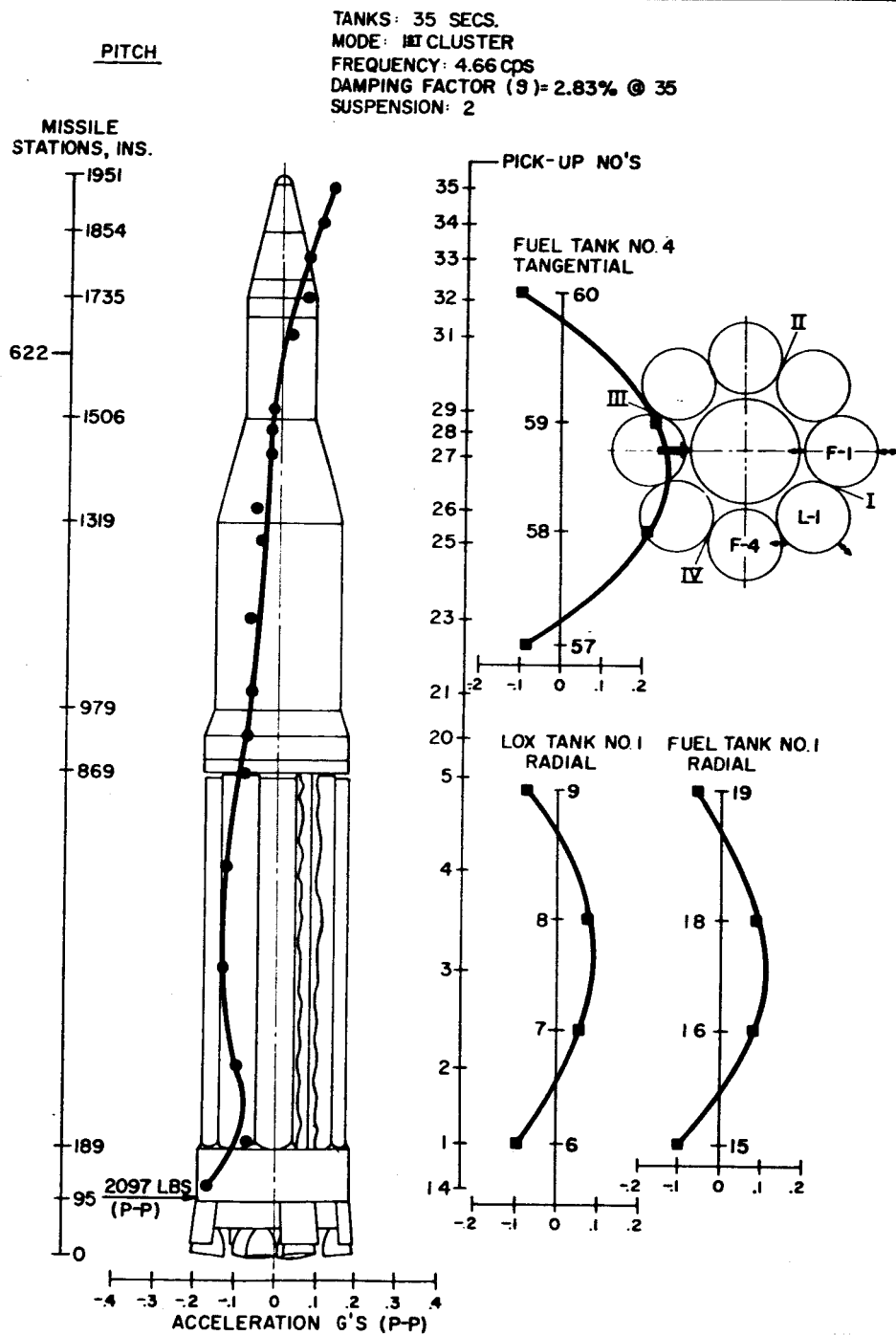


FIGURE 33. LATERAL BENDING MODES (PITCH PLANE)

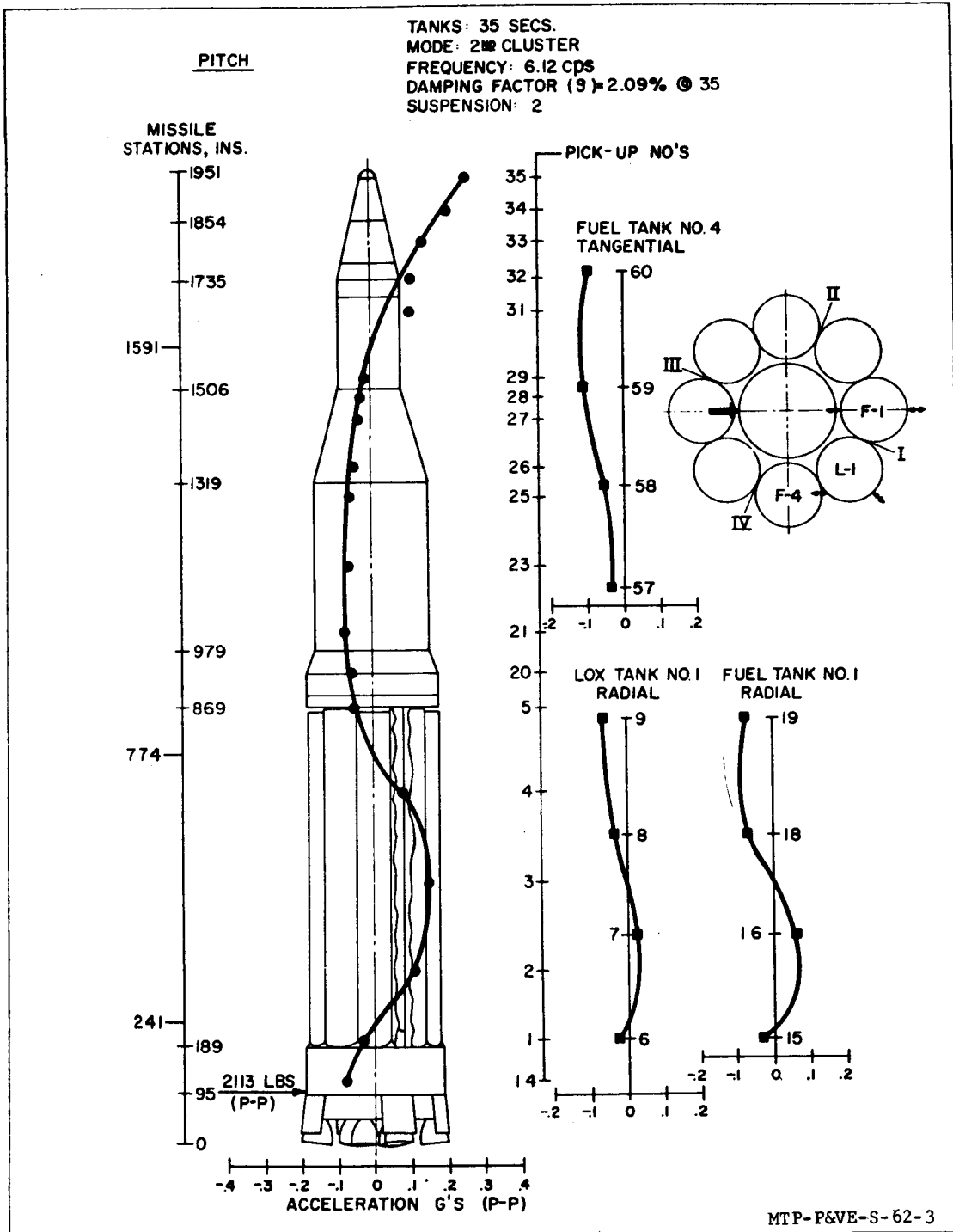


FIGURE 34. LATERAL BENDING MODES (PITCH PLANE)

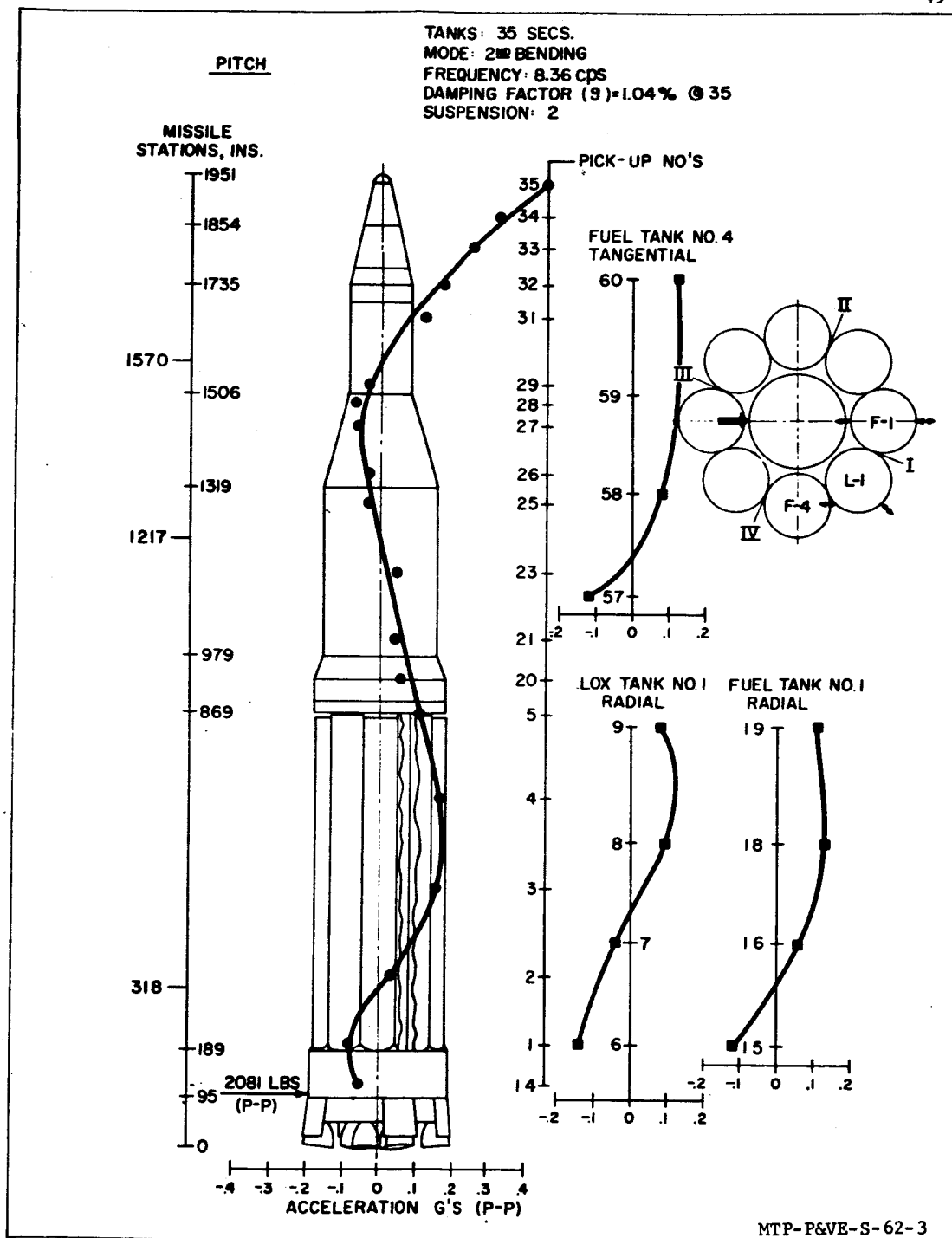


FIGURE 35. LATERAL BENDING MODES (PITCH PLANE)

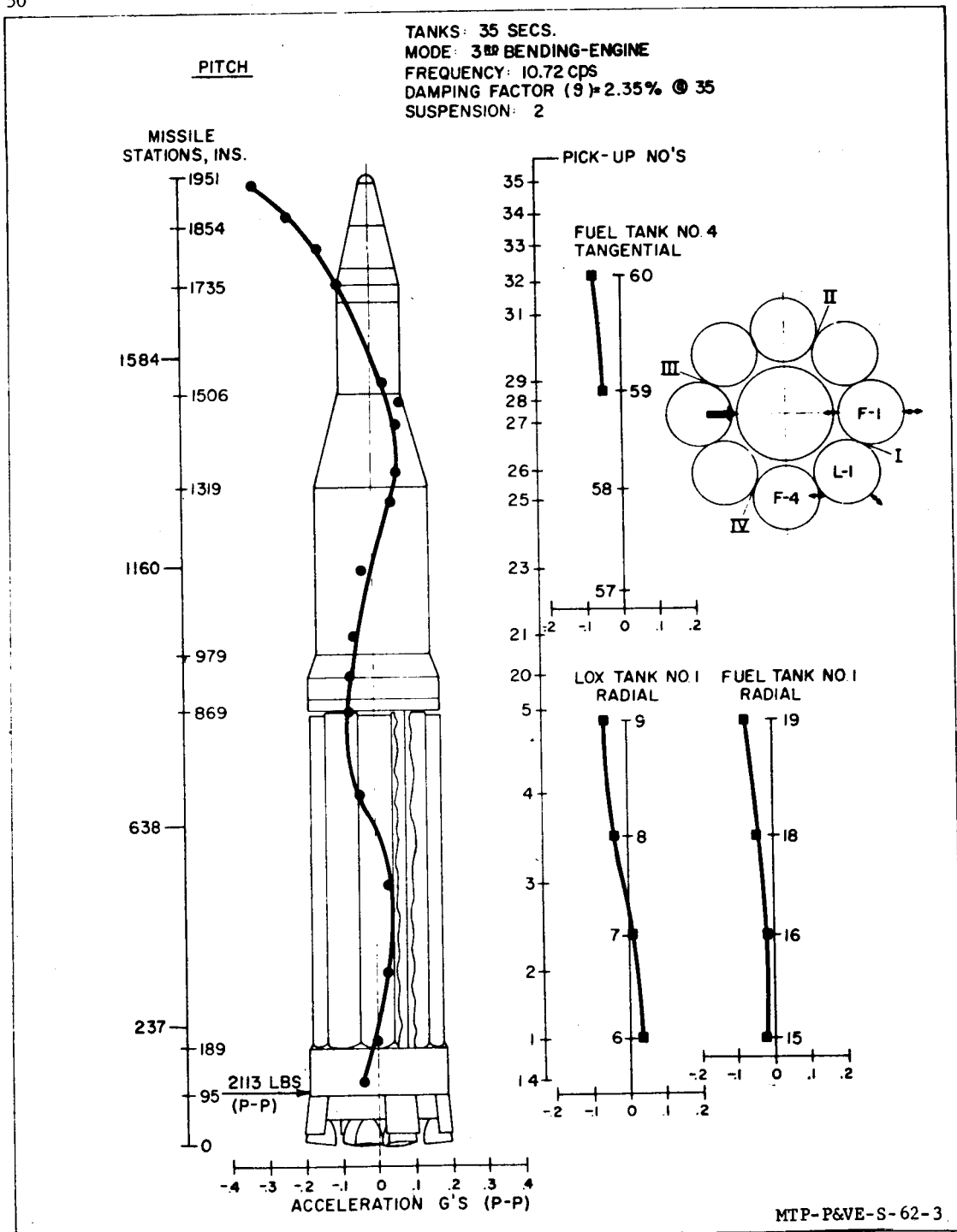


FIGURE 36. LATERAL BENDING MODES (PITCH PLANE)

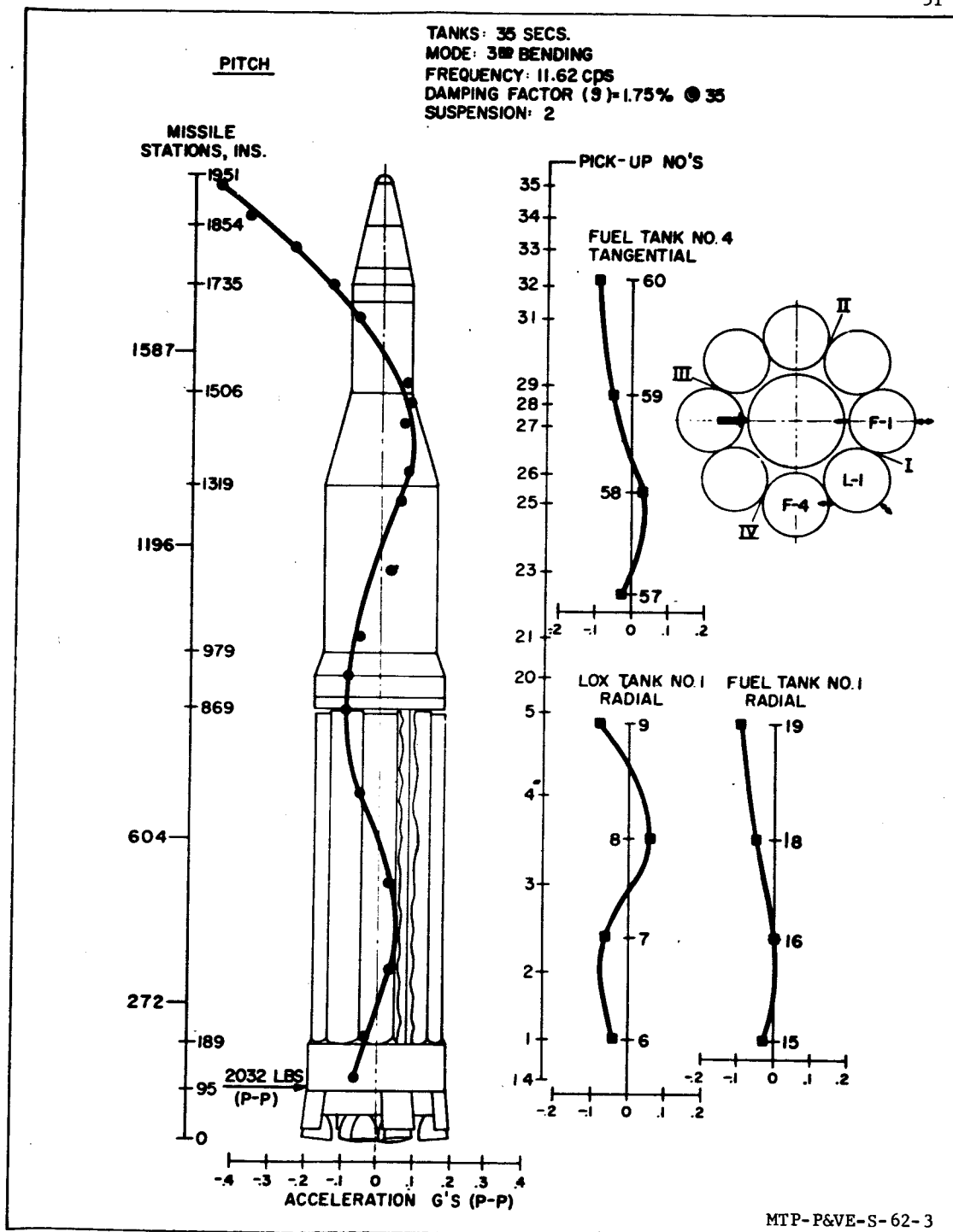


FIGURE 37. LATERAL BENDING MODES (PITCH PLANE)

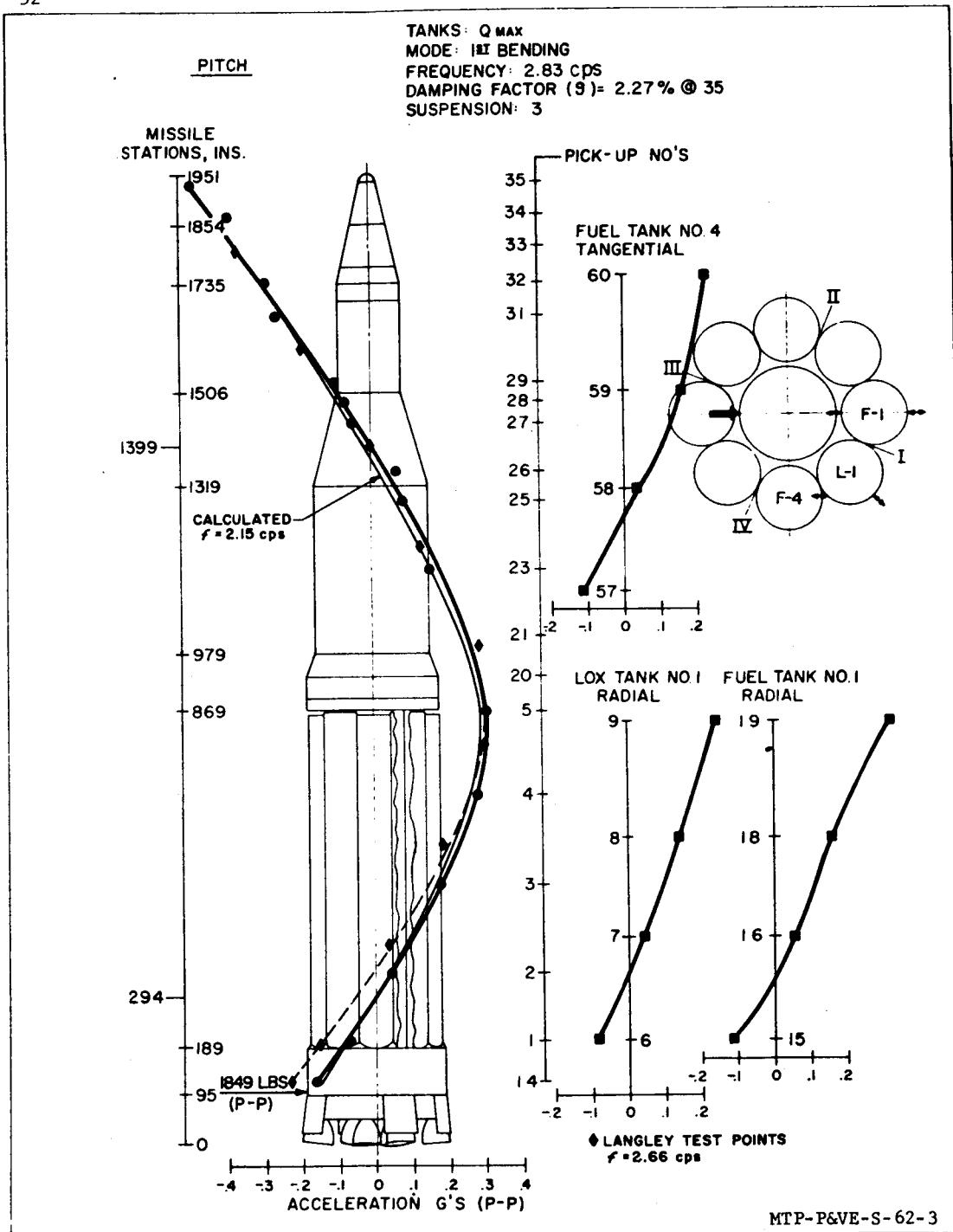


FIGURE 38. LATERAL BENDING MODES (PITCH PLANE)

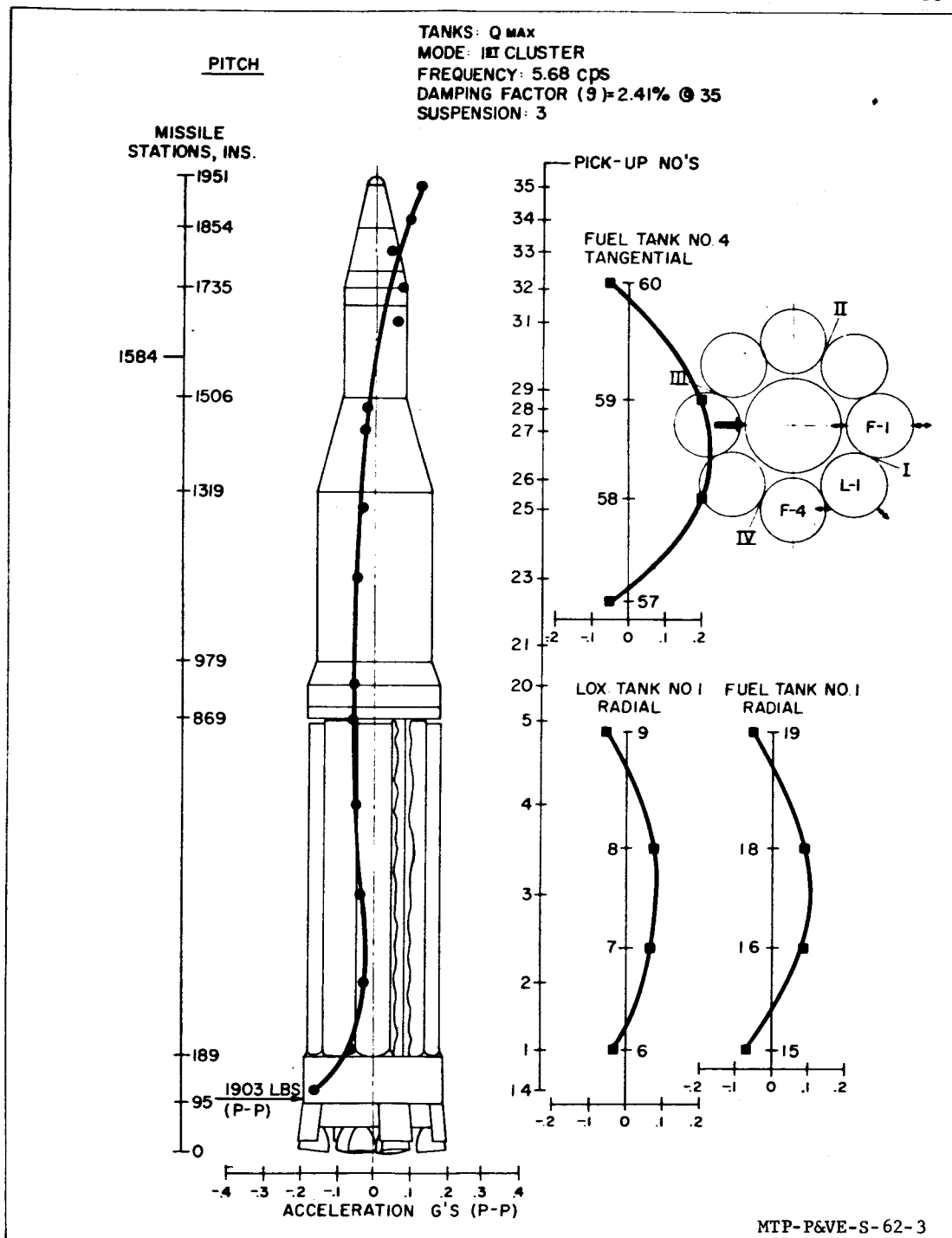


FIGURE 39. LATERAL BENDING MODES (PITCH PLANE)

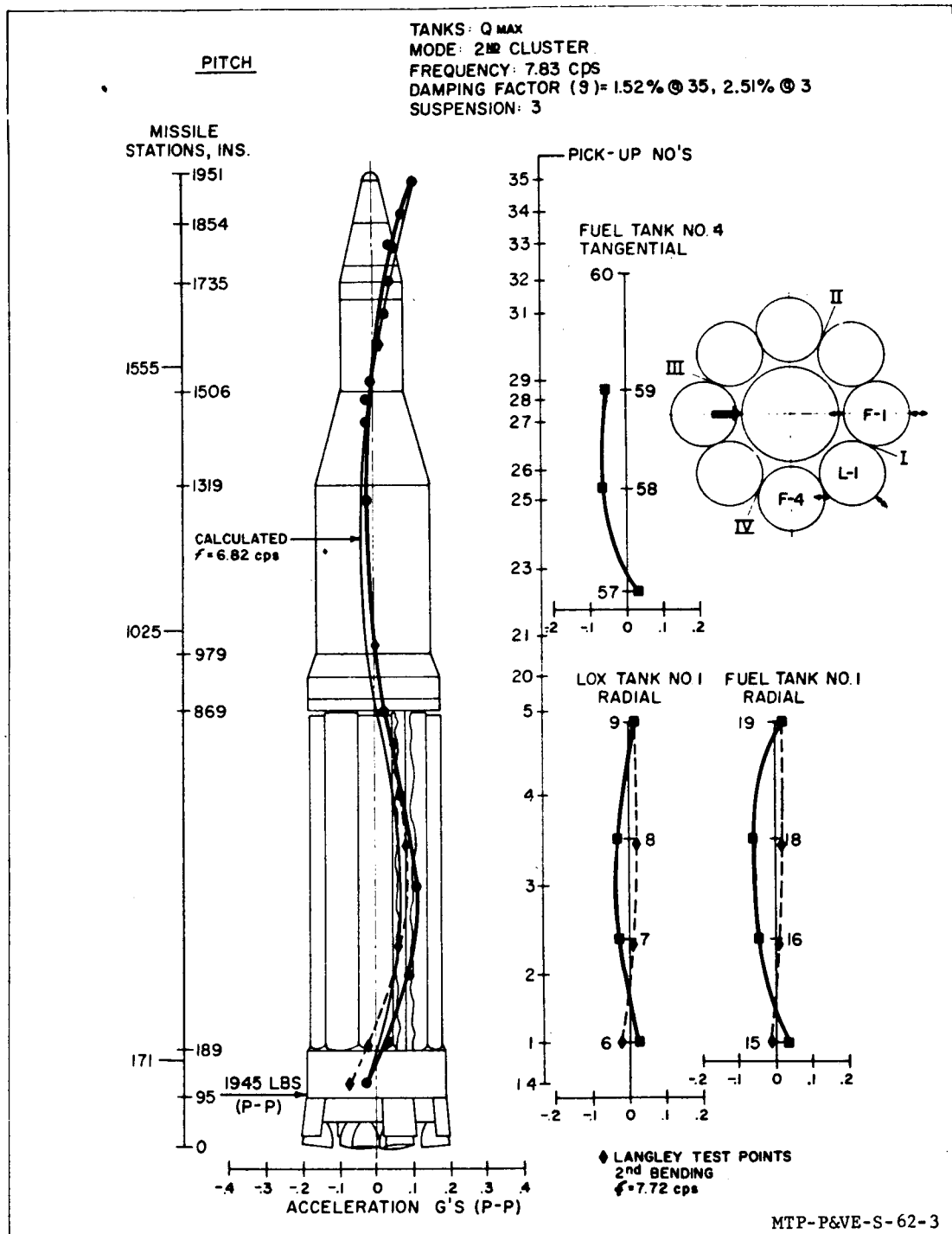


FIGURE 40. LATERAL BENDING MODES (PITCH PLANE)

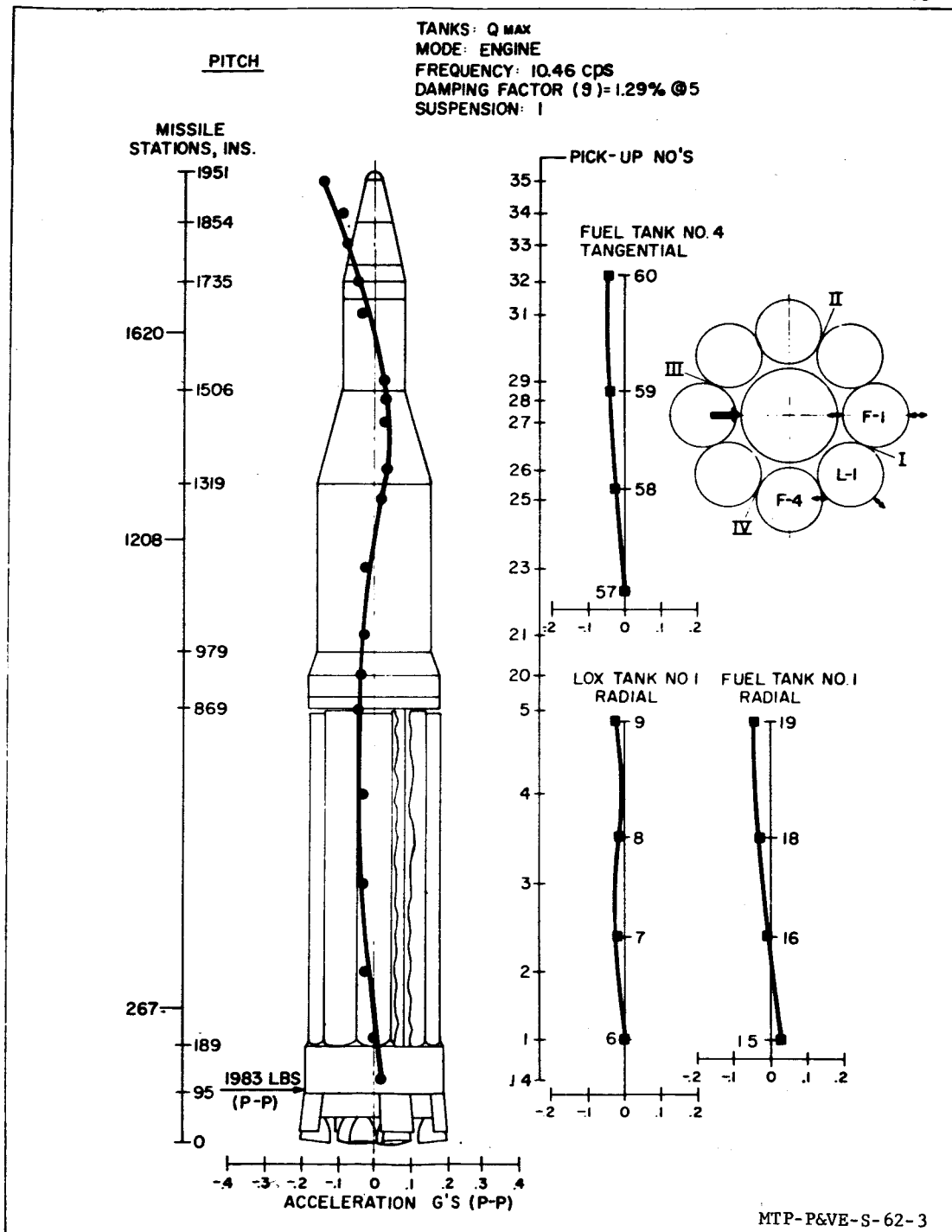


FIGURE 41. LATERAL BENDING MODES (PITCH PLANE)

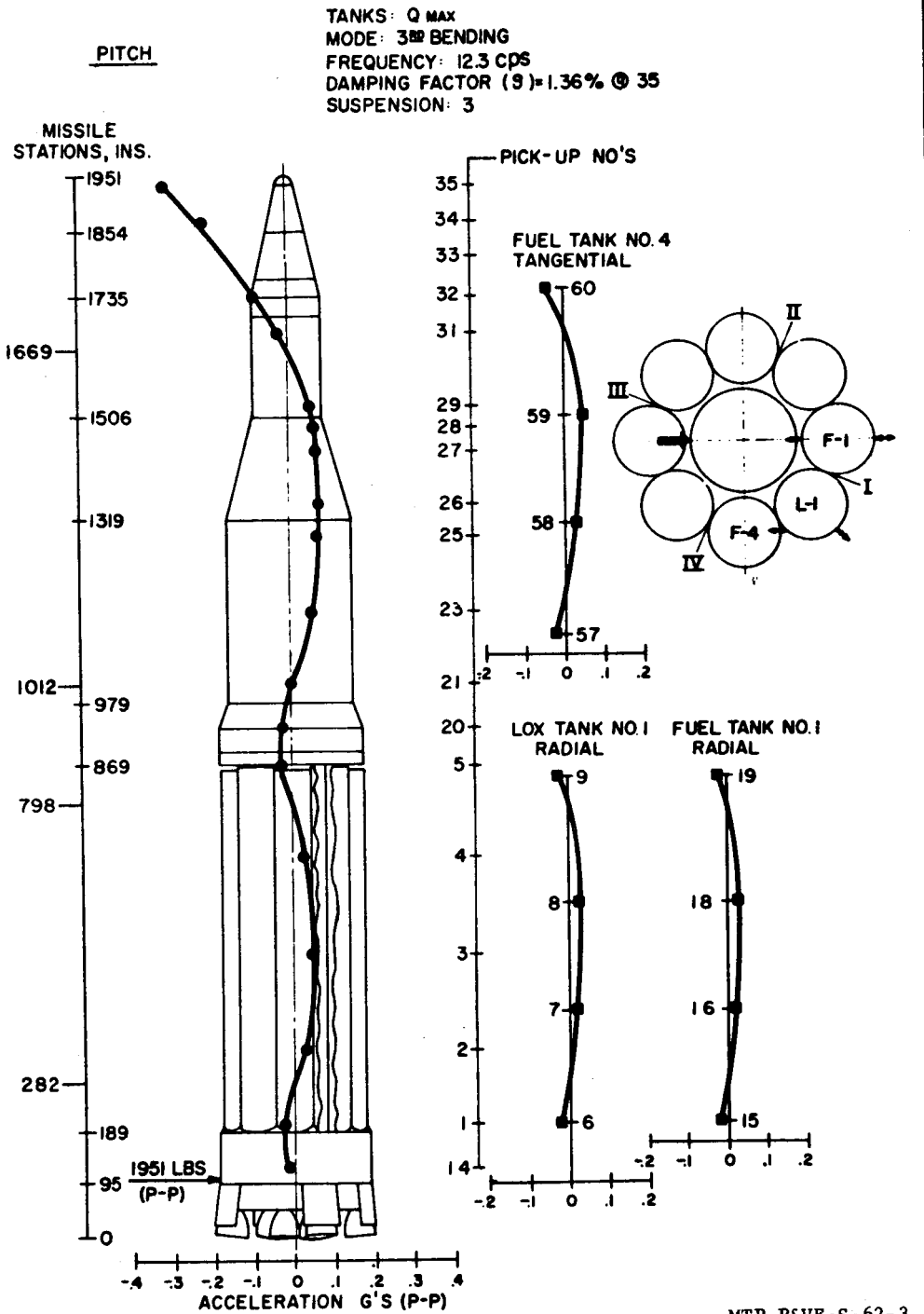


FIGURE 42. LATERAL BENDING MODES (PITCH PLANE)

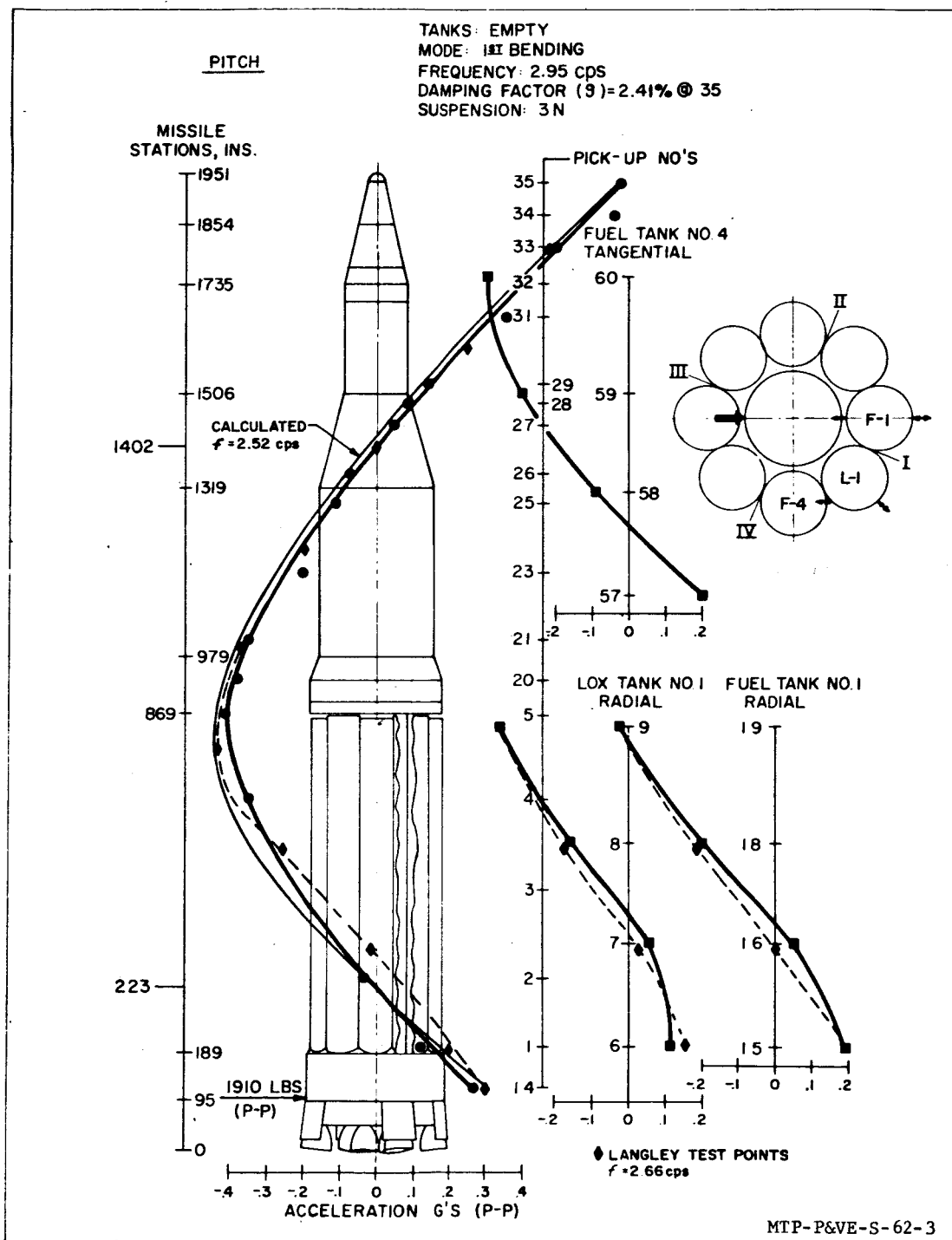


FIGURE 43. LATERAL BENDING MODES (PITCH PLANE)

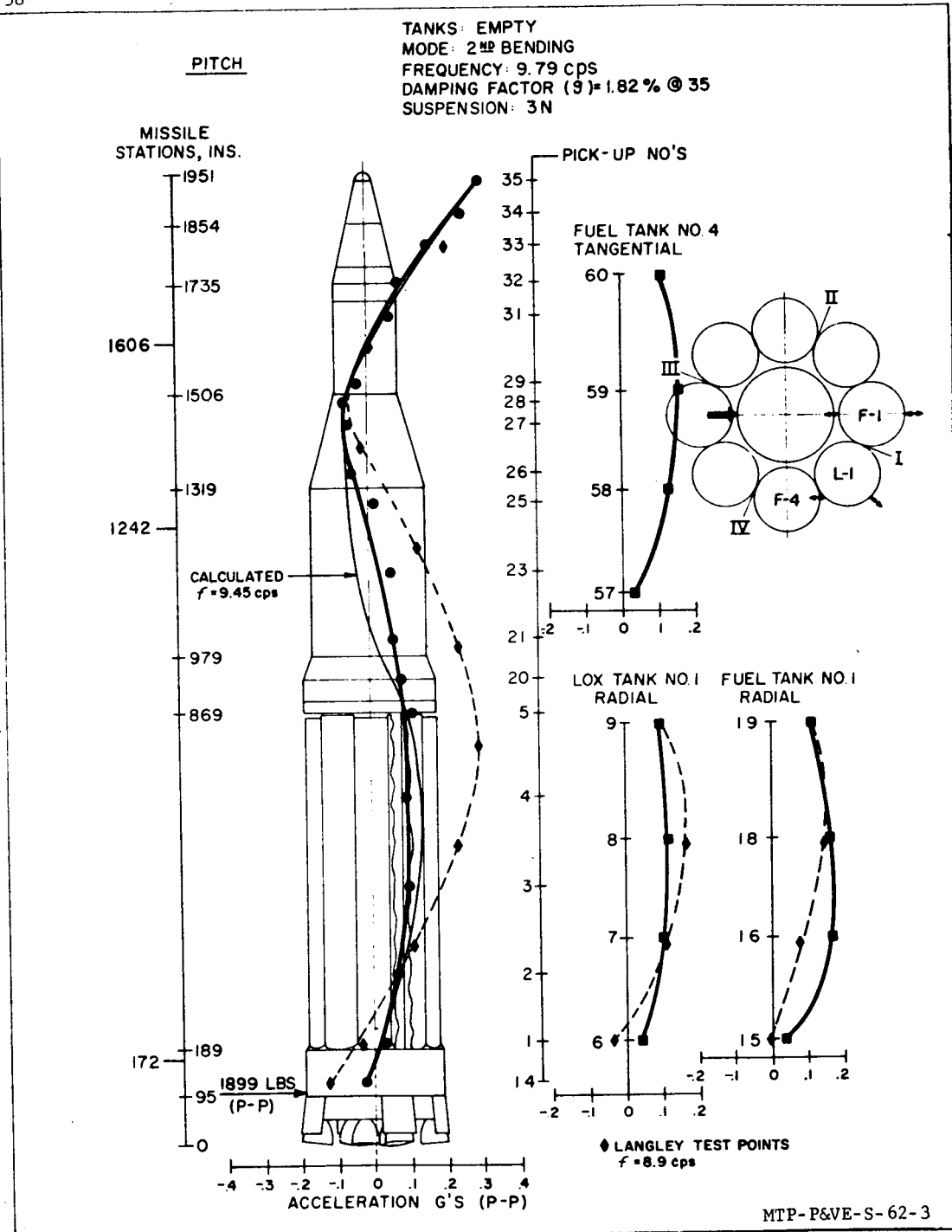


FIGURE 44. LATERAL BENDING MODES (PITCH PLANE)

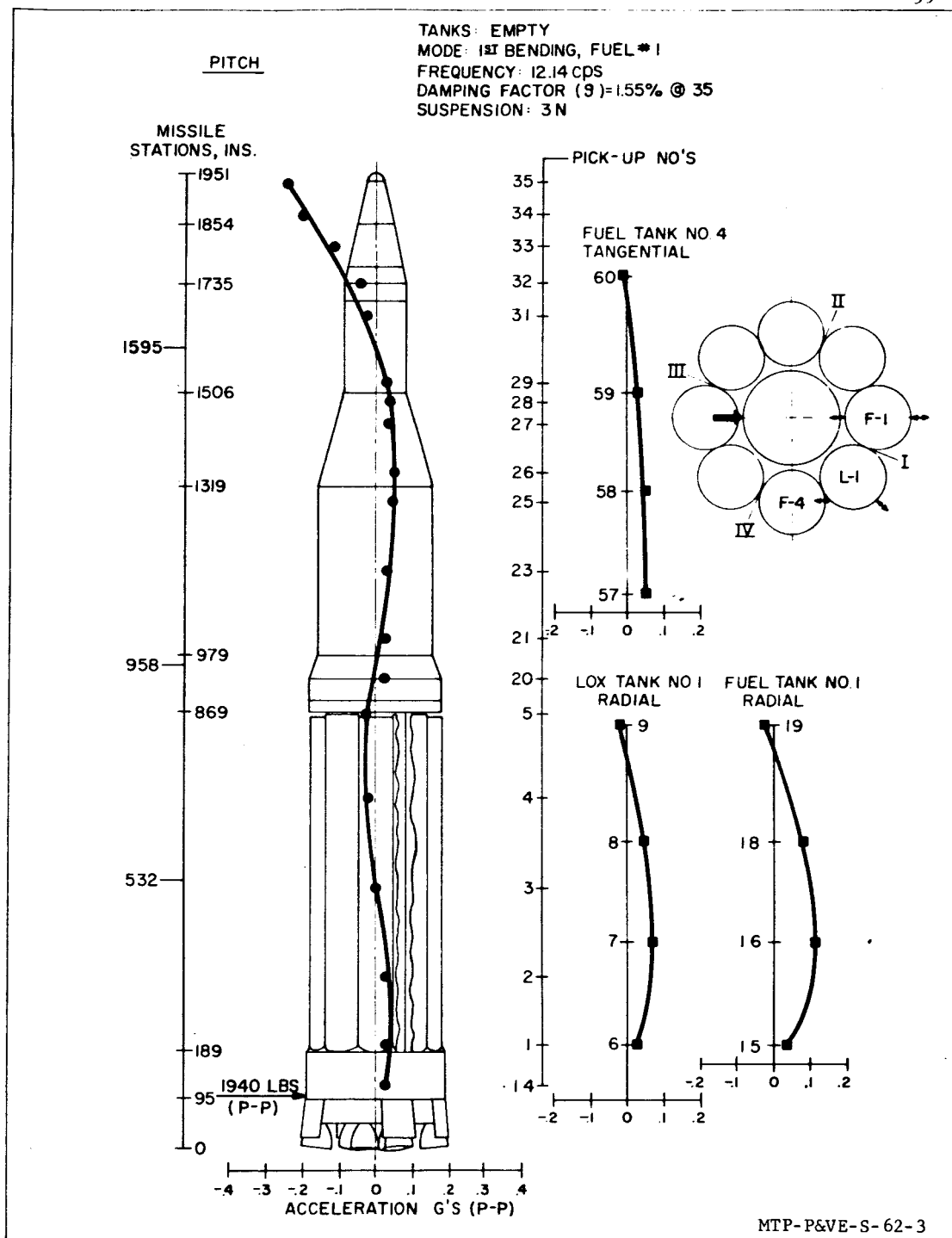


FIGURE 45. LATERAL BENDING MODES (PITCH PLANE)

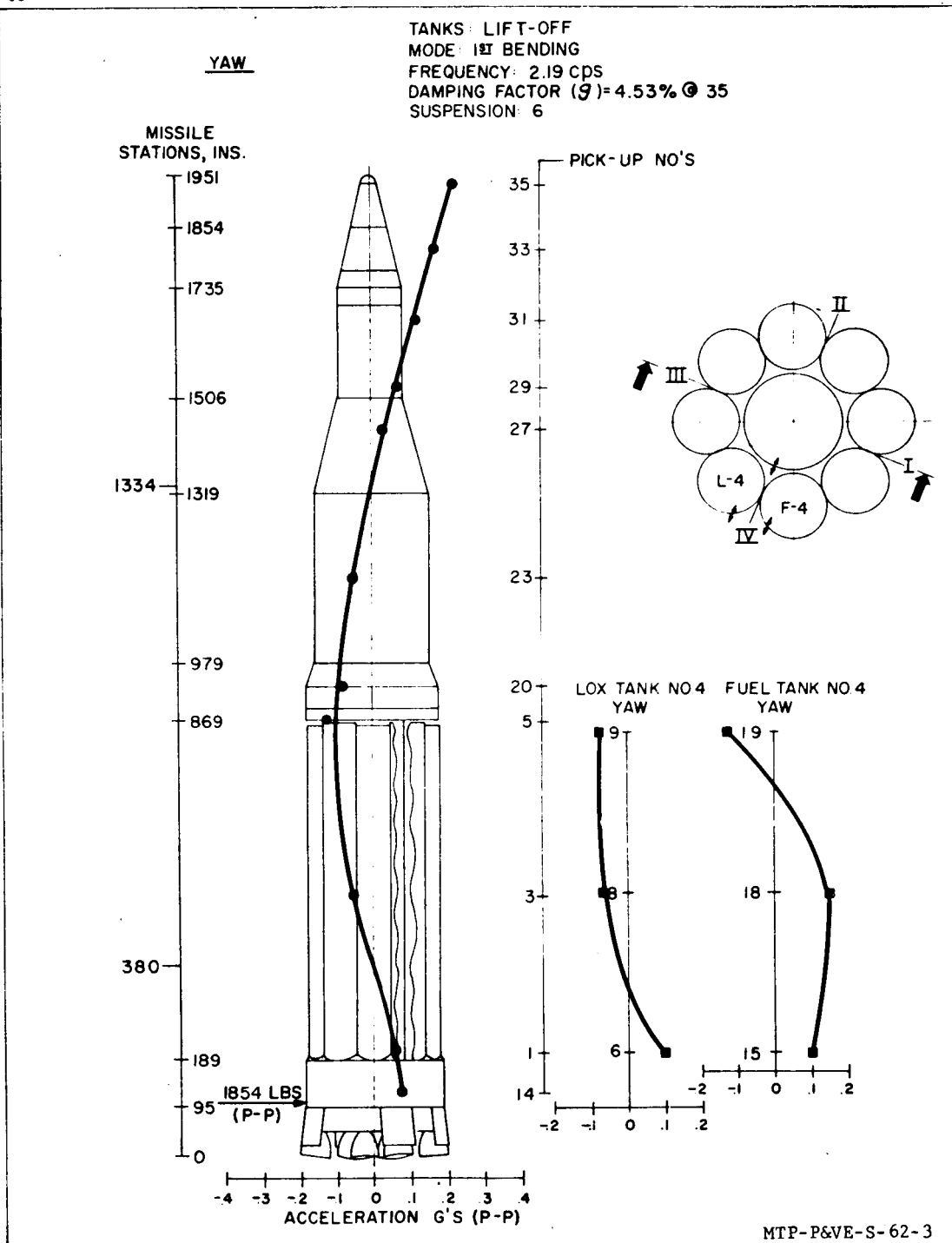


FIGURE 46. LATERAL BENDING MODES (YAW PLANE)

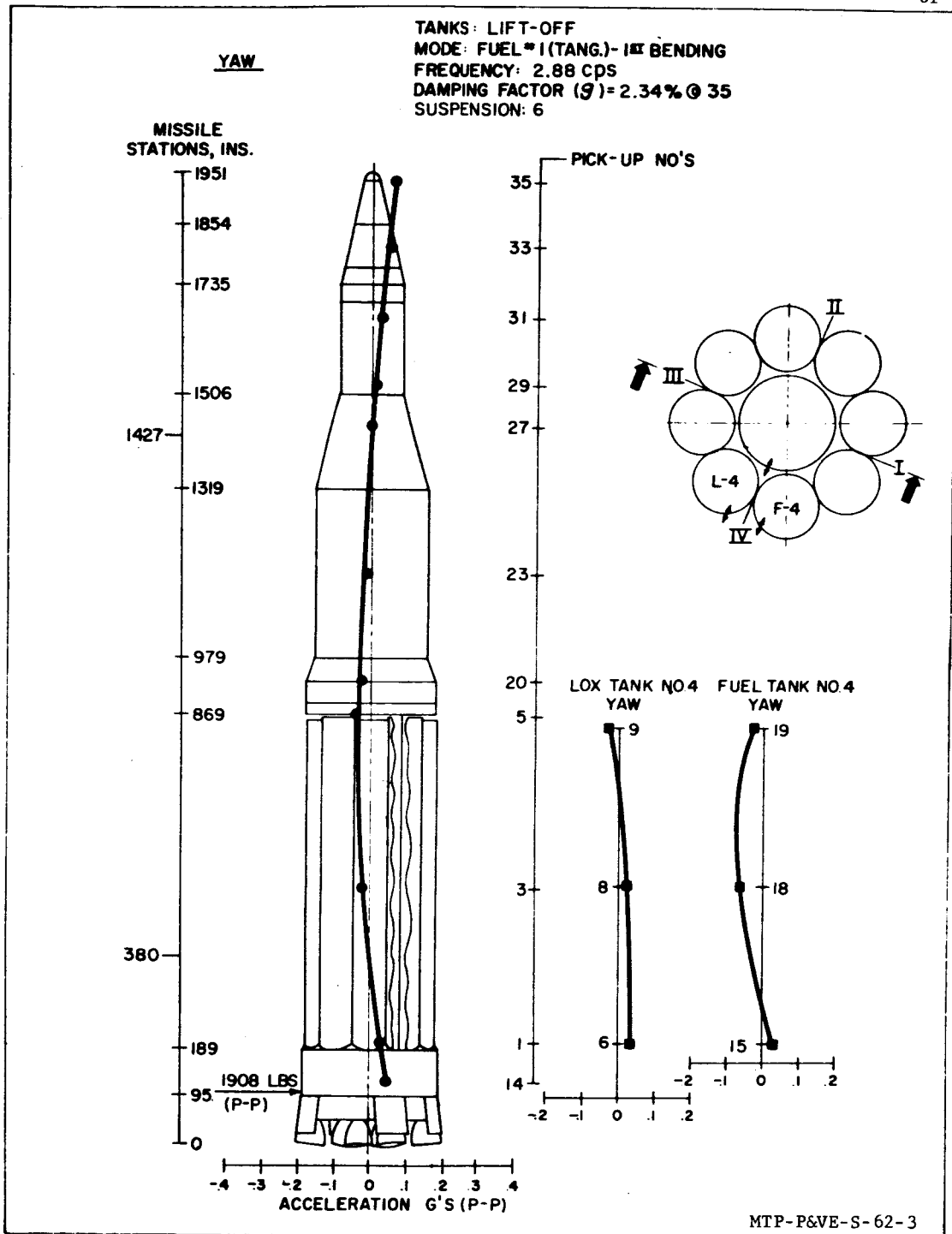


FIGURE 47. LATERAL BENDING MODES (YAW PLANE)

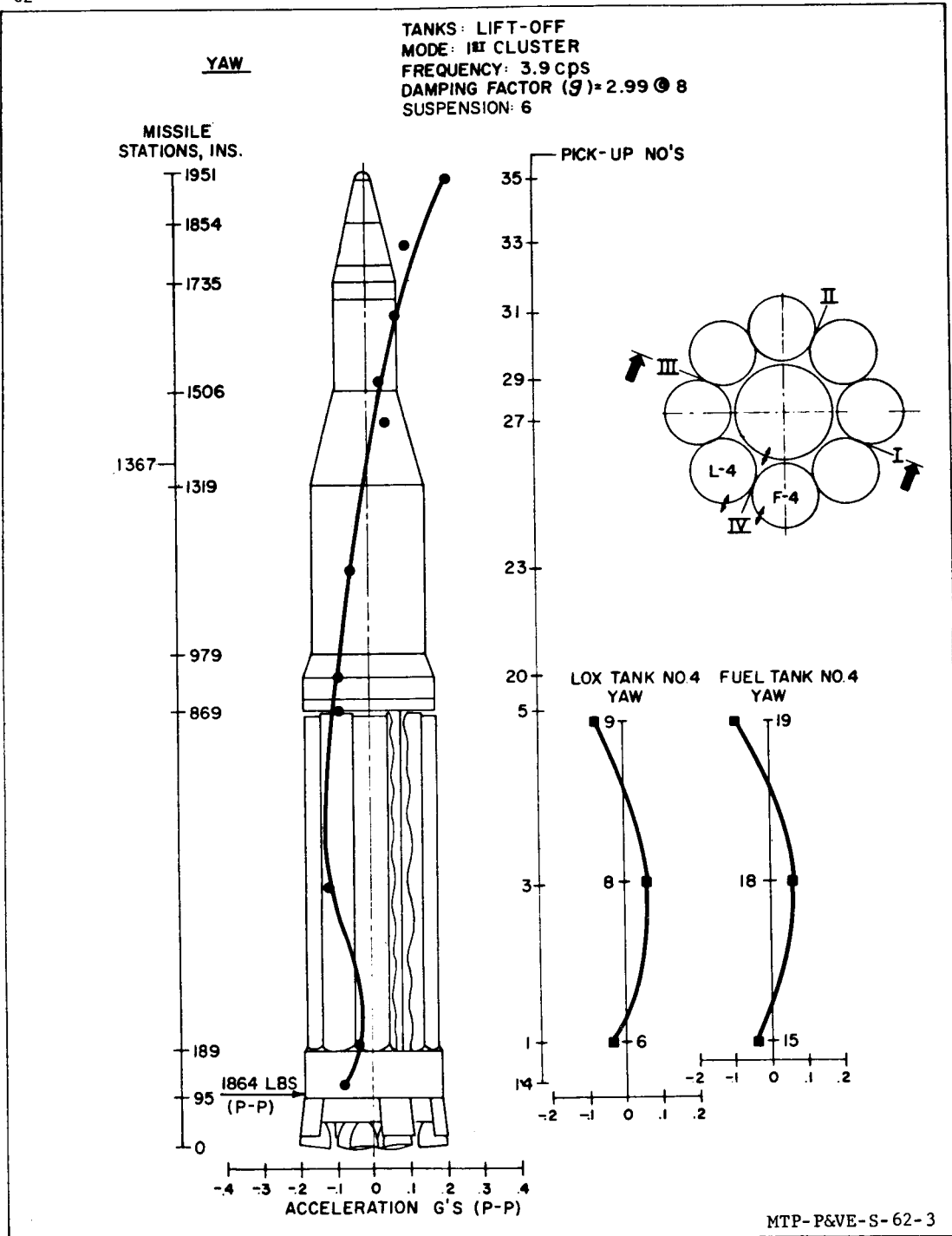


FIGURE 48. LATERAL BENDING MODES (YAW PLANE)

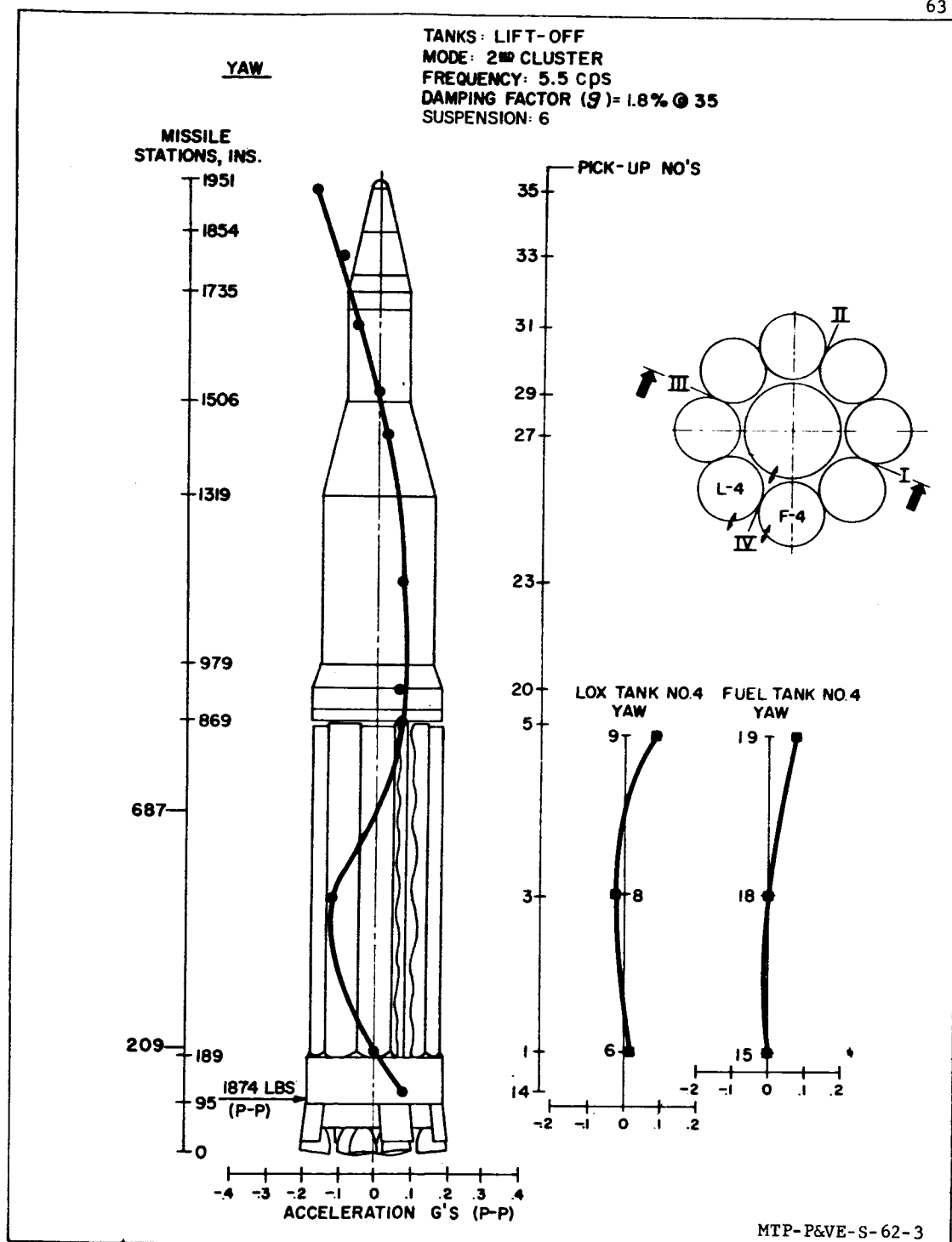


FIGURE 49. LATERAL BENDING MODES (YAW PLANE)

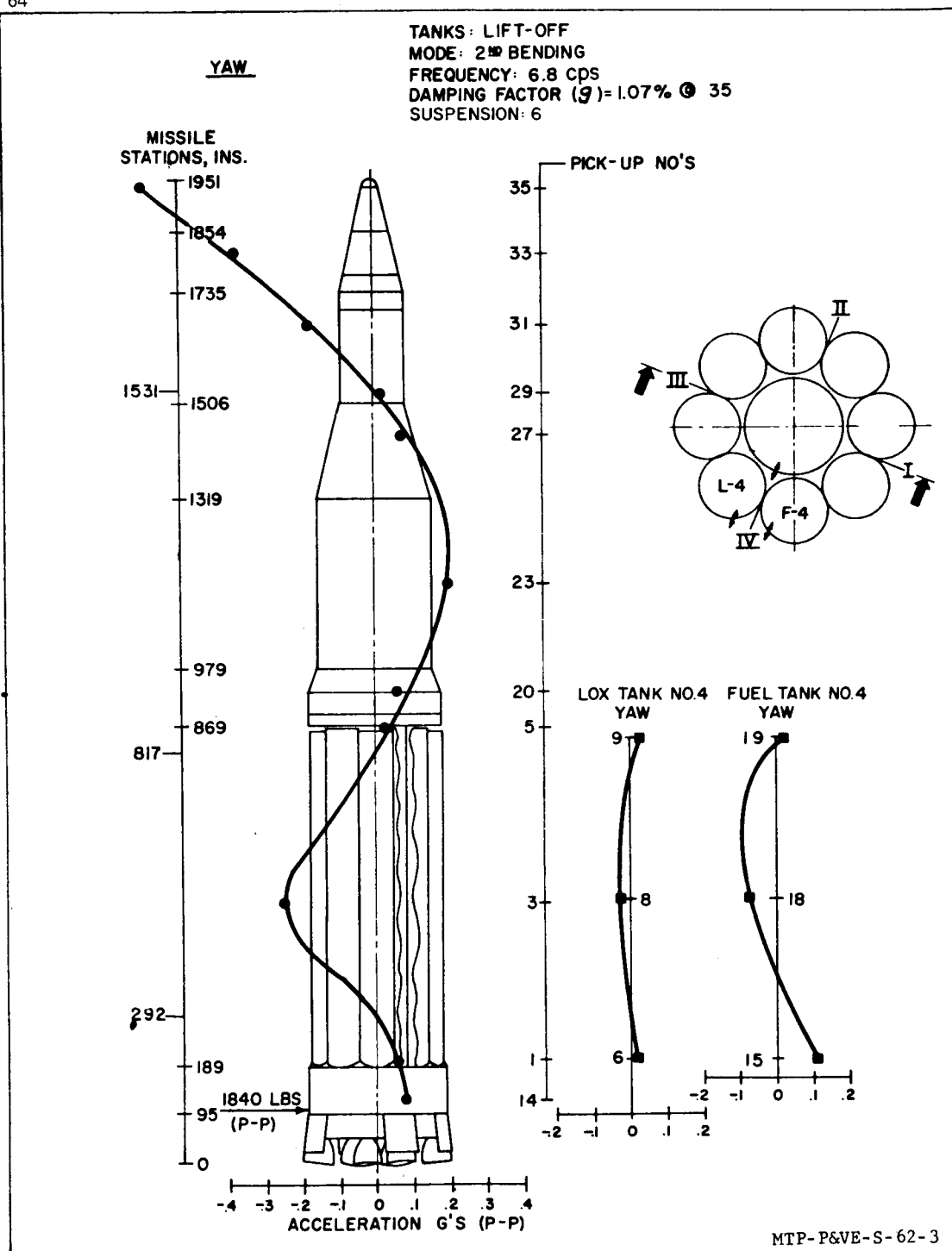


FIGURE 50. LATERAL BENDING MODES (YAW PLANE)

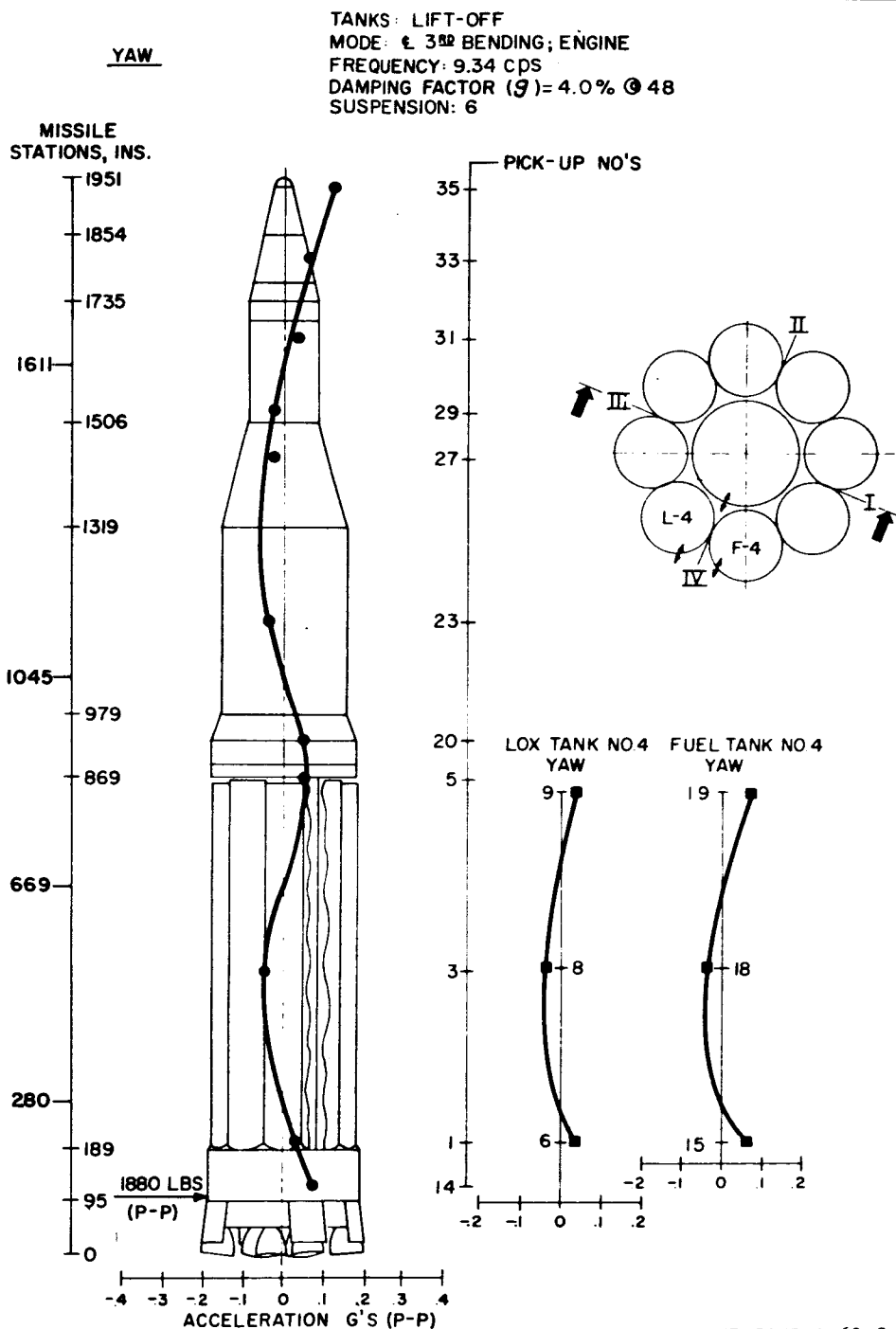


FIGURE 51. LATERAL BENDING MODES (YAW PLANE)

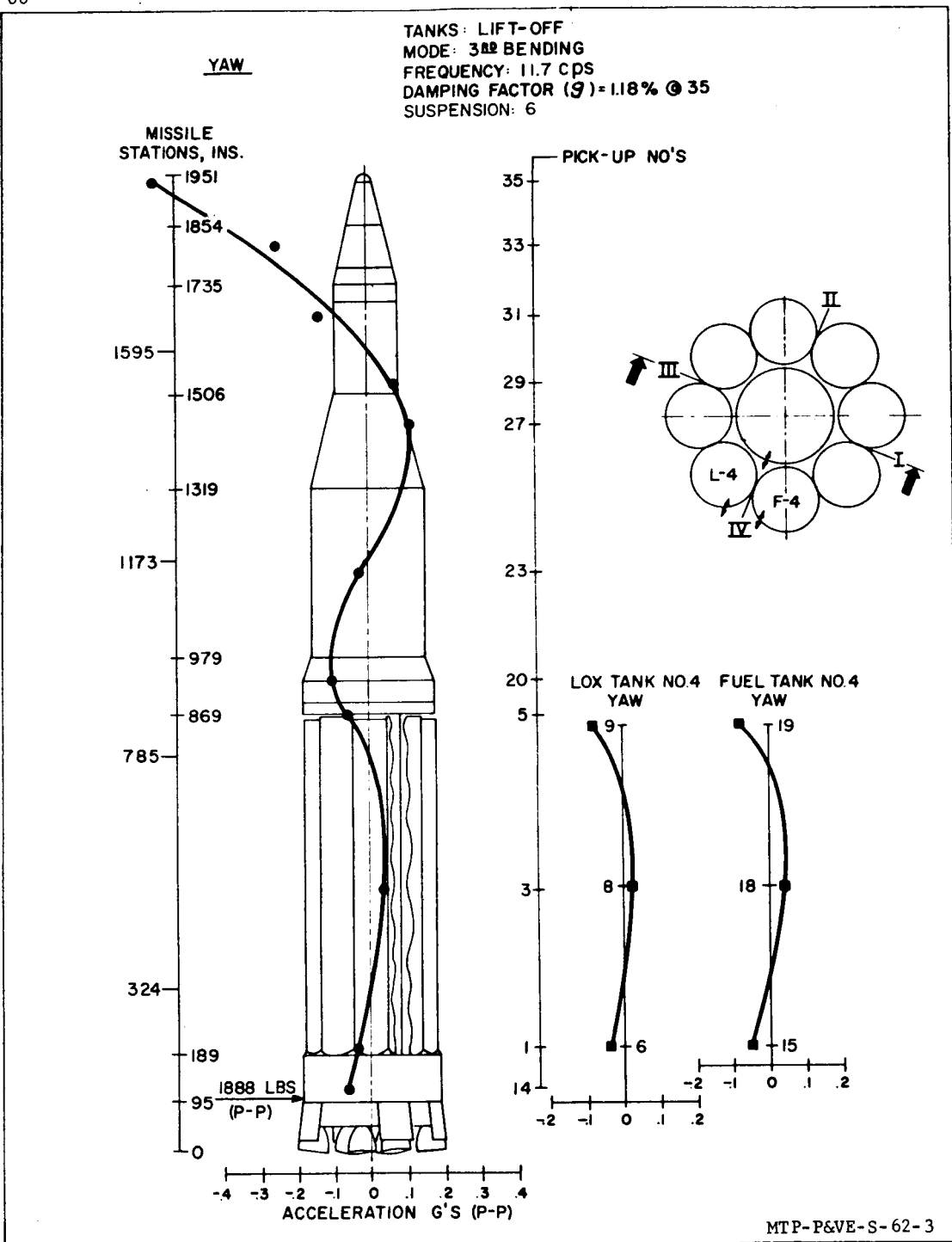


FIGURE 52. LATERAL BENDING MODES (YAW PLANE)

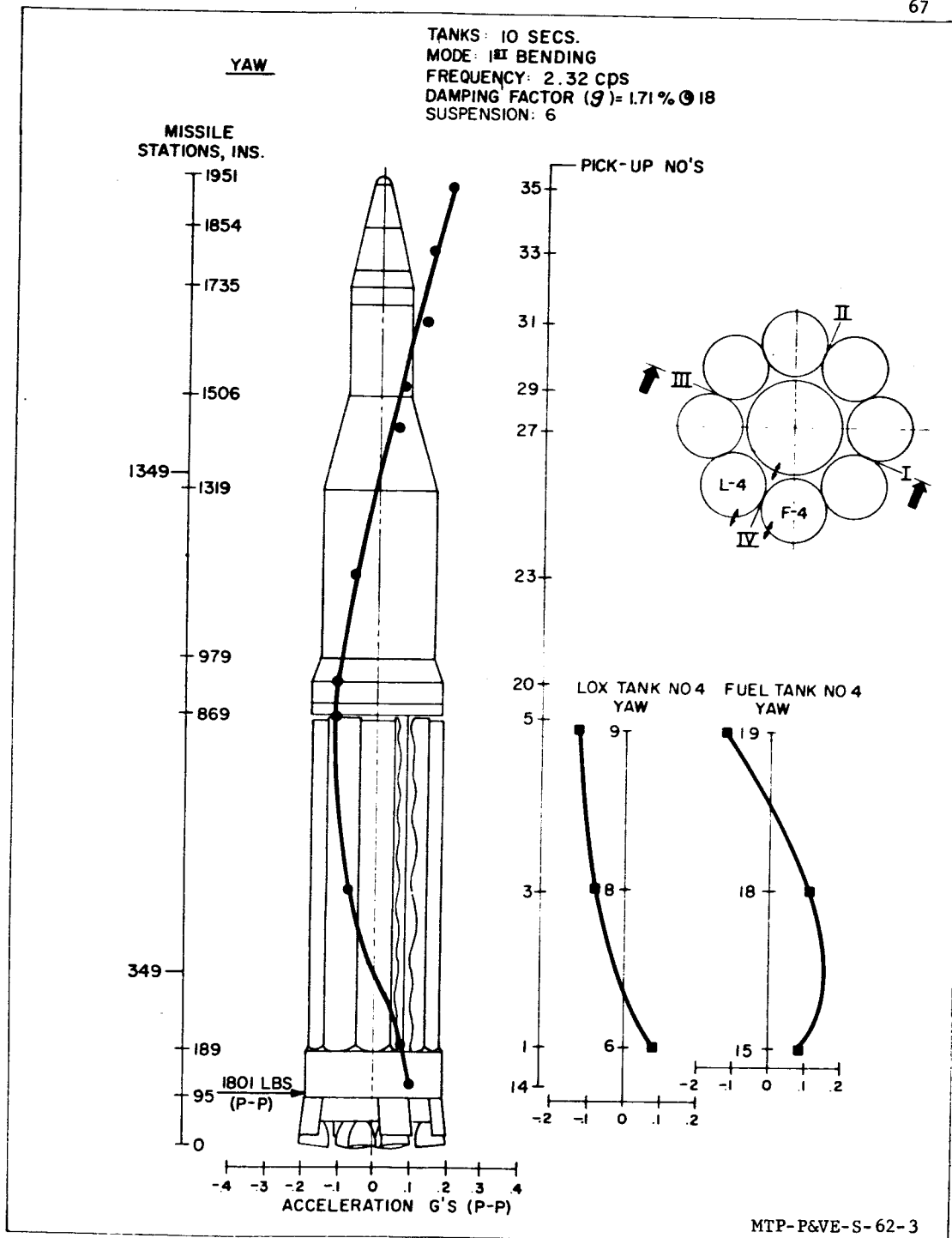


FIGURE 53. LATERAL BENDING MODES (YAW PLANE)

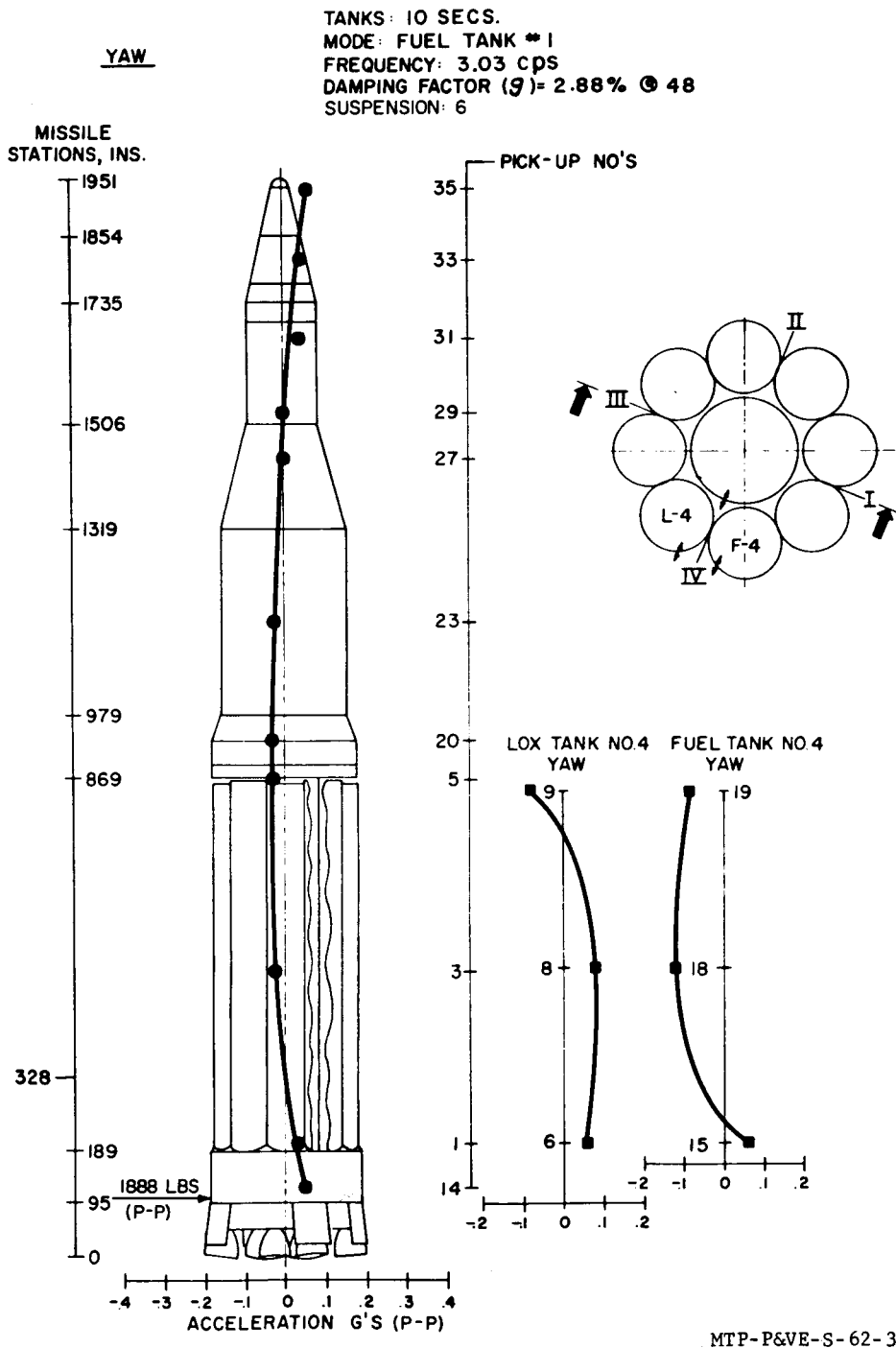


FIGURE 54. LATERAL BENDING MODES (YAW PLANE)

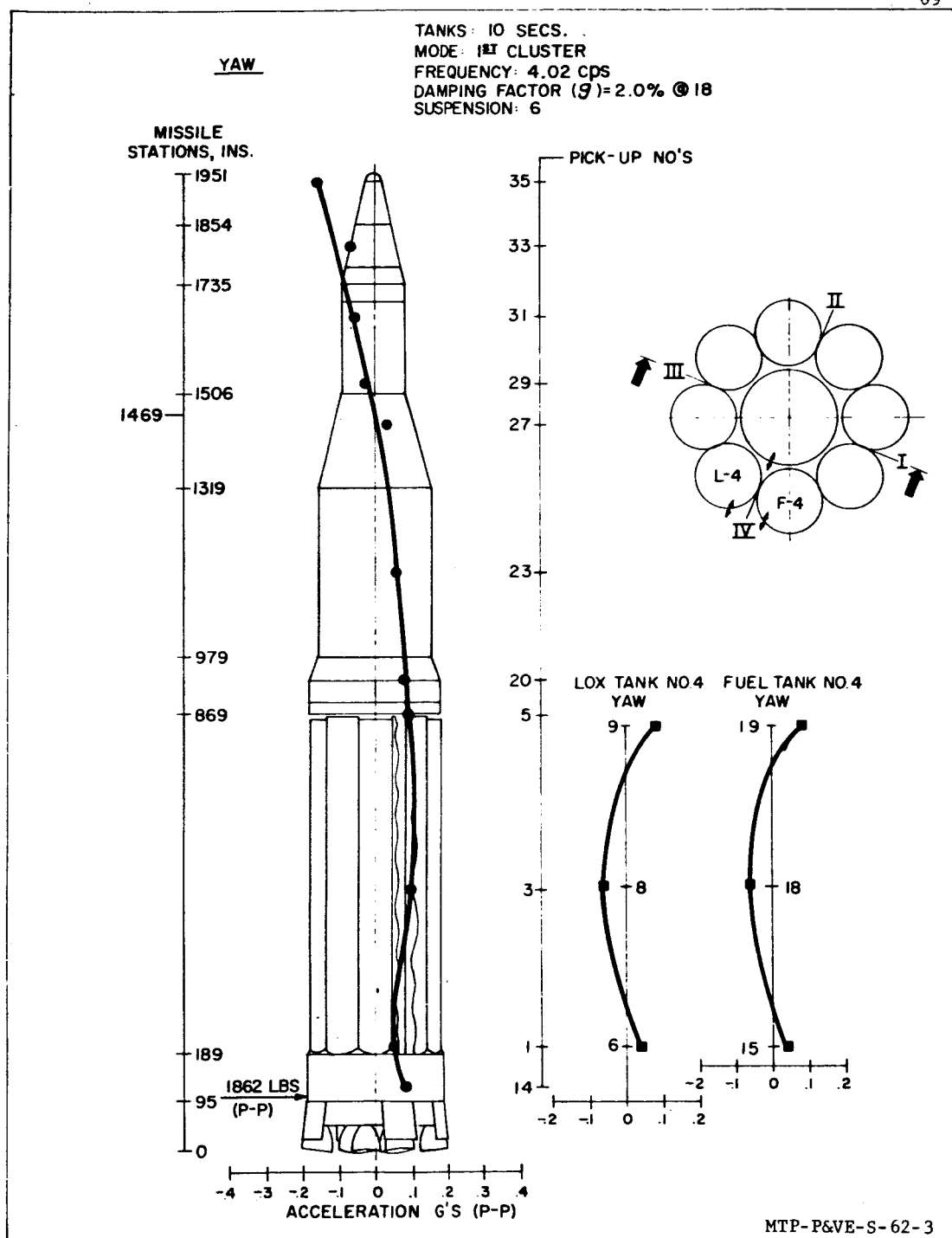


FIGURE 55. LATERAL BENDING MODES (YAW PLANE)

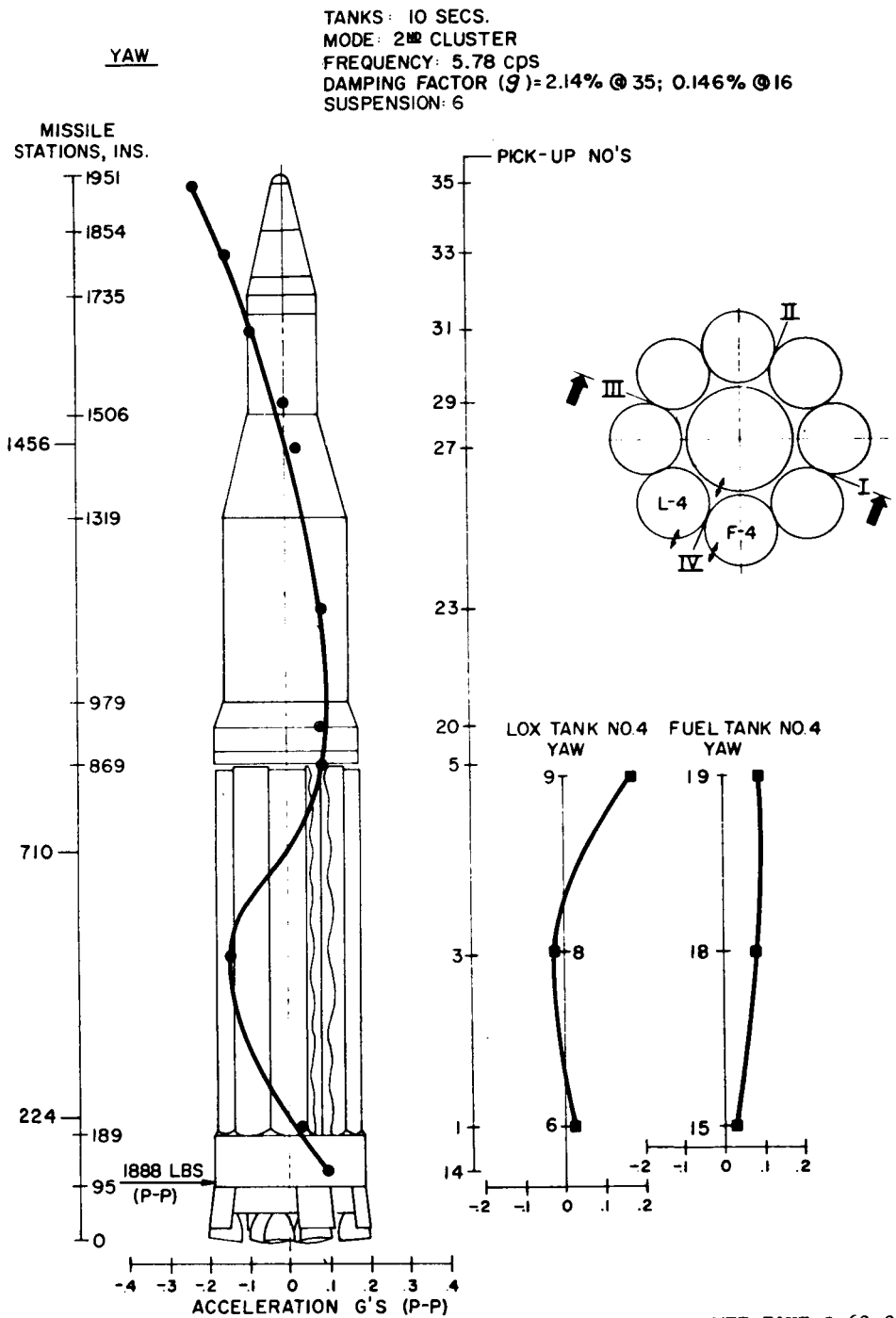


FIGURE 56. LATERAL BENDING MODES (YAW PLANE)

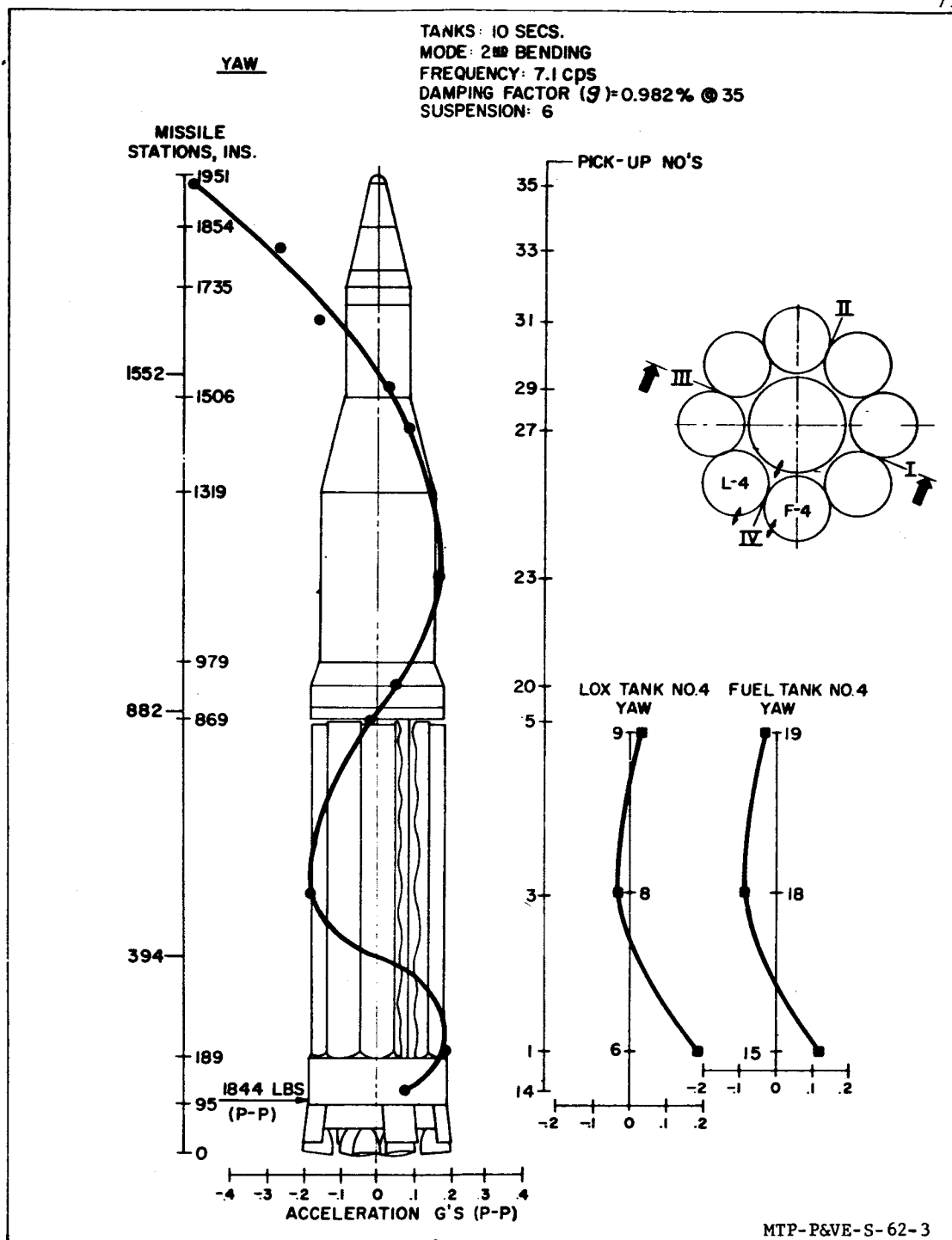


FIGURE 57. LATERAL BENDING MODES (YAW PLANE)

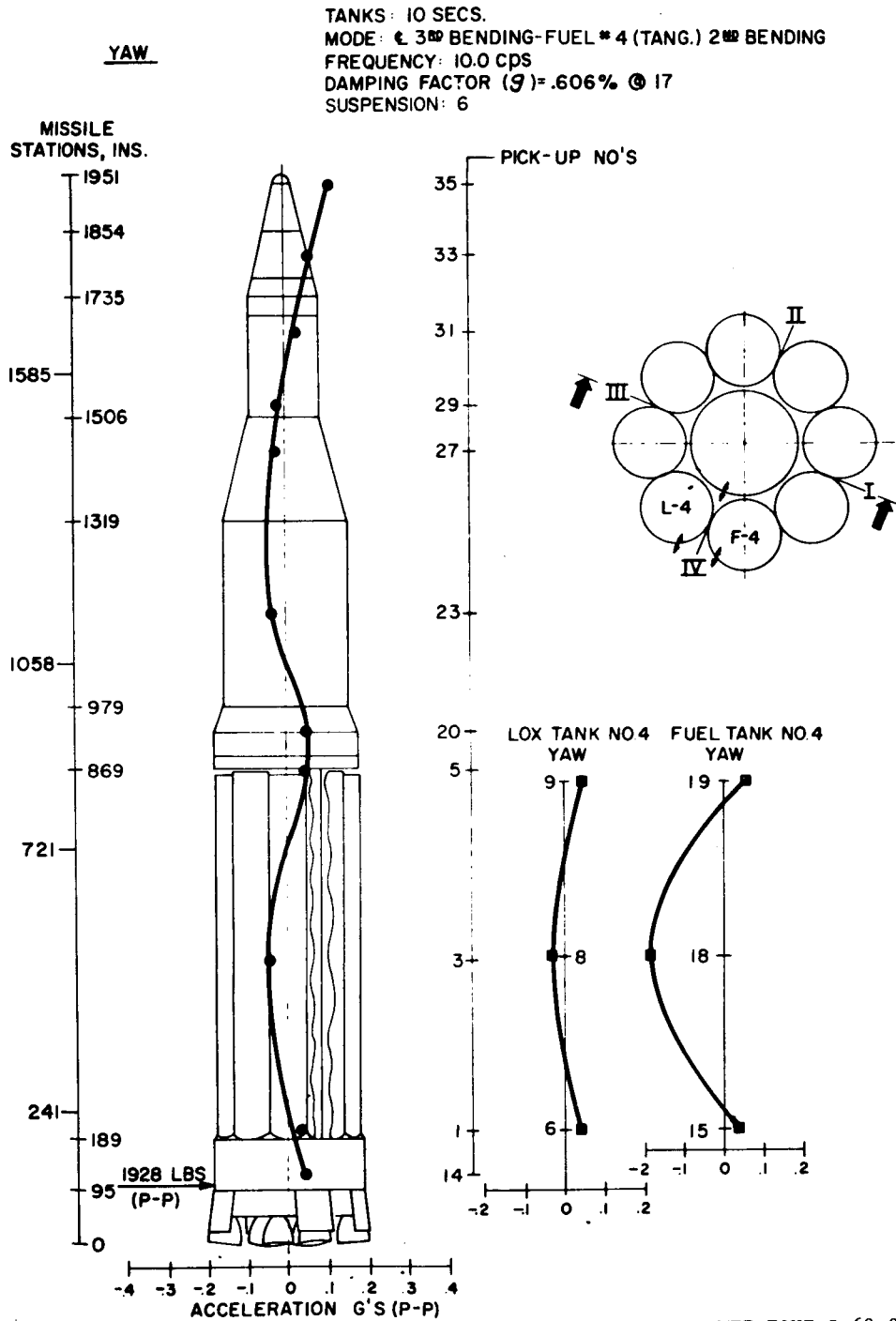


FIGURE 58. LATERAL BENDING MODES (YAW PLANE)

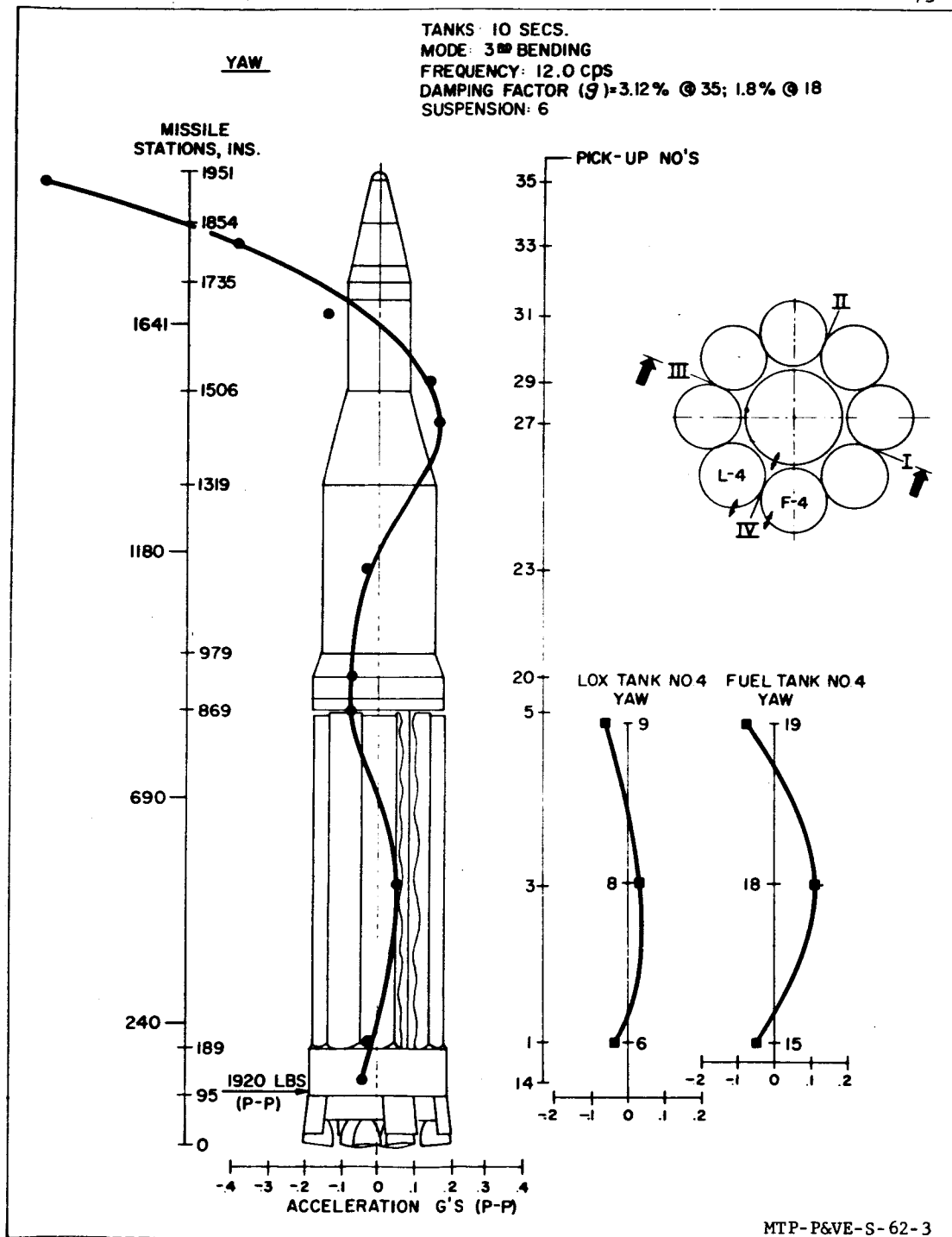


FIGURE 59. LATERAL BENDING MODES (YAW PLANE)

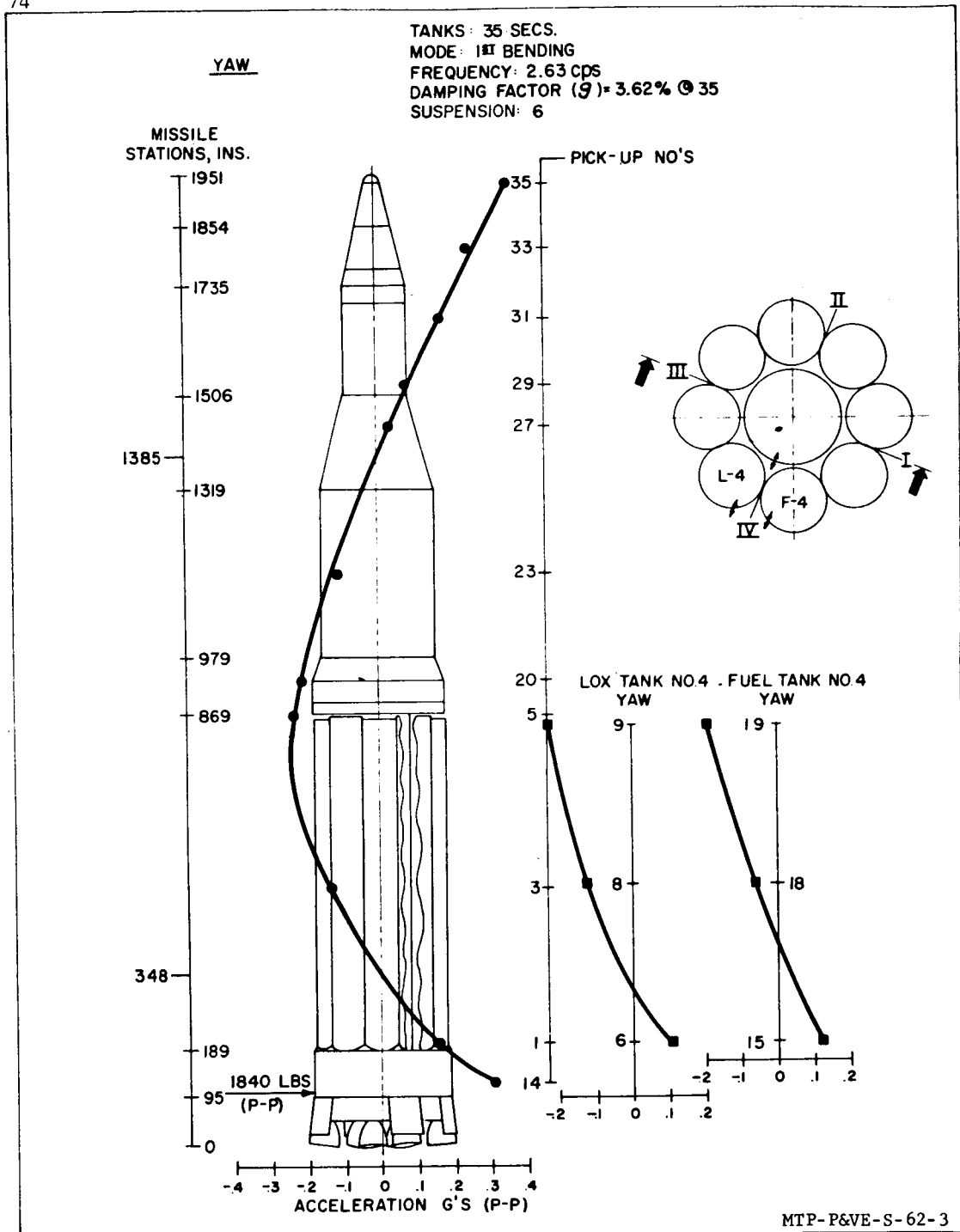


FIGURE 60. LATERAL BENDING MODES (YAW PLANE)

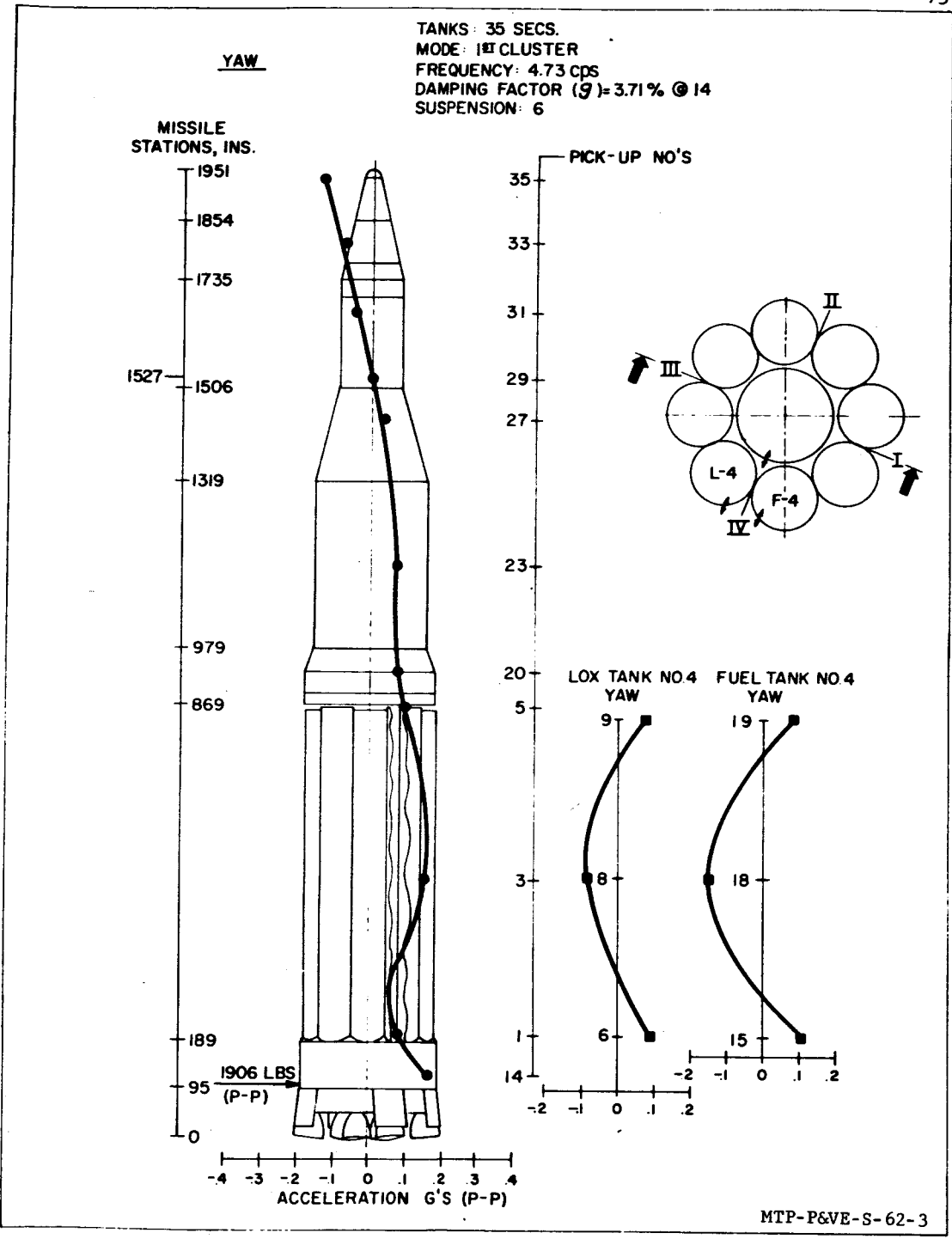
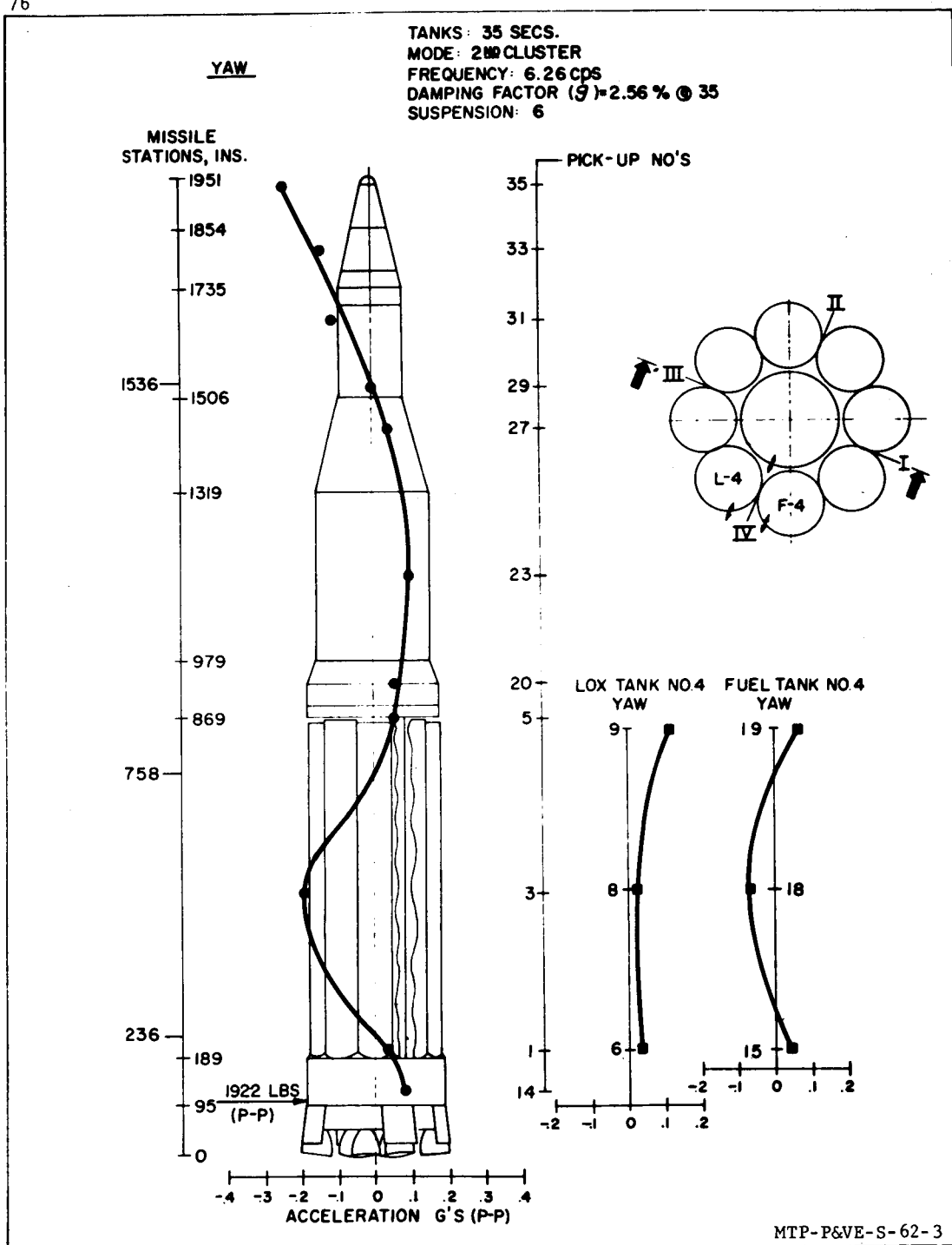


FIGURE 61. LATERAL BENDING MODES (YAW PLANE)



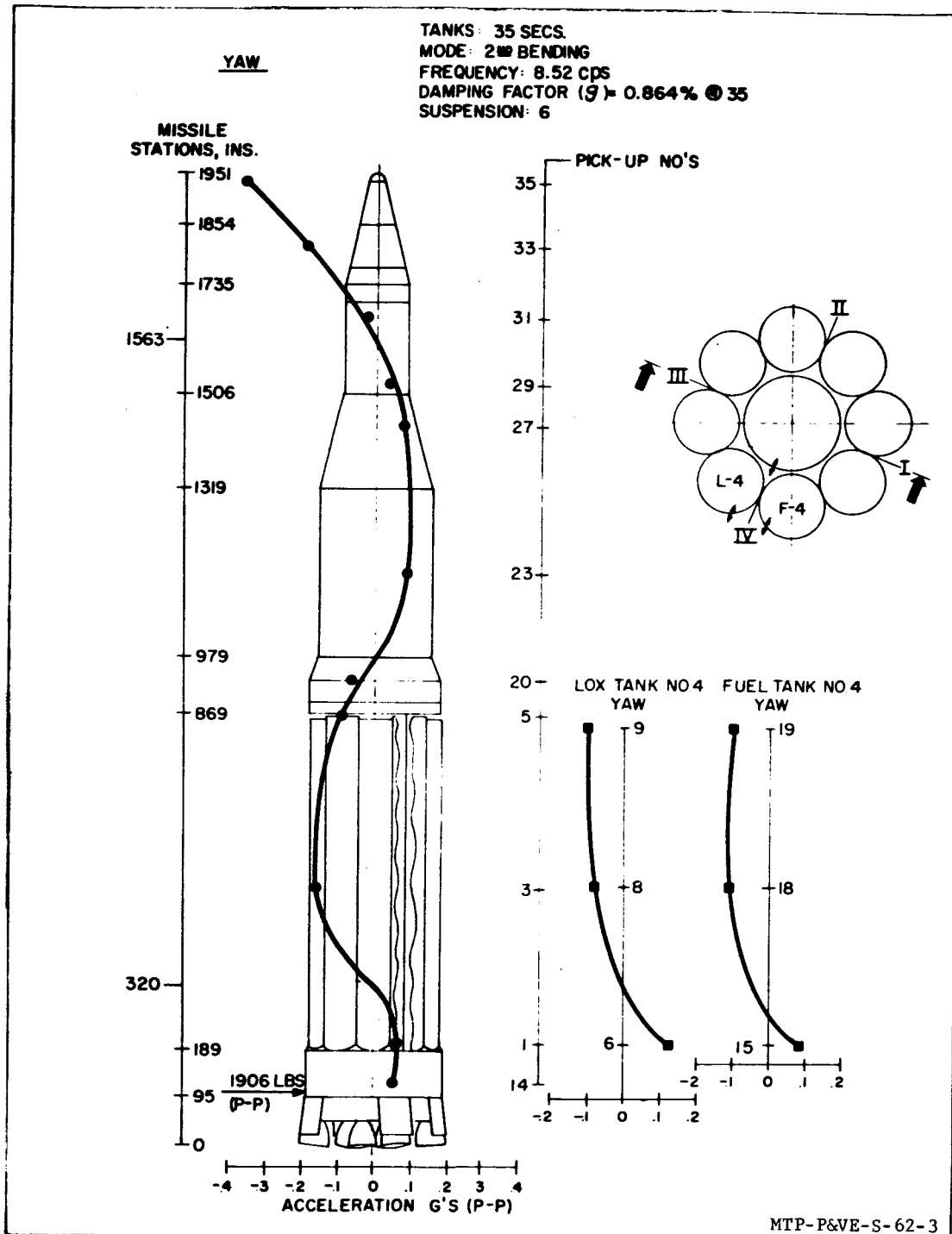


FIGURE 63. LATERAL BENDING MODES (YAW PLANE)

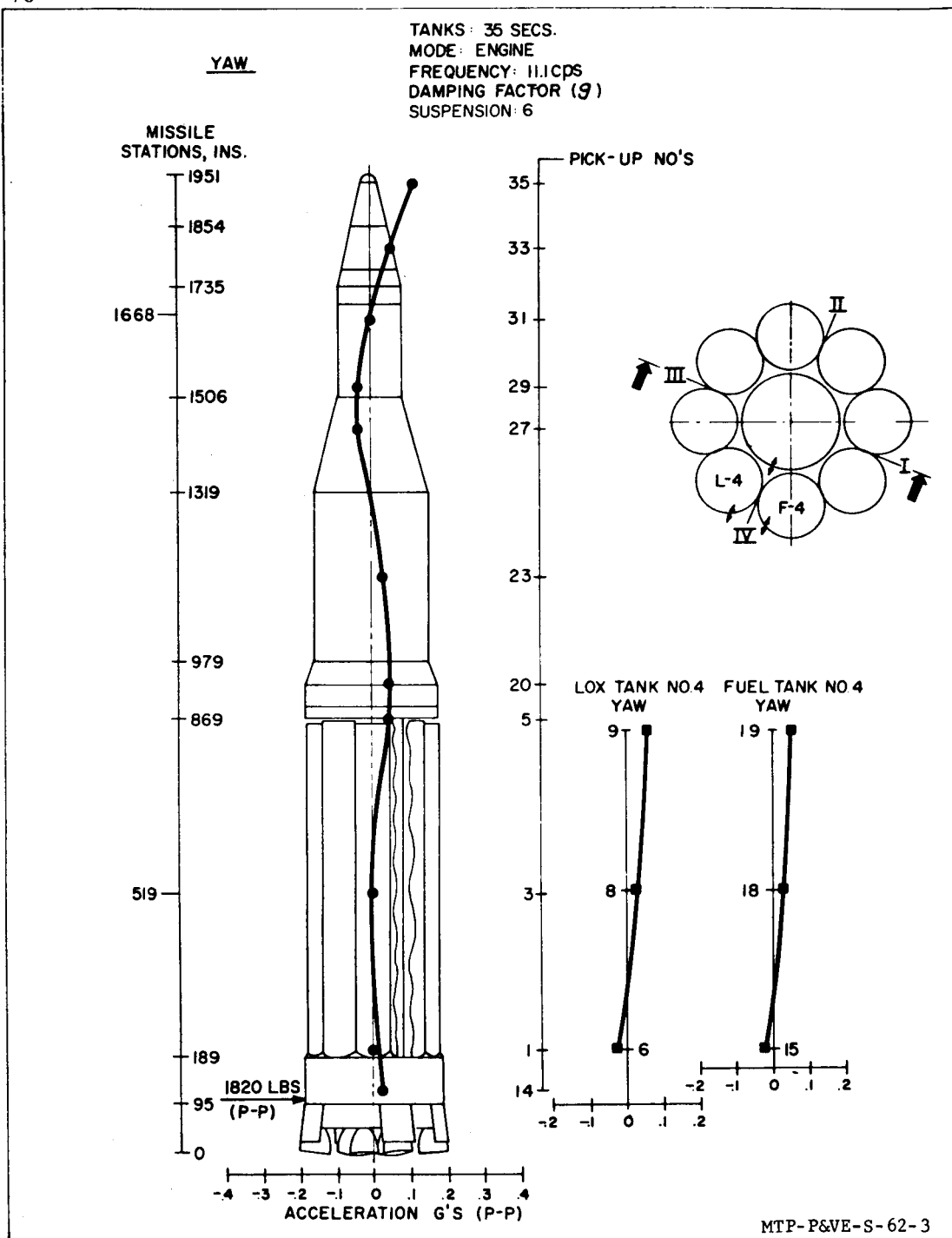


FIGURE 64. LATERAL BENDING MODES (YAW PLANE)

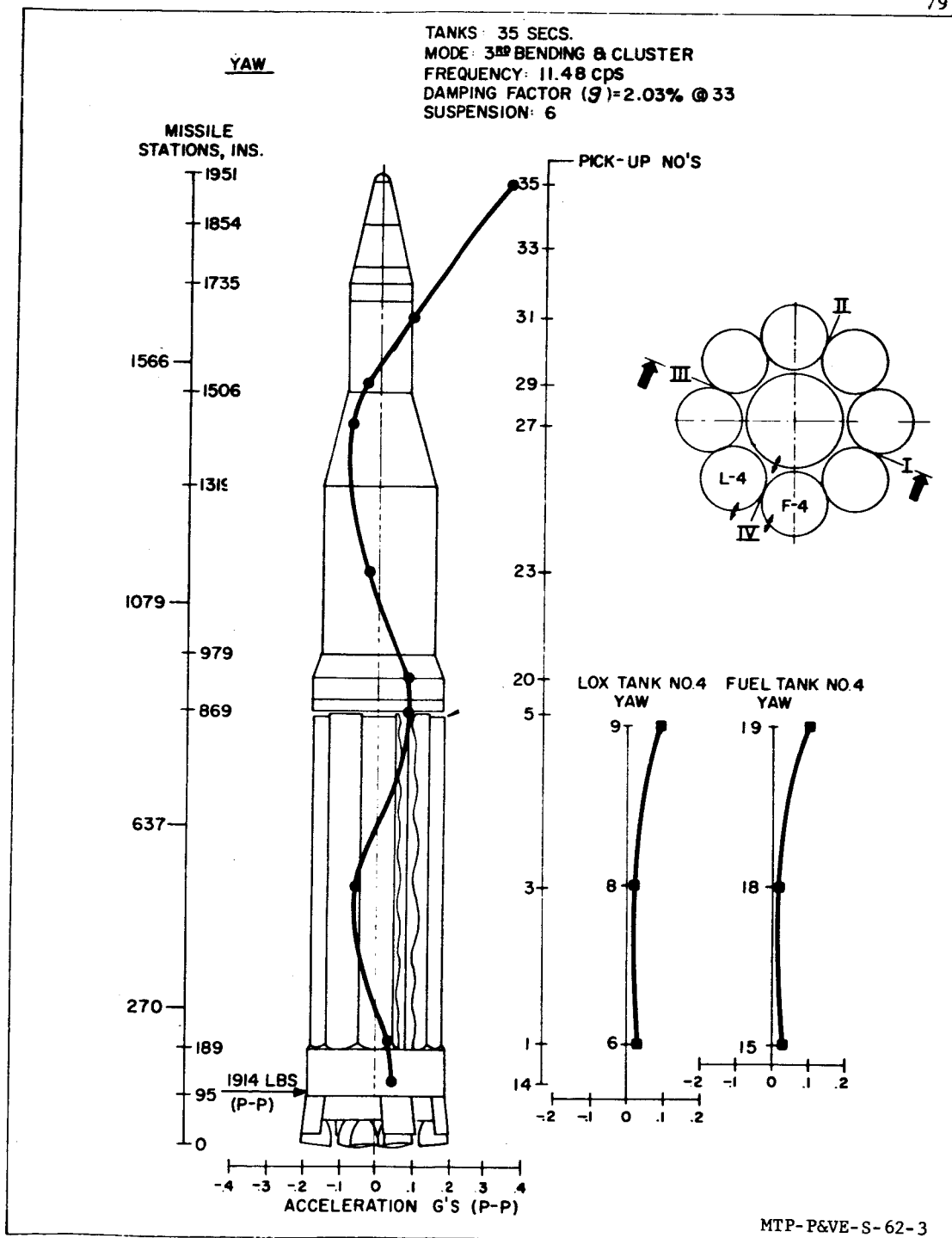


FIGURE 65. LATERAL BENDING MODES (YAW PLANE)

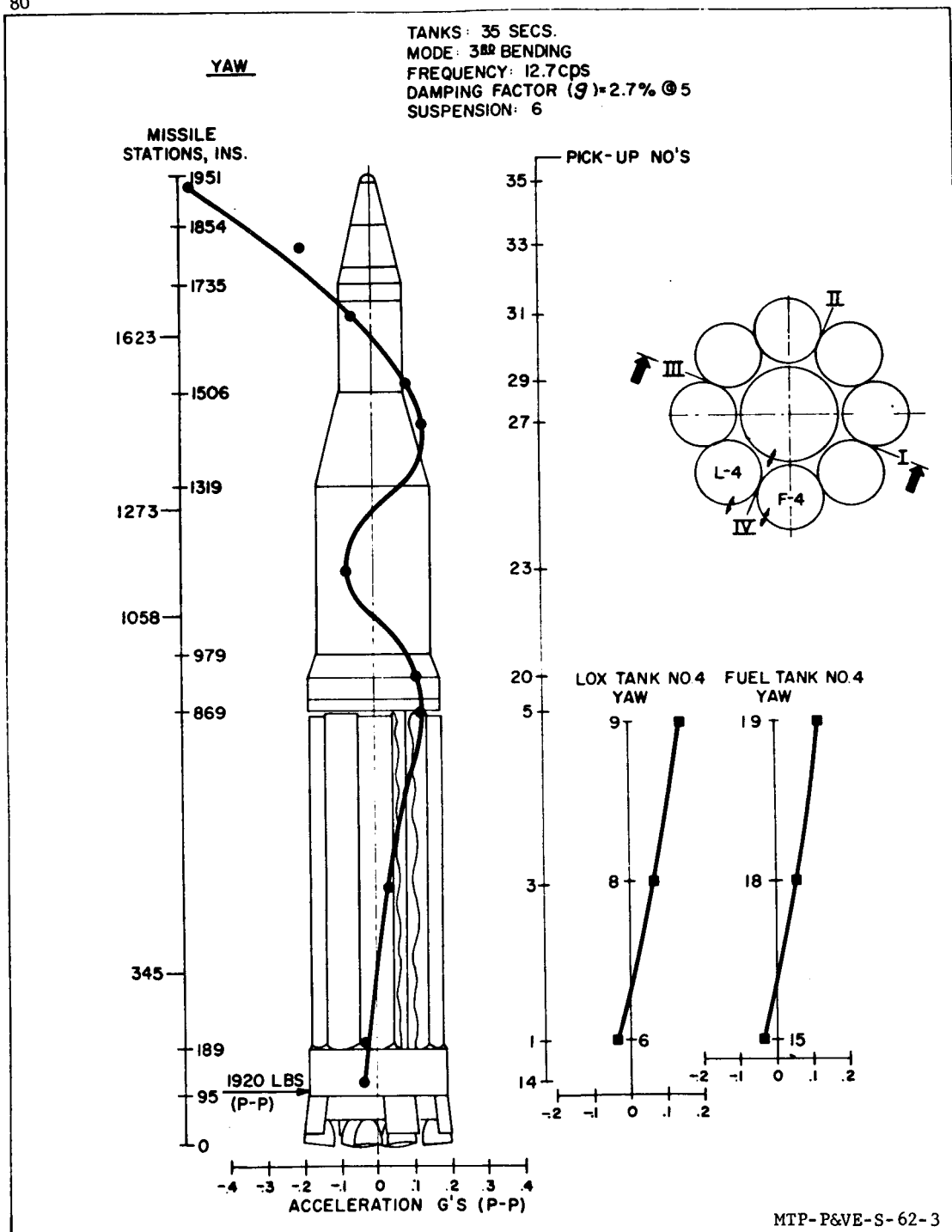


FIGURE 66. LATERAL BENDING MODES (YAW PLANE)

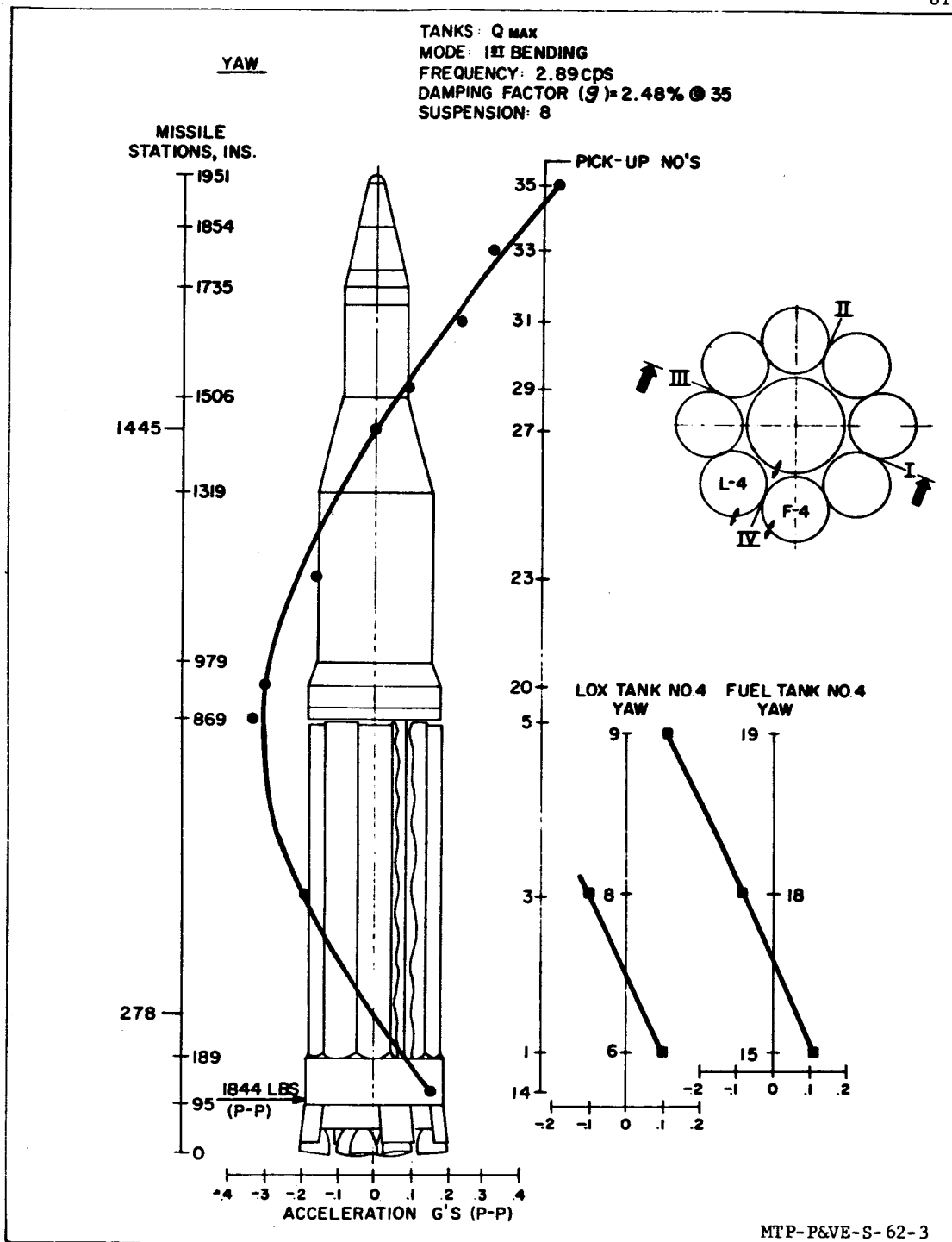


FIGURE 67. LATERAL BENDING MODES (YAW PLANE)

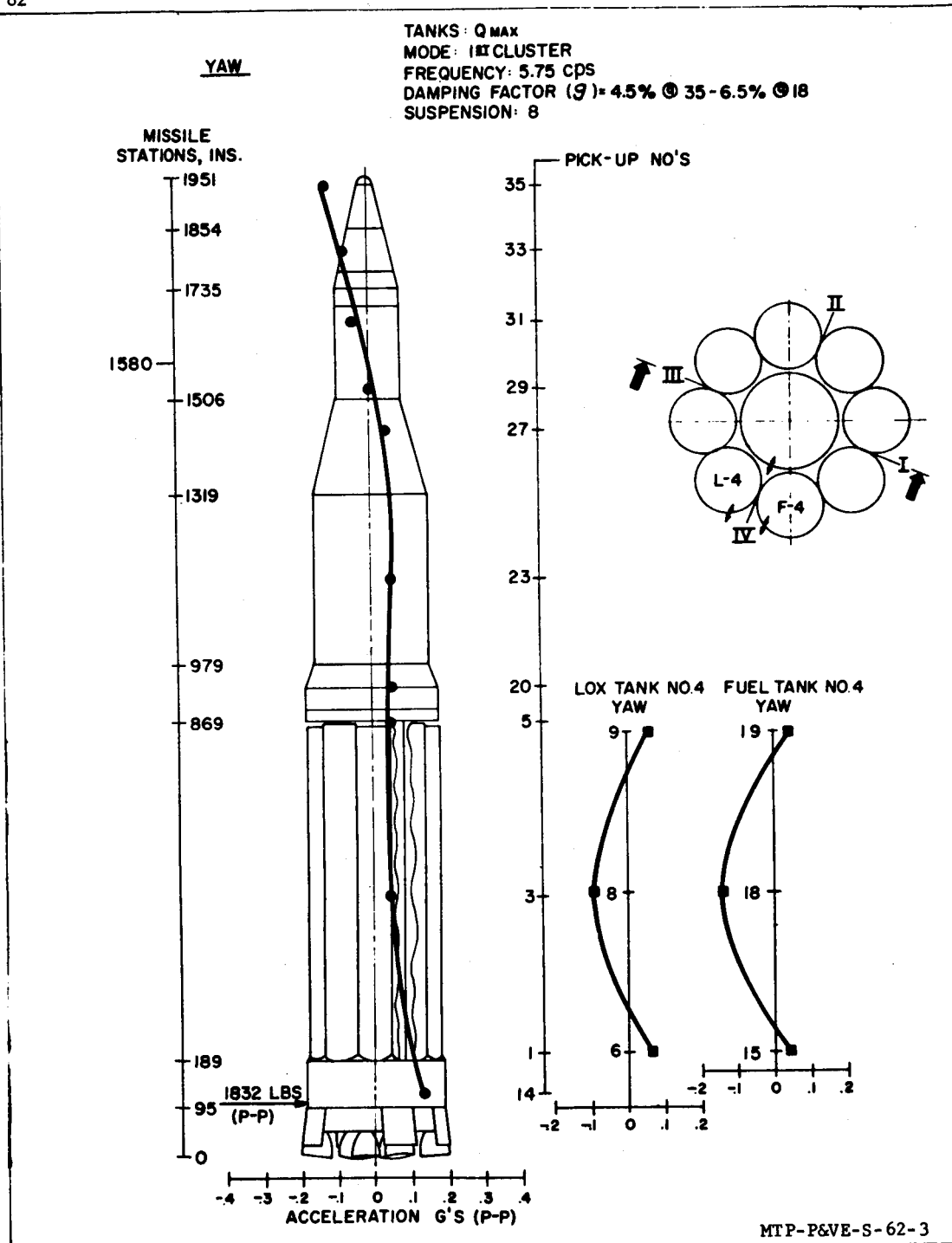


FIGURE 68. LATERAL BENDING MODES (YAW PLANE)

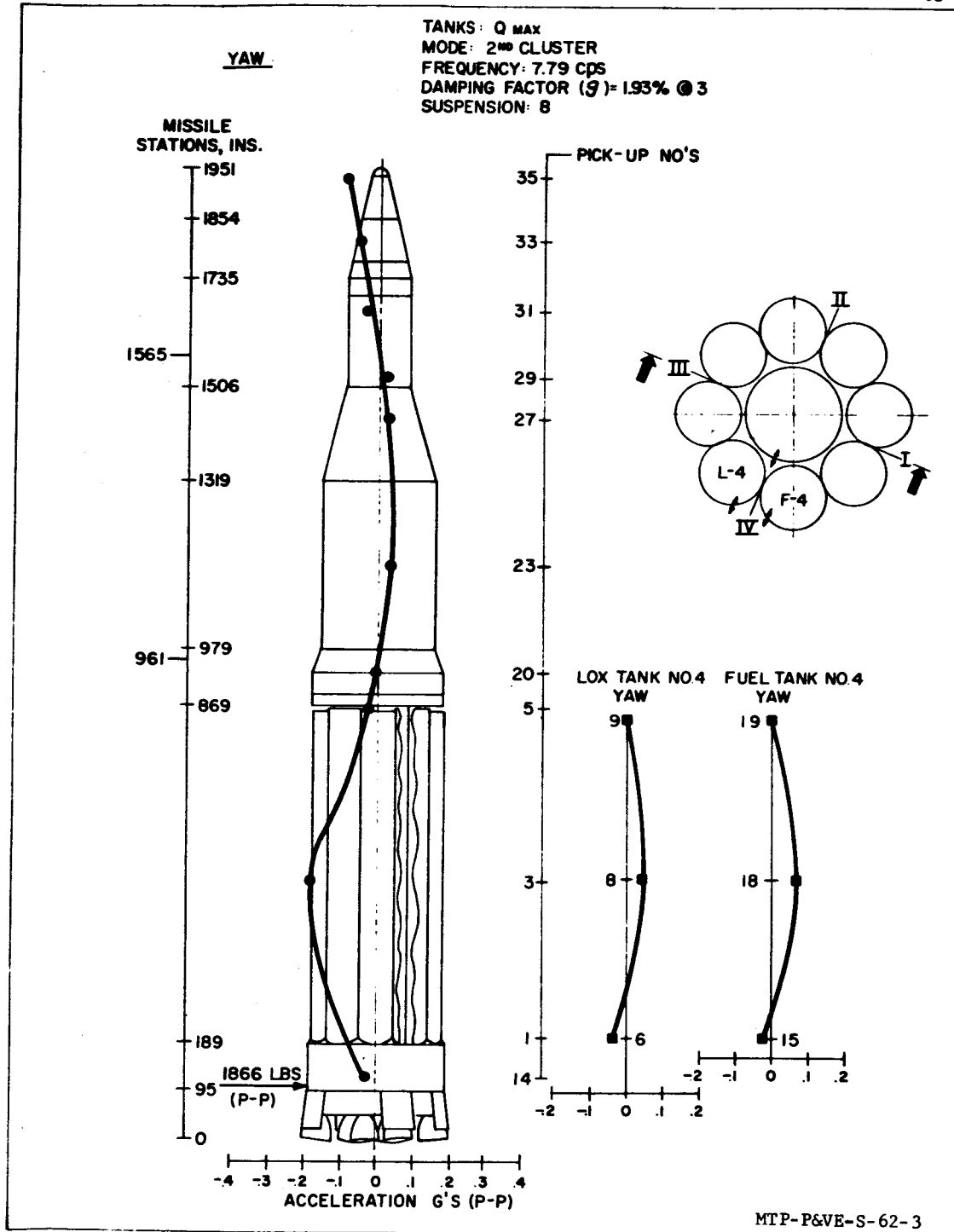


FIGURE 69. LATERAL BENDING MODES (YAW PLANE)

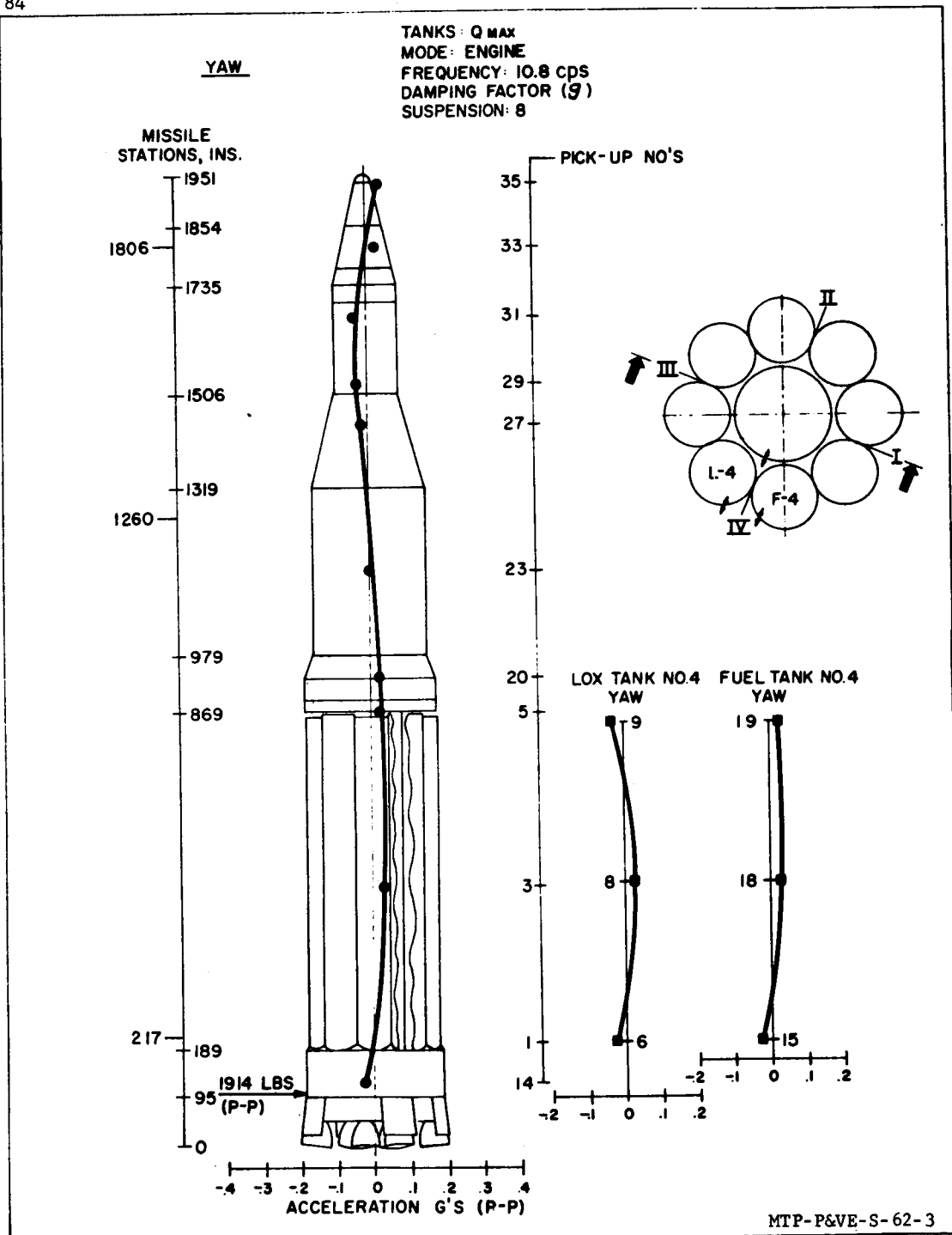


FIGURE 70. LATERAL BENDING MODES (YAW PLANE)

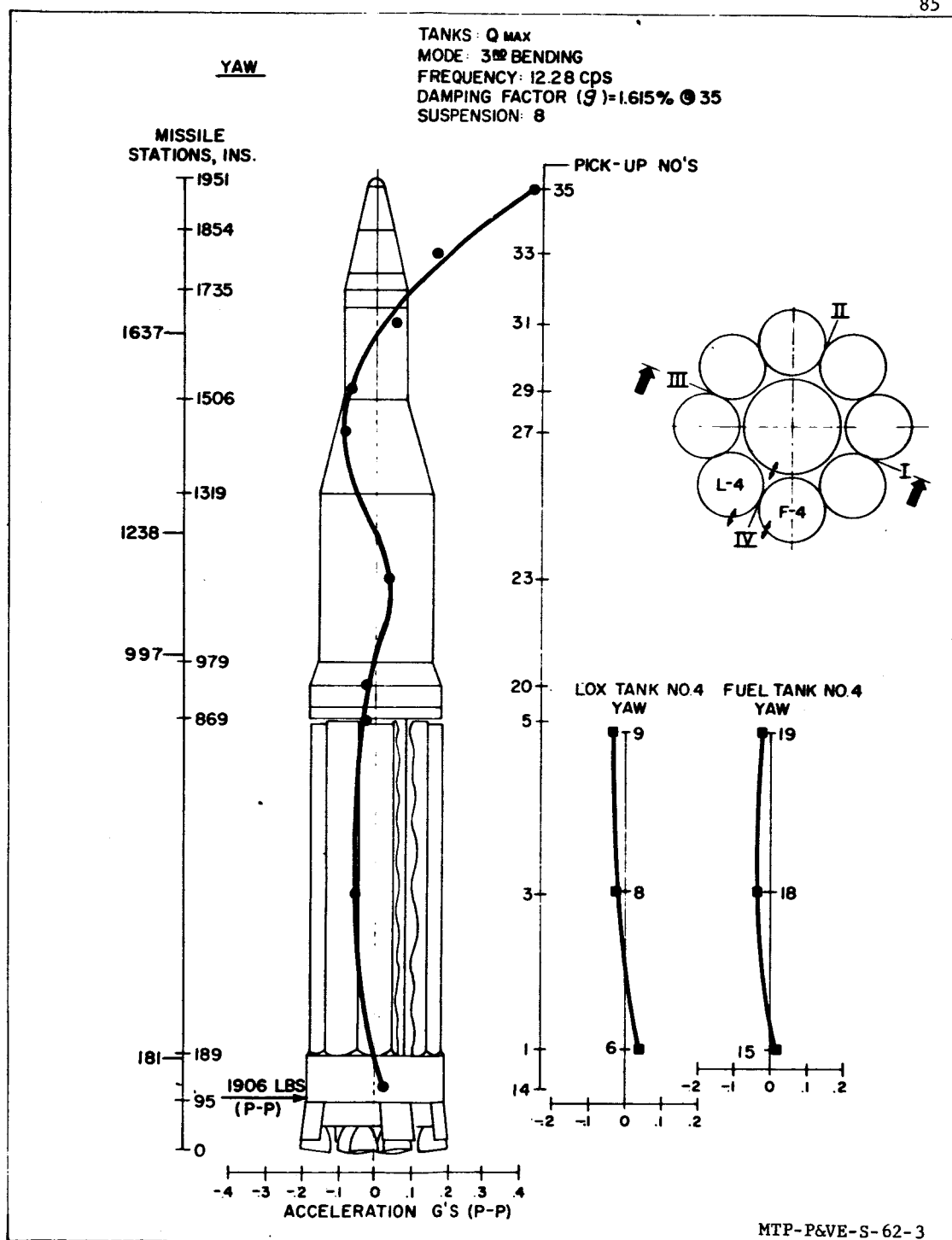


FIGURE 71. LATERAL BENDING MODES (YAW PLANE)

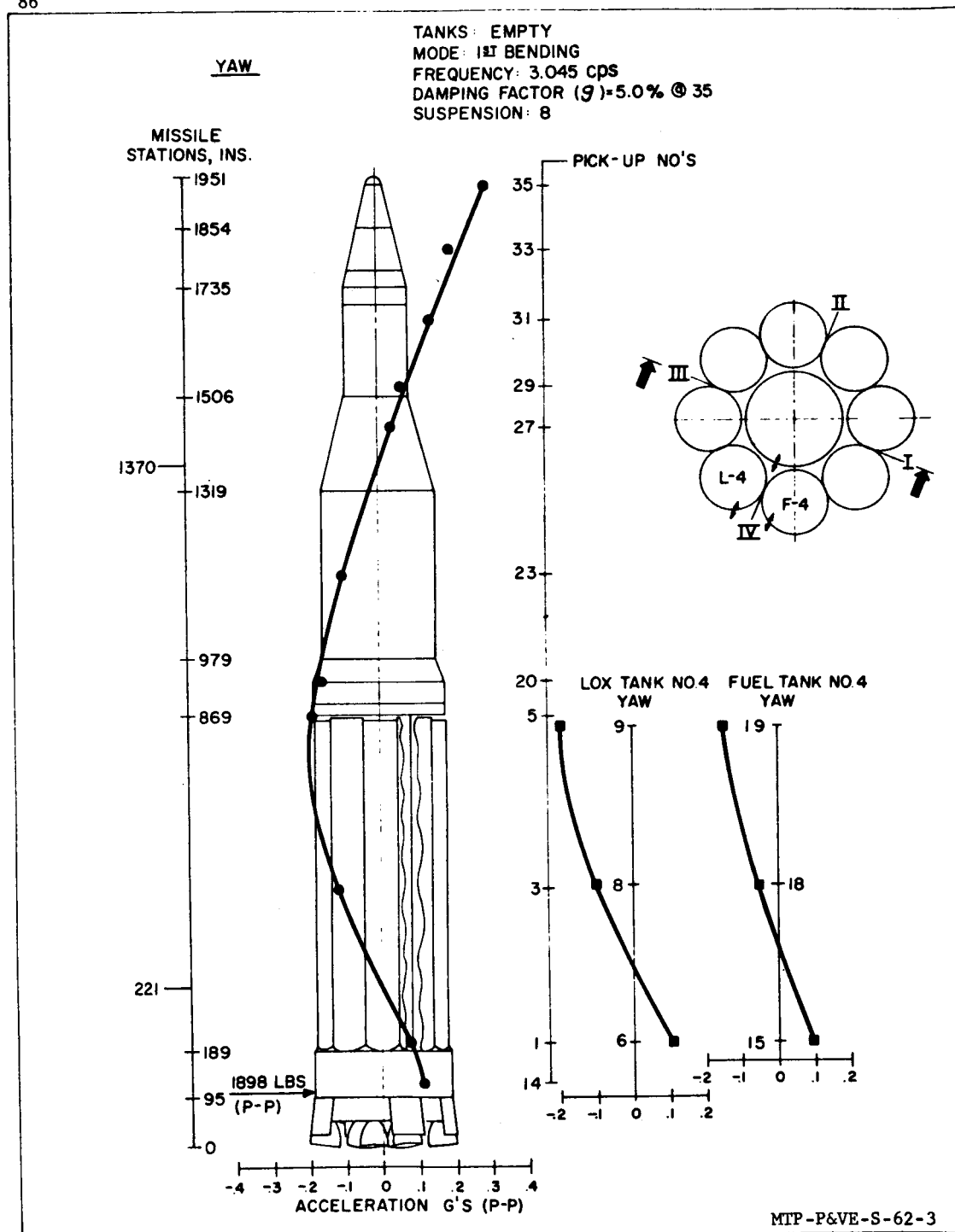


FIGURE 72. LATERAL BENDING MODES (YAW PLANE)

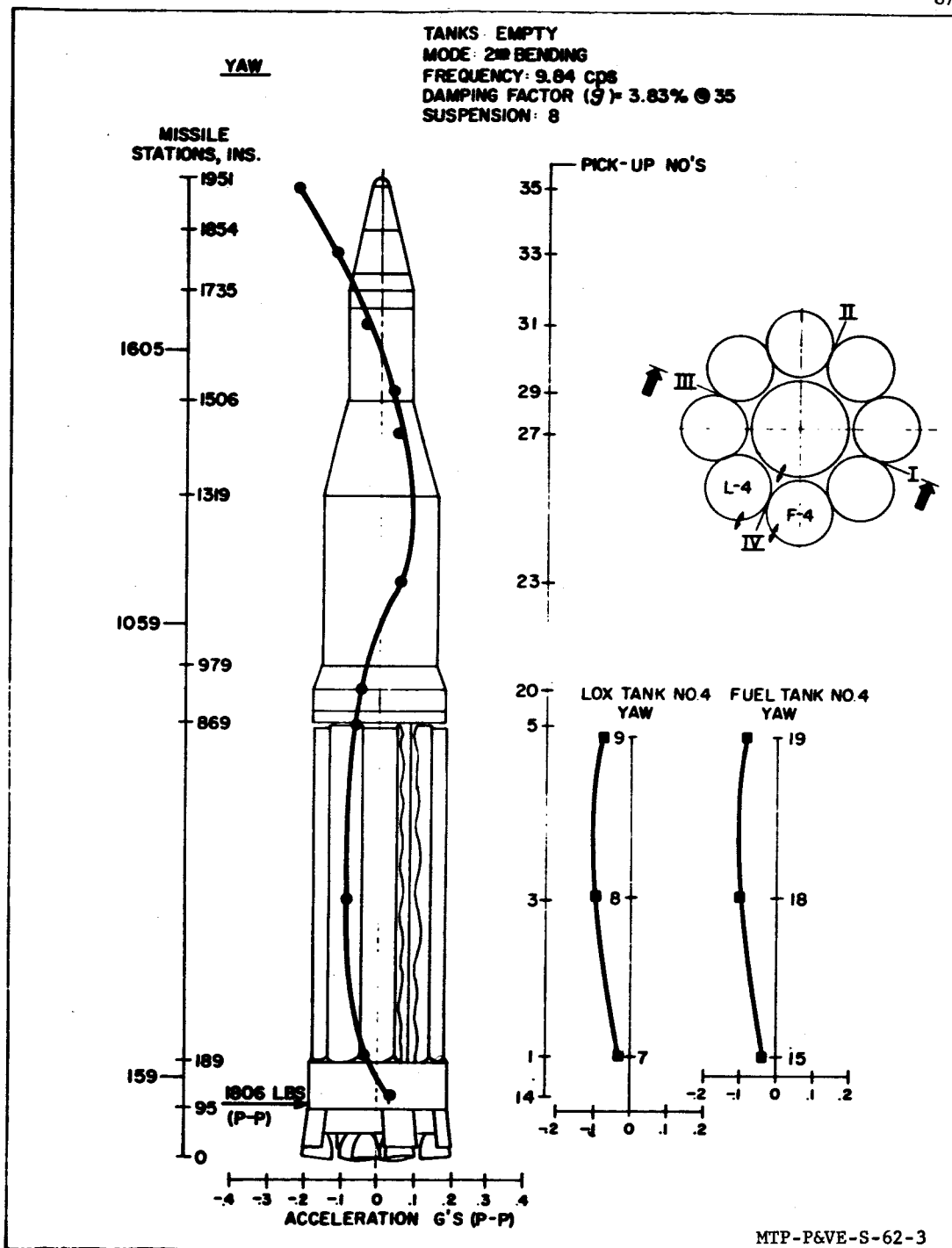


FIGURE 73. LATERAL BENDING MODES (YAW PLANE)

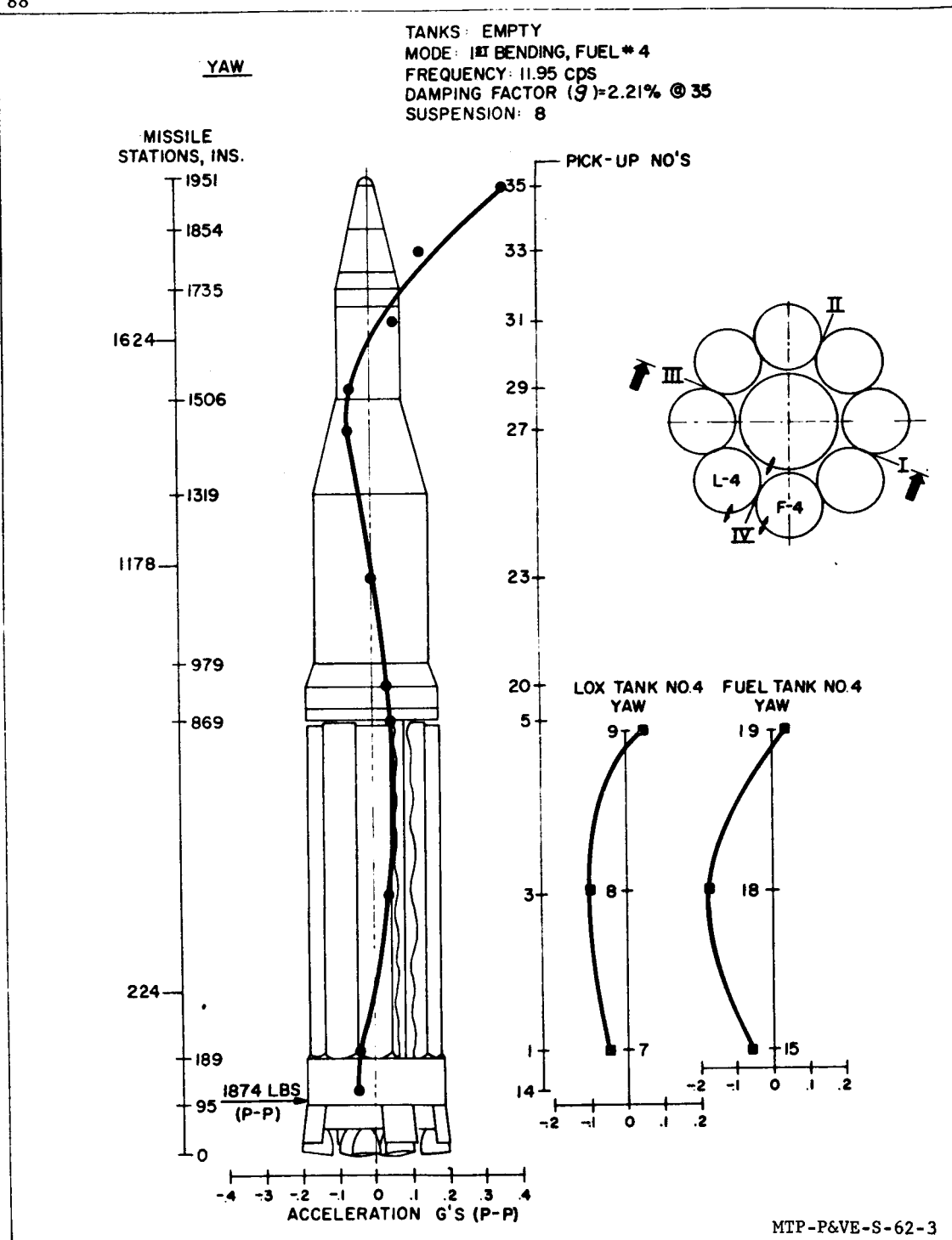
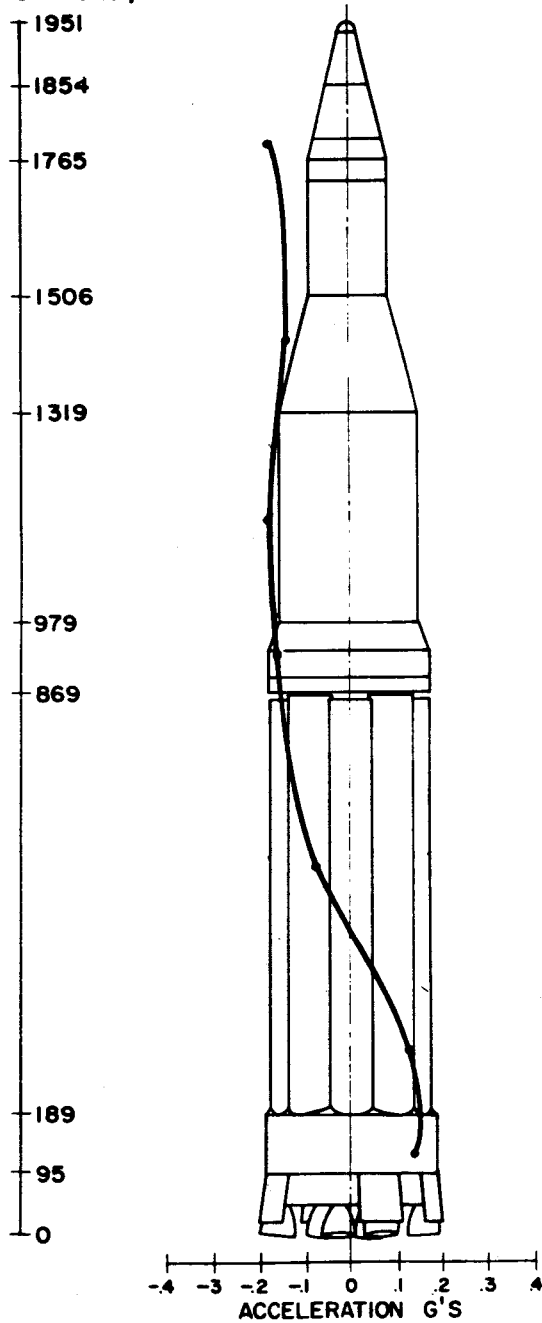


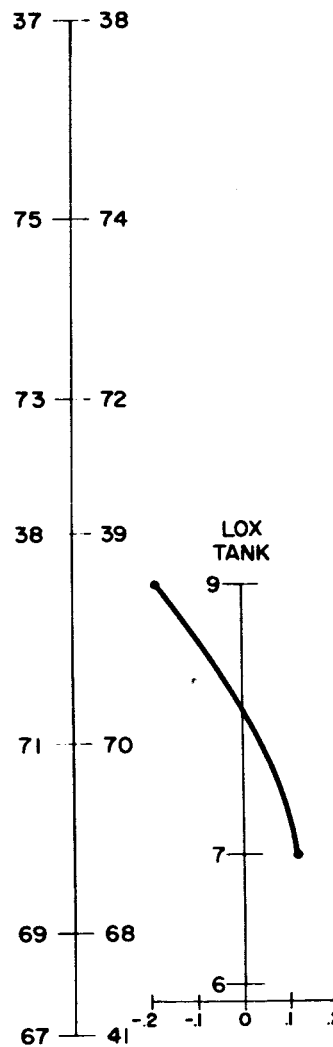
FIGURE 74. LATERAL BENDING MODES (YAW PLANE)

TANKS: LIFT OFF
 MODE: FIRST TORSION
 FREQUENCY: 5.69 CPS
 DAMPING FACTOR (S): 2.67 %
 SUSPENSION: 2

MISSILE STATIONS, INS.



PICK-UP NO'S

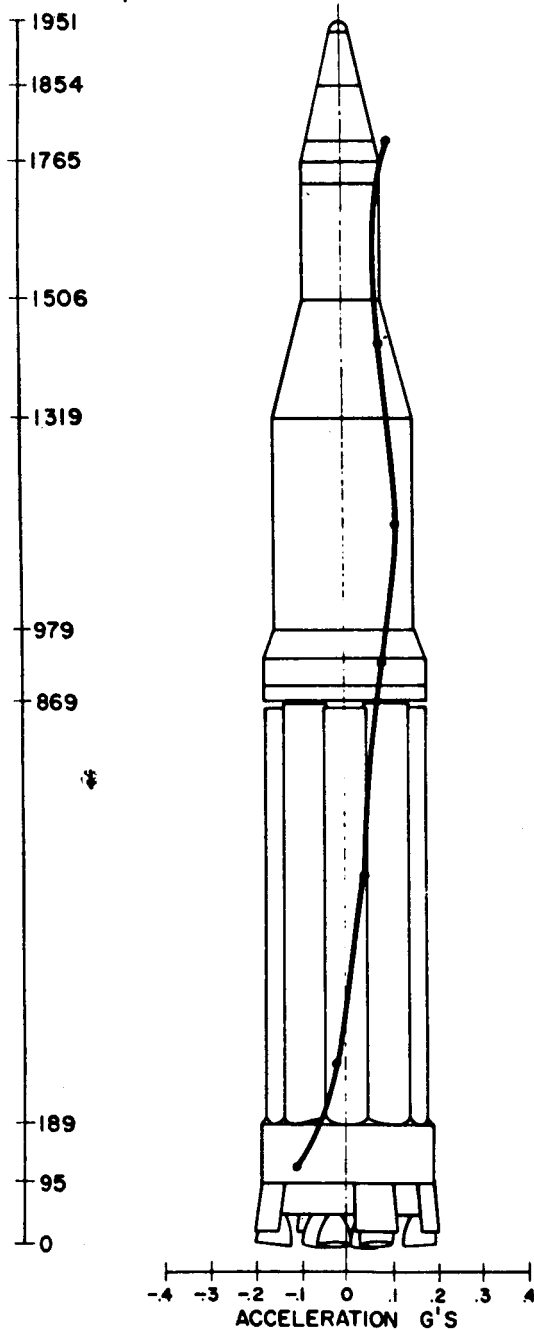


MTP-P&VE-S-62-3

FIGURE 75. TORSIONAL BENDING MODES

TANKS: 35 SEC.
 MODE: FIRST TORSION
 FREQUENCY: 6.38 CPS
 DAMPING FACTOR (ζ): 1.64 %
 SUSPENSION: 2

MISSILE STATIONS, INS.



PICK-UP NO'S

37 - 38

75 - 74

73 - 72

38 - 39

71 - 70

69 - 68

67 - 41

LOX
TANK

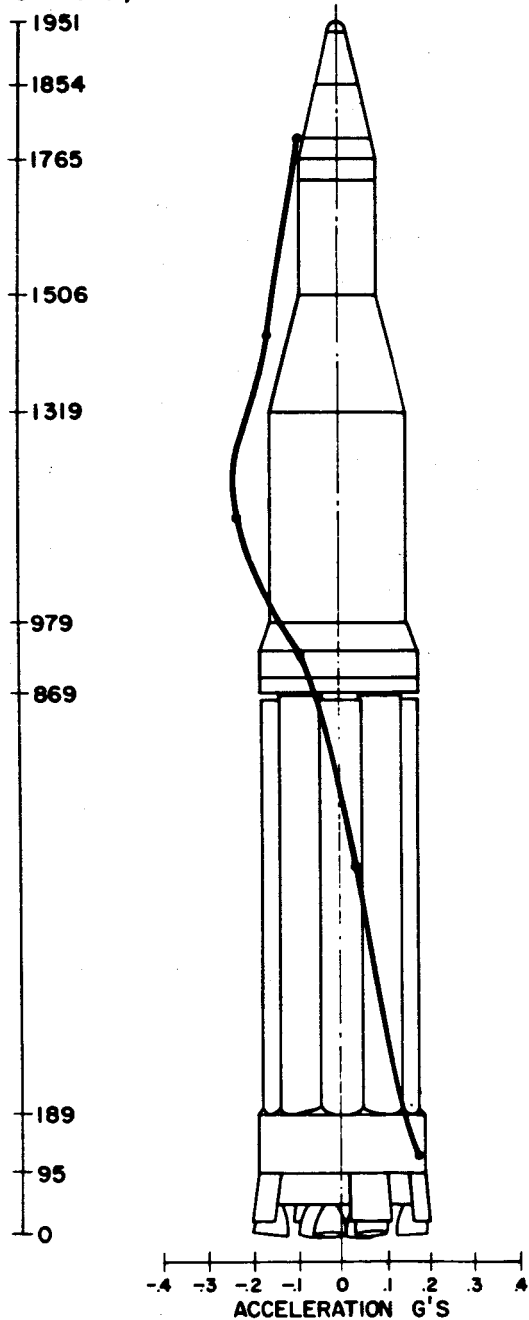


MTP-P&VE-S-62-3

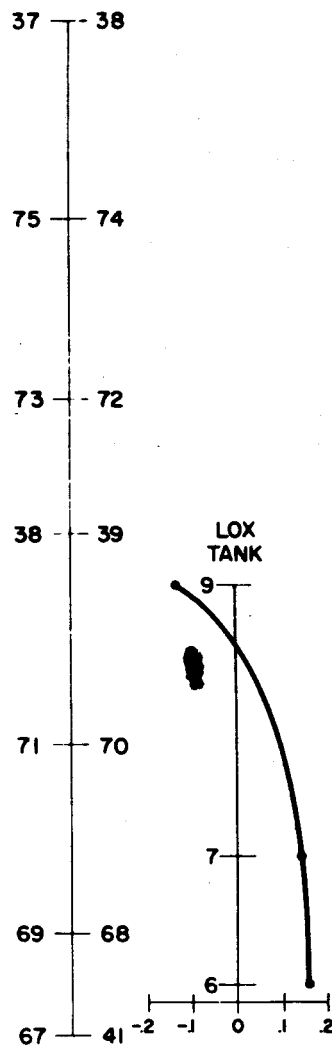
FIGURE 76. TORSIONAL BENDING MODES

TANKS: EMPTY
 MODE: FIRST TORSIONAL
 FREQUENCY: 7.91 CPS
 DAMPING FACTOR (S): 18%
 SUSPENSION: 3

MISSILE STATIONS, INS.



PICK-UP NO'S



MTP-P&VE-S-62-3

FIGURE 77. TORSIONAL BENDING MODES

APPENDIX

PREDICTED SUSPENSION CABLE CHARACTERISTICS FOR SA-D5 DYNAMIC TESTS

The curves plotted in FIGURE A-1 show the predicted first and second vehicle resonant bending frequencies (the ordinate) together with expected cable frequencies versus cable tension for various time conditions and suspension systems (four or eight lifting points). The cable frequencies are seen to go above both the first mode at all conditions and all the second modes, except with an empty booster. This large increase in cable frequency is created by having the lower connecting link fastened rigidly to the vehicle becoming an integral part of the tail assembly, thereby shortening the cable and decreasing the effective moving cable weight, the former having the greatest influence in raising the frequency.

In the event that some cable frequencies coincide with vehicle resonant bending frequencies because of the inability to predict the multitude of resonant points existing in this frequency range a device, referred to as a cable flexure, can be installed near the midpoint of each cable. Cable flexures are made so as to rigidly fix the midpoint of the cable in a radial and tangential direction but have negligible effect on the lateral stiffness of the overall suspension system. This makes it possible to tune the cable resonant frequency away from a vehicle frequency.

A short test program was conducted using cable flexures on the SA-D1 test setup. It was found that the flexures were capable of raising the cable frequencies approximately 0.5 cps with negligible effect on the gain through the vehicle. This frequency change would be sufficient to remove the effects of cable resonance on vehicle resonance because both vehicle and cables have very sharp resonant peaks and narrow band widths of excitation.

Cable frequency response curves plotted in FIGURE A-2 show both the increase in frequency and decrease in cable amplitude from a test without flexures to a test using them.

COMPARISON OF CABLE RESONANCE WITH & WITHOUT FLEXURES

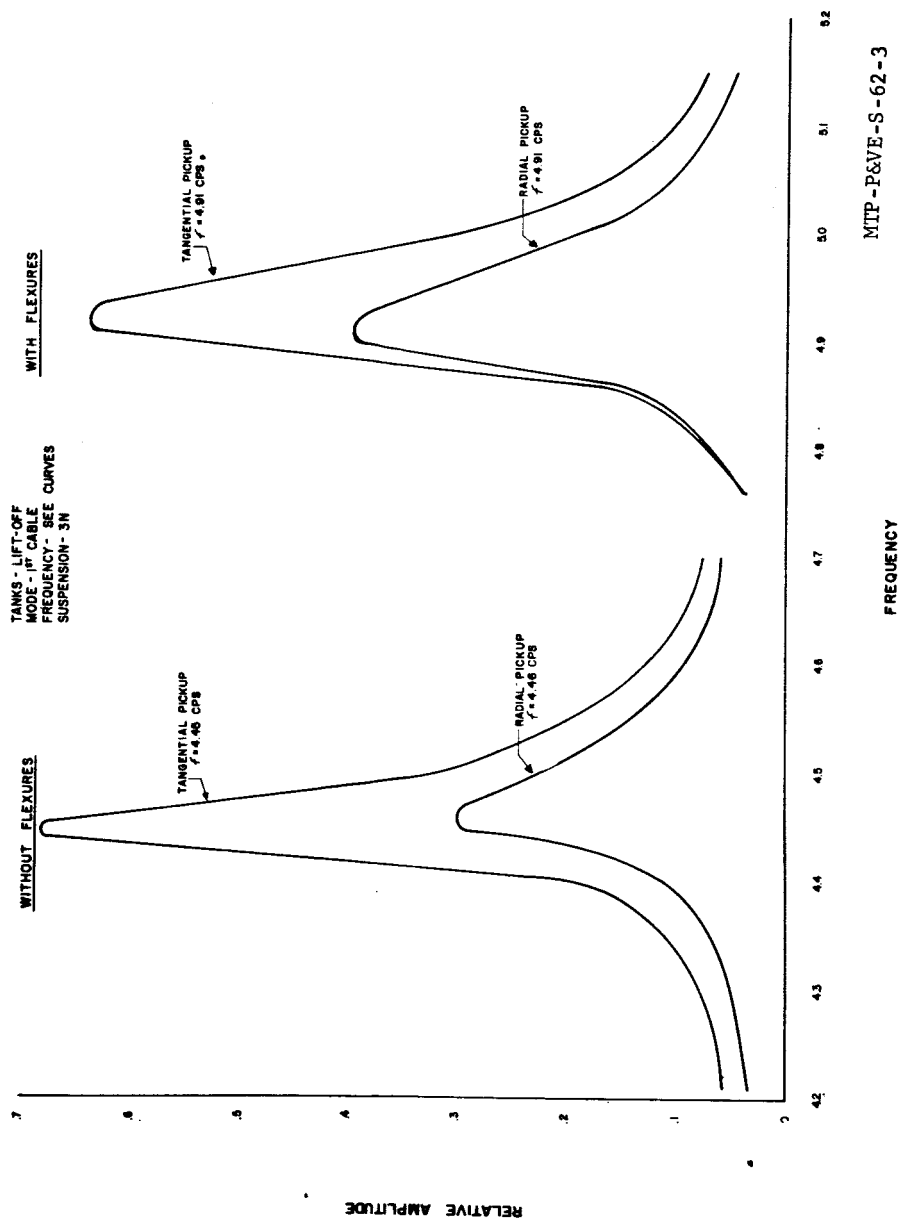
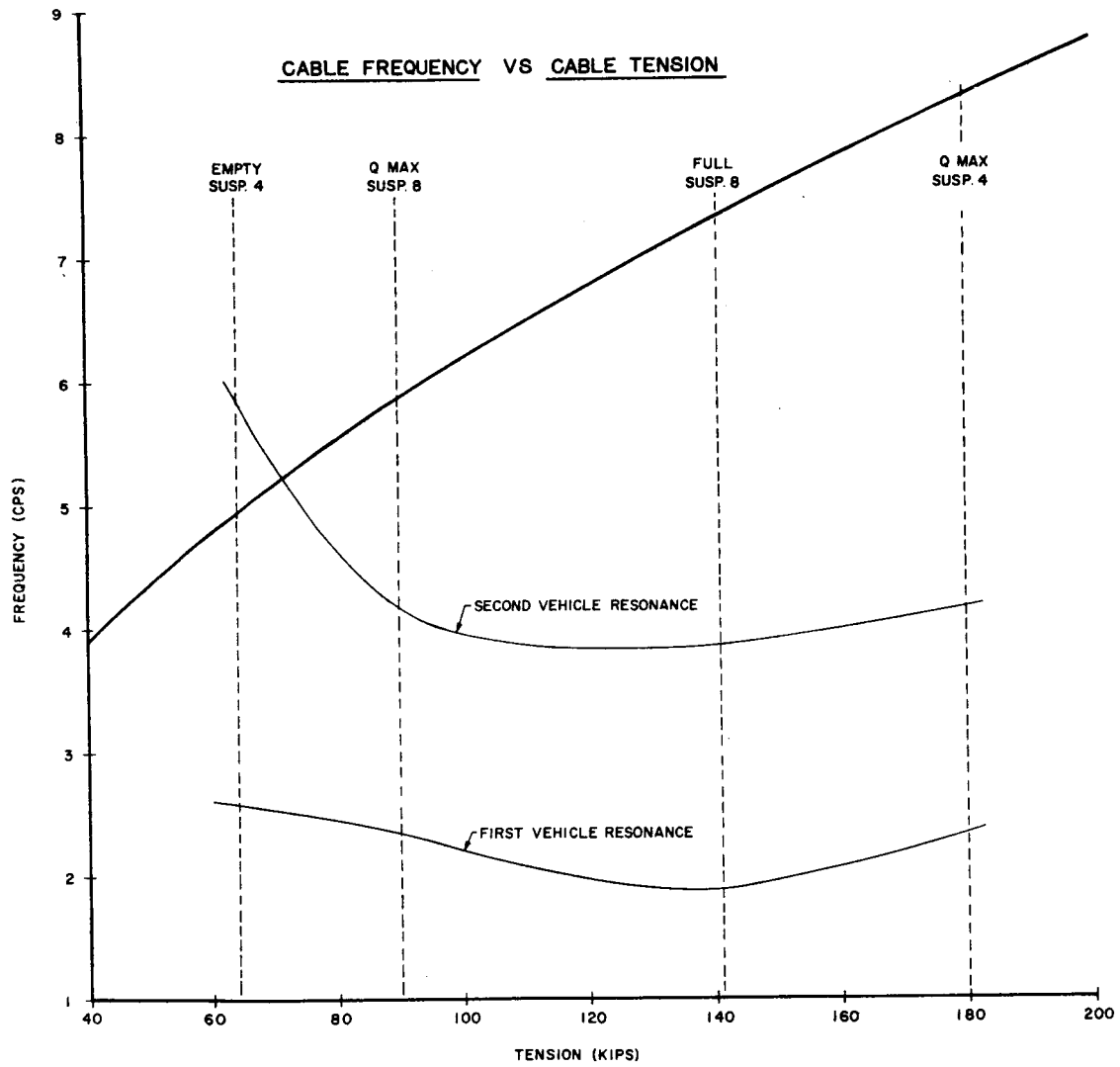


FIGURE A-1. CABLE RESONANT RESPONSE (SA-D5)



MTP-P&VE-S-62-3

FIGURE A-2. CABLE FREQUENCY VS. CABLE TENSION (SA-D5)

Rate gyro output, with and without cable flexures, for three locations on the vehicle and an average increase in response of 3.0 percent is found with the flexures are given below.

RATE GYRO OUTPUT VS. VEHICLE STATION
WITH AND WITHOUT CABLE FLEXURES

RATE GYRO OUTPUT degrees/sec/lb.		
RATE GYRO STATION	W/O FLEXURES f - 2.946 cps	WITH FLEXURES f - 2.953 cps
100	8.65×10^{-4}	9.23×10^{-4}
940	5.54×10^{-4}	5.64×10^{-4}
1765	10.28×10^{-4}	10.26×10^{-4}

Cable flexures of a known spring constant would be used and their effect on the entire suspension system could be evaluated mathematically, if it became necessary.

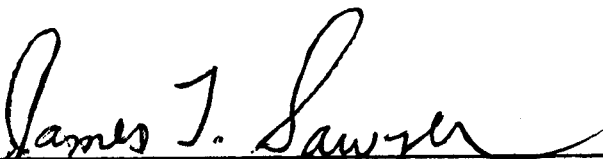
APPROVAL

MTP-P&VE-S-62-3

EXPERIMENTAL VIBRATION PROGRAM ON A FULL SCALE SATURN SPACE VEHICLE

By Charles E. Watson & Kay W. Slayden

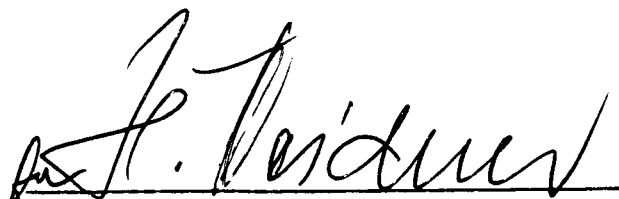
The information in this report has been reviewed for security classification. Review of any information concerning Department of Defense or Atomic Energy Commission programs has been made by the MSFC Security Classification Officer. This report, in its entirety, has been determined to be unclassified.



J. T. SAWYER
Chief, Experimental Structures Section



G. A. KROLL
Chief, Structures Branch



W. A. MRAZEK
Director, Propulsion & Vehicle Engineering Division